

2003

Simplified live-load moment distribution factors for simple span slab on I-girder bridges

Wesley D. Hevener
West Virginia University

Follow this and additional works at: <https://researchrepository.wvu.edu/etd>

Recommended Citation

Hevener, Wesley D., "Simplified live-load moment distribution factors for simple span slab on I-girder bridges" (2003). *Graduate Theses, Dissertations, and Problem Reports*. 1377.
<https://researchrepository.wvu.edu/etd/1377>

This Thesis is protected by copyright and/or related rights. It has been brought to you by the The Research Repository @ WVU with permission from the rights-holder(s). You are free to use this Thesis in any way that is permitted by the copyright and related rights legislation that applies to your use. For other uses you must obtain permission from the rights-holder(s) directly, unless additional rights are indicated by a Creative Commons license in the record and/ or on the work itself. This Thesis has been accepted for inclusion in WVU Graduate Theses, Dissertations, and Problem Reports collection by an authorized administrator of The Research Repository @ WVU. For more information, please contact researchrepository@mail.wvu.edu.

**SIMPLIFIED LIVE-LOAD MOMENT DISTRIBUTION FACTORS FOR SIMPLE
SPAN SLAB ON I-GIRDER BRIDGES**

Wesley D. Hevener

**Thesis submitted to the
College of Engineering and Mineral Resources
at West Virginia University
in partial fulfillment of the requirements
for
Master of Science
in
Civil Engineering**

**Karl E. Barth, Ph.D., Chair
Julio F. Davalos, Ph.D.
Indrajit N. Ray, Ph.D.**

Department of Civil and Environmental Engineering

**Morgantown, West Virginia
2003**

Keywords: Load Distribution, Bridges, FEA

Live load distribution factors have been used in the design of highway bridges since the first edition of the AASHTO Standard Specifications were introduced in 1931. Revisions were made to the AASHTO Standard Specifications in 1943 based on work conducted by Newmark. These changes lead to the $S/5.5$ factor. In 1988, an effort was made to revise the AASHTO Standard Specification equation for live load distribution to produce less conservative results. NCHRP Report 12-26 successfully developed an equation involving girder spacing, girder span length, girder stiffness, and slab thickness; and was adopted into the AASHTO LRFD Specifications.

The primary goal of this effort is to identify and assess various methods of computing live load distribution factors and to use the results of laboratory and field tests to compare these methods. It is further a goal of this work to use these methods to perform a parametric study over a wide range of typical slab on steel I-girder bridges to assess the accuracy of both the AASHTO Standard and AASHTO LRFD specifications and to propose an empirical model that correlates better with the analytical results within the range of parameters that are to be studied.

These studies include: (1) a verification study into the FEA techniques used in modeling bridge geometry, (2) selection of procedure of calculating load distribution factors from FEA data, (3) a verification study of the selected procedure, (4) a parametric study to assess the influence of bridge parameters on the contribution to load distribution factors, (5) the development, using regression techniques, of a new equation for live load distribution factors, and (6) a comparison of proposed distribution factors against FEA, AASHTO LRFD, and AASHTO Standard Specifications.

Results from this work that over a wide range of typical bridge parameters both the AASHTO Standard and LRFD Specifications may produce conservative results and indicate the proposed equation provides a good foundation for the development of new equations for live load distribution factors. Girder spacing and girder span length were found to have the most influence of load distribution. The proposed equation developed showed good correlation to the FEA data and also correlated well against actual DOT bridge inventories used in the development of the AASHTO LRFD equation for live load distribution factors in slab on steel I-girder bridges.

ACKNOWLEDGEMENTS

I would like to express my sincere gratitude to Dr. Karl Barth for the opportunity to pursue my master's degree at West Virginia University under his guidance and direction. The encouragement and support shown throughout my graduate study along with the valuable instruction will be instrumental in my future endeavors.

I would also like to thank Dr. Julio Davalos and Dr. Indrajit Ray for their participation on my graduate advisory committee.

Funding for this project was provided by the West Virginia Department of Transportation Division of Highways and is gratefully acknowledged.

TABLE OF CONTENTS

Title Page.....	i
Abstract.....	ii
Acknowledgements.....	iii
Table of Contents.....	iv
List of Tables.....	vii
List of Figures.....	viii
Chapter 1: Introduction.....	1
1.1 General.....	1
1.2 Problem Statement.....	1
1.3 Scope of Work.....	2
1.4 Organization of Thesis.....	4
Chapter 2: Literature Review.....	5
2.1 Introduction.....	5
2.2 AASHTO Standard Specifications.....	5
2.3 AASHTO LRFD Specifications.....	8
2.4 Ontario Highway Bridge Code [OHBC] and the Canadian Highway Bridge Code [CSA].....	10
2.5 European Codes.....	10
2.6 Australian Bridge Code.....	11
2.7 Refined Analysis.....	11
2.8 Studies Evaluating Current Distribution Factors.....	12
2.8.1 Analytical Studies.....	13
2.8.2 Field Studies.....	15
2.9 Factors Influence Live Load Distribution.....	16
2.9.1 Girder Spacing.....	16
2.9.2 Span Length.....	17
2.9.3 Girder Stiffness.....	17
2.9.4 Deck Thickness.....	19
2.9.5 Girder Location.....	19
2.9.6 Continuity Conditions.....	20
2.9.7 Skew.....	20
2.9.8 Cross Frame Characteristics.....	21
2.9.9 Secondary Stiffening Elements.....	21
2.9.10 Composite Behavior.....	22
Chapter 3: Development of Current AASHTO Load Distribution Factor Equations.....	23
3.1 Introduction.....	23
3.2 Method of Analysis Selection.....	23
3.3 Sensitivity Studies.....	24

3.4	Parametric Study.....	25
3.4.1	Database of State DOT Bridges.....	25
3.4.2	Parametric Study Bridges.....	26
3.5	Proposed Equations.....	26
3.6	Determination of Accuracy of Proposed Equations.....	28

Chapter 4: Computation of Distribution Factors for Slab-on-Steel

	Girder Bridges.....	63
4.1	Introduction.....	63
4.2	Barker Method.....	63
4.3	Stallings Method.....	67
4.4	Bakht Method.....	68
4.5	Mabsout Method.....	69
4.6	Example Calculations.....	70
4.6.1	Barker Method 1 for Positive Moment Region.....	71
4.6.2	Barker Method 1 for Negative Moment Region.....	74
4.6.3	Barker Method 2 for Positive Moment Region.....	76
4.6.4	Barker Method 2 for Negative Moment Region.....	76
4.6.5	Stallings Method for Positive Moment Region.....	77
4.6.6	Stallings Method for Negative Moment Region.....	78
4.6.7	Bakht Method for Positive Moment Region.....	78
4.6.8	Bakht Method for Negative Moment Region.....	79
4.6.9	Mabsout Method for Positive Moment Region.....	80
4.6.10	Mabsout Method for Negative Moment Region.....	81
4.7	Conclusions.....	81

Chapter 5: Verification Studies..... 89

5.1	Introduction.....	89
5.2	Description of FEA modeling tools.....	90
5.3	Verification Studies.....	91
5.3.1	Comparison with Newmark Bridge.....	91
5.3.2	Comparison with FHWA-AISI Bridge.....	92
5.3.3	Comparison with Bakht Medium Span Length Bridge.....	94
5.3.4	Comparison with Stallings Bridges.....	96
5.3	Conclusions.....	97

Chapter 6: Parametric Studies..... 110

6.1	Introduction.....	110
6.2	Range of Parameters.....	110
6.3	General Results.....	113
6.3.1	Influence of girder spacing.....	114
6.3.2	Girder span length.....	114
6.3.3	Steel yield strength.....	114
6.3.4	Span to depth ratio.....	115
6.4	Further Data Reduction.....	115

Chapter 7: General Results and Development of Proposed Moment	
Distribution Factors.....	127
7.1 Introduction.....	127
7.2 Development of Proposed Equation.....	127
7.3 Comparisons of Proposed Equation.....	129
7.4 Conclusions.....	130
Chapter 8: Summary and Concluding Remarks.....	134
8.1 Scope of Work.....	134
8.2 Summary Results.....	135
8.3 Future Work.....	136
Reference Cited.....	137

LIST OF TABLES

Table 3.1	Parametric values used in development of LRFD distribution factors for beam-and-slab bridges.....	30
Table 3.2	NCHRP 12-26 database of bridges.....	31
Table 3.3	Parameter ranges for NCHRP 12-26 bridge database.....	46
Table 3.4	NCHRP 12-26 parametric study database.....	47
Table 3.5	Representative AASHTO LRFD distribution factors (Partial Reprint from AASHTO Table 4.6.2.2.2b-1).....	54
Table 4.1	Bottom-flange strains, stresses, and D values for AISI-FHWA bridge calculations.....	83
Table 4.2	Mabsout method results showing the element stress, area, distance from neutral axis, and calculated moments for the positive moment region.....	83
Table 4.3	Mabsout method results showing the element stress, area, distance from neutral axis, and calculated moments for the negative moment region.....	84
Table 4.4	Results from example distribution factor calculation.....	84
Table 5.1	Example distribution factors for Newmark bridge.....	99
Table 5.2	Design factors for Bakht medium span bridge.....	99
Table 5.3	Distribution factors for Stallings’s bridge.....	100
Table 6.1	Key parameters for WVU parametric bridges.....	116
Table 6.2	Summary of FEA results distribution factors calculated from WVU parametric study.....	119
Table 7.1	Comparison of distribution factors comparing proposed, AASHTO LRFD, and AASHTO Standard specification done on four bridges from the WVU small bridge inventory, Bakht, and Stallings.....	131

LIST OF FIGURES

Figure 3.1	Histogram of relative frequency for span length.....	55
Figure 3.2	Histogram of relative frequency for clear roadway width.....	55
Figure 3.3	Histogram of relative frequency for skew.....	56
Figure 3.4	Histogram of relative frequency for number of girders.....	56
Figure 3.5	Histogram of relative frequency for girder spacing.....	57
Figure 3.6	Histogram of relative frequency for slab thickness.....	57
Figure 3.7	Histogram of relative frequency for girder depth.....	58
Figure 3.8	Histogram of relative frequency for roadway width (out-to-out).....	58
Figure 3.9	Histogram of relative frequency for deck overhang.....	59
Figure 3.10	Histogram of relative frequency for girder area.....	59
Figure 3.11	Histogram of relative frequency for girder moment of inertia.....	60
Figure 3.12	Histogram of relative frequency for eccentricity.....	60
Figure 3.13	Histogram of relative frequency for bridge construction date.....	61
Figure 3.14	Comparison of proposed distribution factors vs. analytical results.....	61
Figure 3.15	Comparison of proposed distribution factors vs. MSI results.....	62
Figure 4.1	Diagram of variables found in Eqn. 4.3 for least squares method.....	85
Figure 4.2	Diagram of the componets used to compute elastic moment calculated in Eqns. 4.5 to 4.8.....	85
Figure 4.3	AISI-FHWA bridge cross-section.....	86
Figure 4.4	AISI-FHWA bridge plan view showing the location of flange transitions.....	86
Figure 4.5	Cross section of girder profiles for AISI-FHWA bridge.....	87
Figure 4.6	Transverse load positions for AISI-FHWA bridge.....	87

Figure 4.7	Hypothetical loading position of a line of wheels for the calculation of Mabsout M^{truck}	88
Figure 5.1	Typical FEA mesh discretization for a WVU bridge model.....	101
Figure 5.2	Newmark bridge cross-section with horizontal loading positions.....	101
Figure 5.3	Plan view of the Newmark Bridge showing the longitudinal dimensions and loading.....	102
Figure 5.4	Comparison of deflection between Newmark experimental testing and WVU FEA for the Newmark bridge in Section 5.2.1.....	102
Figure 5.5	Bottom-Flange Stress for 0.44L-1 Lane-Loaded comparing Actual Data, Tiedeman et al. FEA results, and WVU FEA results.....	103
Figure 5.6	Bottom-Flange Stress for 0.44L-3 Lanes-Loaded comparing Actual Data, Tiedeman et al. FEA results, and WVU FEA results.....	103
Figure 5.7	Bottom-Flange Stress for 0.65L-1 Lane-Loaded comparing Actual Data, Tiedeman et al. FEA results, and WVU FEA results.....	104
Figure 5.8	Bottom-Flange Stress for 0.65L-3 Lanes-Loaded comparing Actual Data, Tiedeman et al. FEA results, and WVU FEA results.....	104
Figure 5.9	Cross-section view of Bakht medium span length bridge.....	105
Figure 5.10	Plan view of Bakht bridge showing girder transitions and cross-frame locations.....	105
Figure 5.11	Cross-sections for Bakht medium span length bridge.....	106
Figure 5.12	Plan view showing the location of longitudinal loading for each load case involving a (a) Kenworth and (b) Mack truck.....	106
Figure 5.13	Plan view showing the location of transverse loading positions for each load case involving a (a) Kenworth and (b) Mack truck.....	107
Figure 5.14	Comparison of deflection from the Bakht field-testing and WVU FEA model for the 3 load cases presented in Section 5.2.3.....	108
Figure 5.15	Stalling bridge cross-section and horizontal truck loading positions.....	108
Figure 5.16	Cross-section for Stallings's bridges.....	109

Figure 5.17	Plan view of Stalling bridges showing longitudinal dimensions and loading for two truck tests.....	109
Figure 6.1	Cross-section view and horizontal loading positions for all bridges included in the WVU parametric study for cross-section 1.....	122
Figure 6.2	Cross-section view and horizontal loading positions for all bridges included in the WVU parametric study for cross-section 2.....	122
Figure 6.3	Cross-section view and horizontal loading positions for all bridges included in the WVU parametric study for cross-section 3.....	123
Figure 6.4	Hypothetical girder elevation for girder configurations found in Table 6.1.....	123
Figure 6.5	Elevation and longitudinal loading positions for girders found in Table 6.1.....	124
Figure 6.6	Sensitivity study comparing girder stiffness against span length for the WVU parametric study, LRFD parametric study, NCHRP DOT inventory, and WVU small DOT inventory.....	124
Figure 6.7	Sensitivity study comparing design factor, D, against girder spacing for the WVU parametric study.....	125
Figure 6.8	Sensitivity study comparing design factor, D, against span length for the WVU parametric study.....	125
Figure 6.9	Sensitivity study comparing design factor, D, against girder spacing for the WVU parametric study.....	126
Figure 7.1	Comparison of actual FEA design factor values plotted against proposed design factor values.....	132
Figure 7.2	Histogram of proposed distribution factors over the actual FEA distribution factors.....	132
Figure 7.3	Histogram of the AASHTO LRFD distribution factors over the actual FEA distribution factors.....	133
Figure 7.4	Histogram of the AASHTO Standard distribution factors over the actual FEA distribution factors.....	133

CHAPTER 1

INTRODUCTION

1.1 General

Analytical studies were performed for simply supported, slab-on-stringer bridges ranging in girder spacing, span length, steel yield strength, and span-to-depth ratio. The main objectives of the studies were to verify finite element data from previous researchers, compare results of analytical modeling with data obtained from field-testing, and develop an improved equation for calculating the distribution of wheel loads on highway bridges.

1.2 Problem Statement

Live load distribution factors (also referred to as girder distribution factors and load distribution factors) are commonly used by bridge engineers in order to simplify the complex, three-dimensional behavior of a bridge system. Specifically, these factors allow for the designer or analyst to consider bridge girders individually by determining the maximum number of lines of wheels (or vehicles) that may act on a given girder. Current American specifications give relatively simple, empirical equations for calculation of these distribution factors; however they contain parameters which are difficult for the design engineer to work with primarily for initial member sizes.

Although, several researchers have shown through analytical and field studies that these equations can be inaccurate in some circumstances. The relatively recent adoption of the LRFD specifications has resulted in enhanced accuracy for bridges having geometries similar to those considered in developing the equations. However, for bridges with span lengths, girder spacings, etc. outside of these ranges, overly conservative results are often obtained. Therefore, there is a need to develop more comprehensive distribution factors that will provide a more accurate approximation of live load response and maintain simplicity of use.

The goal of this research study is to develop less complex live-load distribution equations with accuracy appropriate for design. These new equations will be less restrictive in their ranges of applicability than the present LRFD distribution factors, represent a more reasonable range of bridges being designed today, and provide a more simplistic approach. The proposed ranges of applicability will minimize the need for more refined analysis and will help to facilitate the use of the traditional line girder approach.

1.3 Scope of Work

The current bridge design codes and evaluation methods are often overly conservative for computing the live load distribution factors. As a result, a number of existing bridges can be over designed creating for more uneconomical designs. Therefore, this study attempts to create an improved methodology for computing a more

accurate live load distribution factor to use in design, and to eventually propose the modification of the current provisions for the design and evaluation of existing bridges.

The specific objectives of this research are:

1. To review previous work done by other researchers on live load distribution factors to determine the importance of particular parameters, gain an understanding on the analysis methods previously used, and to understand how the existing methods were derived.
2. To determine an accurate approach to compute distribution factors from finite element data.
3. To verify the selected approach against laboratory and field test data as well as to compare results with analytical models developed by other researchers.
4. To compute distribution factors from a parametric study of bridges ranging in length, steel strength, and span-to-depth ratios. The distribution factors from previous researchers are also computed, especially the NCHRP Report 12-26.
5. To determine a more simplistic approach to computing distribution equations from the previously calculated distribution factors using a regression method.
6. To recalculate the distribution factors of all previously modeled bridges and compare with the previous methods prescribed by the codes.
7. To document the results and present in an orderly fashion for proposal of improving the existing specifications.

1.4 Organization of Thesis

The thesis is organized into eight chapters. Chapter 1 presents an overview of the problem along with a summary of background information, along with the scope and objectives of this study. Chapter 2 presents a literature review of previous research focused on live load distribution factors for slab on steel I-girder bridges.

Chapter 3 discusses the development of the current AASHTO LRFD load distribution factor equation. The chapter focuses on the selection of analysis tools, development of sensitivity and parametric studies, the proposed equations, and the verification methods utilized in NCHRP 12-26 (1988), the primary research project undertaken to develop current AASHTO LRFD load distribution factor equations. Chapter 4 contains the computation of live load distribution factors for slab on steel girder bridges using different methods prescribed by previous researchers to aid in the selection of a method for use in this study. Chapter 5 provides a verification study done recreating bridges from previous analytical and field-testing research to compare the methods described in Chapter 4 with the recorded results from the research to select an effective method to compute live load distribution factors. Chapter 6 presents a parametric study of simply supported bridges focused on assessing load distribution factors using a discrete range of parameters. Summary information is provided regarding trends in key design parameters and comparisons are made between analytical values and current code predictions. Chapter 7 discusses the development of a more accurate and simplistic method of computing live load distribution factors. Chapter 8 provides a summary and conclusion for the work done and results obtained for this thesis.

CHAPTER 2

LITERATURE REVIEW

2.1 Introduction

This section contains a concise summary of the development of present live load distribution factors. These factors have been incorporated in American bridge codes since the publication of the first edition of the AASHTO Standard Specifications in 1931 (AASHTO, 1931). The current Standard Specifications (AASHTO, 1996) still include these original distribution factors with relatively minor modifications. In 1994, AASHTO adopted the LRFD Bridge Design Specifications. These Specifications contained a new form of distribution factors that represented the first major change to these equations since 1931. A description of the distribution factors contained in these two codes of practice and their historical development is presented in this section. A brief overview of the methods specified for live load distribution in selected foreign bridge codes is also included.

2.2 AASHTO Standard Specifications

Distribution factors in the Standard Specifications are typically given in the form S/D ; where S is the distance between girders (in ft.) and D is a constant that varies depending on the bridge type. Also, slightly more complex equations are given for precast multibeam bridges (AASHTO article 3.23.4), spread box girder bridges

(AASHTO article 3.28) and steel box girder bridges (AASHTO article 10.39.2).

Distribution factors for these bridge types are not solely a function of girder spacing, and instead parameters such as the number of design lanes, number of girders, stiffness parameters, span length, and roadway width also influence the distribution factor.

The current distribution factor for composite steel I-beam bridges with two or more design lanes (S/5.5) was developed by Newmark and Siess (1943) providing a major revision to load distribution factor procedures presented in the first two editions of the AASHTO Standard Specifications. Newmark and Siess approached the slab on girder study using a beam on elastic foundation approach. Specifically, they considered a portion of the slab to act as a beam supported by girders that were approximated as elastic supports. They then used moment distribution to determine the beam response and suggested the following general expression for live load distribution in interior girders (Newmark and Siess, 1942)

$$D = 4.4 + 0.42 \frac{L}{10\sqrt{H}} \quad (\text{Eqn. 2.1})$$

where L = span length

H = stiffness parameter defined as $\frac{E_b I_b}{LEI}$

E_b = modulus of elasticity of the material of the beam

I_b = moment of inertia of the cross section of the beam

E = modulus of elasticity of the slab material

I = moment of inertia per unit of width of the cross section of the slab.

By examining typical values of L and H for simple span bridges having span lengths of 20 to 80 ft. and girder spacings of 5 to 8 ft., the distribution factor was further simplified

to the current form of $S/5.5$ (Newmark and Siess, 1943). The accuracy of this resulting distribution factor was verified experimentally using quarter scale right bridges (Newmark, 1949). Subsequent experimental tests were done on quarter scale right and skewed bridges (Newmark et al., 1946; Newmark et al., 1948) to determine the relevance of the $S/5.5$ with close comparisons shown for small skew angles. Over the years, the range of applicability of Newmark's expression has been increased.

Specifically, Newmark and Siess considered only simply supported, non-skewed bridges, with span lengths ranging from 20 to 80 feet. The girder spacing of the bridges used to develop this distribution factor ranged from 5 to 8 ft., while today the equation is considered valid for girder spacings up to 14 ft. Also, at the time the $S/5.5$ factor was developed, the standard design lane was 10 ft. wide, while today 12 ft. design lanes are customary.

Throughout the past seventy years, there have been numerous studies related to load distribution of vehicular loads. As a result of the findings of some of these efforts, modifications have been made to the distribution factors provided in the Standard Specifications, with the goal of providing improved accuracy. There have been many instances, however, where this has led to inconsistencies in the manner in which distribution factors are calculated. Sanders (1984) summarizes these conflicts as follows.

- The majority of the distribution factors have been determined by considering only a limited number of parameters (typically floor type, beam type, and girder spacing), while additional parameters have been included for other bridge types (stiffness parameters, span length, etc.).
- There is a variation in the format of the distribution factors for bridges of similar construction (i.e., steel I-girders, composite box beams, precast multibeams, and spread box beams).

- The Standard Specifications include provisions for a reduction in live load intensity as the number of design lanes increases. This provision has been inconsistently considered during the development of various distribution factors.
- Changes in the number, position, and width of traffic lanes have been randomly incorporated in the distribution factor expressions.
- Lastly, there are discrepancies regarding the level of research performed for various distribution factors.

2.3 AASHTO LRFD Specifications

The load distribution factors presented in the AASHTO LRFD Specifications are in a large part based on work conducted in the NCHRP Report 12-26. The equation was developed based on parameters from a parametric study developed from a set of 364 existing bridges from several differing geographic regions represented by ten different states comprised of three different types of bridges: prestressed T-beam, concrete I-girder, and steel I-girder.

One of the initial tasks in NCHRP 12-26 was to conduct modeling studies to assess the capabilities of various software packages to predict lateral load distribution in bridge superstructures. Models were created for fifteen bridges using grillage, equivalent orthotropic plate, concentrically stiffened plate, eccentrically stiffened plate, and folded plate models.

Sensitivity studies were conducted in order to assess the effect of various parameters on live load distribution using an “average” reinforced concrete T-beam bridge where only one parameter at a time was varied. Parameter ranges used in the sensitivity studies were based on the 364 bridge database. After analyzing the sensitivity

of the distribution factors, the only parameters used in the parametric study were girder spacing, span length, girder stiffness, and slab thickness. The database of existing bridges was again used to determine representative values for these four parameters in order to develop a parametric study.

The results of both the sensitivity studies and the parametric studies were used to develop new equations for live load distribution. Based on the results of the sensitivity studies, equations were developed for moment with one design lane, moment with two or more design lanes, end shear with one design lane, and end shear with two or more design lanes for bridges within the range of parameters used in the sensitivity study.

Alternatively, results from the parametric study were used to develop equations for moment and shear for one and multiple design lanes using a multidimensional space interpolation (MSI) method. The equations derived using the MSI methods are not presented in the NCHRP reports.

The accuracy of the distribution factor equations developed as a result of the sensitivity studies was evaluated using two methods. First, analytical methods were created using randomly selected bridges from the database and the resulting distribution factor was compared with that from the proposed equations. The distribution factors were compared to the corresponding factors developed using the MSI method for a large number of randomly selected bridges from the database.

Chapter 3 gives a thorough description and layout of the process used in the development of the AASHTO LRFD Specification equation for live load distribution factors.

2.4 Ontario Highway Bridge Code [OHBC] and the Canadian Highway Bridge Code [CSA]

The Ontario Highway Bridge Code uses live load distribution factors that have a similar S/D format to the US Standard Specifications (1991). However, the OHBDC prescribes a unique approach for determination of D_d that is based on the research of Bakht and Moses (1988) and Bakht and Jaeger (1990). The value of D_d (and subsequent variables incorporated in expressions for D_d) varies based on the limit state of interest and for moment versus shear.

The recent adoption of the national Canadian Highway Bridge Code (CSA, 2000) has also incorporated the work of Bakht and Moses (1988) and Bakht and Bakht and Jaeger (1990). However, this specification essentially uses a live load distribution factor in which the force effect of interest (i.e., moment of shear) is distributed based on the number of design lanes divided by the number of girders. Modification factors are then applied to these expressions to account for multilane loading and other effects as a function of the limit state of interest.

2.5 European Codes

Most European Common Market countries base their design specifications upon the Euro codes (Dorka, 2001). The Eurocodes are only a framework for national standards. Each country must issue a "national application document (NAD)" which specifies the details of their procedures. A Euro code becomes a design standard only in connection with the respective NAD. Thus, there is considerable variation in the design

specifics from country to country. However, the codes used in many European countries generally do not use simplified methods (such as distribution factors) to determine the live load affect on bridges. Rather, more detailed analysis methods are typically used (Nutt et al., 1988).

2.6 Australian Bridge Code

Similar to the practices of most European countries, the Australian bridge code (Austroads, 1992) does not incorporate distribution factors for live load. Instead, the number of design lanes is determined based on roadway width, and then these lanes are positioned to give the maximum load effect as a result of refined analysis methods. “Multiple lane modification factors” are incorporated (similar to American multiple presence factors) which reduce the load applied to each lane as the number of design lanes increases.

2.7 Refined Analysis

While the use of the empirical equations described above is the most common method of determining distribution factors, both the AASHTO Standard and LRFD Specifications also allow the use of more refined analysis techniques to determine the transverse distribution of wheel loads in a bridge superstructure. Specifically, two other methods with increasing complexity and reliability are given.

The first level of refined analysis permitted in the specifications is to utilize computer aided techniques in order to determine appropriate wheel load distribution factors. Specifically, computer programs have been developed that simplify bridge behavior using influence surface or influence section concepts, which are then used to determine distribution factors.

For bridges that do not meet the geometric limitations required for the use of simplified distribution factors, detailed computer analysis may be used. In these situations, the actual forces occurring in the superstructure are calculated and the use of distribution factors is not necessary. When these methods are employed, it is the responsibility of the designer to determine the most critical location of the live loads. The LRFD Specifications (1998) give several examples of acceptable methods of analysis including (but not limited to): finite element modeling, grillage analogy method, and the folded plate method.

2.8 Studies Evaluating Current Distribution Factors

Several investigators focused on examining the accuracy of the current AASHTO distribution factors based on research conducted. These efforts have included both analytical studies using finite element analysis and field studies of existing bridges.

2.8.1 Analytical Studies

Many studies by various researchers have shown that the lateral distribution of live load predicted by expressions in both the current AASHTO Standard Specifications and LRFD Specifications can be overly conservative. The bulk of these efforts have been focused on limited parameter variations such as the influence of span length, skew, girder spacing, etc.

Hays et al. (1986) and Mabsout et al. (1999) have both investigated the accuracy of the Specifications compared to varying span lengths. A similar range of span lengths was investigated in both studies, with span varying from 30 to 120 ft. Hays et al. compared the results of their analytical study to distribution factors resulting from the Standard Specifications and the OHBDC and show that the Standard Specifications are unconservative for interior girders with span lengths less than 60 ft. They also demonstrate that while the OHBDC is somewhat conservative, it is very accurate in capturing the non-linear relationship of decreasing distribution factor with increasing span length. Mabsout et al. (1999) obtained similar results from their analytical studies. They state that the Standard Specifications are less conservative than the LRFD Specifications for span lengths up to 60 ft. and girder spacing up to 6 ft. Although, as span length and girder spacing increase, the Standard Specifications were found to become more conservative. Mabsout et al. also found their finite element result to be reasonably close the results predicted by the LRFD equations.

Other researchers have investigated the accuracy of the current distribution factors for bridges with varying degrees of skew. One such study was that of Arockiasamy et al.

(1997). The authors investigated angles of skew ranging from 0 to 60 degrees and concluded that the LRFD code is accurate in capturing the effects of skew for beam-and-slab bridges, particularly for skew angles in excess of 30 degrees. Arockiasamy et al. also state that the LRFD equations overestimate the effect of slab thickness.

Analytical studies conducted by Barr et al. (2001) investigated the accuracy of the LRFD distribution factors while varying several parameters. These parameters included: skew, simply supported versus continuous spans, presence of interior and end diaphragms, and presence of haunches. Results of this work indicate that for models similar to those used in developing the LRFD equations (simple-spans, without haunches, interior diaphragms, or end diaphragms), the equations are reliable and are 6% conservative on average. However, when these additional parameters are included in the model, the distribution factors given by the specifications are up to 28% conservative. Specifically, the authors found that: (1) including the presence of haunches and end diaphragms significantly reduced the distribution factors, (2) the effects of including intermediate diaphragms in the model were negligible, and (3) the effects of continuity increased the distribution factor in some cases and decreased it in others. In addition, these researchers also found the effects of skew to be reasonably approximated by the LRFD equations. Also, the OHBDC procedures were shown to capture the effects of skew with high precision. However, these specifications are only valid for angles of skew not exceeding 20 degrees.

In analytical studies by Shahawy and Huang (2001), the focus was on the accuracy of the LRFD equations as a function of span length, girder spacing, width of deck overhang, and deck thickness. The authors found that results from the LRFD

equations can have up to 30% error for some situations, particularly when girder spacing exceeds 8 ft. and deck overhang exceeds 3 ft.

2.8.2 Field Studies

Field-testing of two simply supported, steel I-girder bridges was performed by Kim and Nowak (1997). One bridge, designated as M50/GR had a span length of 48 ft. and a girder spacing of 4 ft. - 9in. The second bridge, referred to as US23/HR, had a span length of 78 ft. and a girder spacing of 6 ft. - 3 in. It was shown that the LRFD distribution factors overestimated the actual distribution by 28% and 19% in the two bridges tested. Furthermore, the distribution factors obtained from the Standard Specifications were 16% and 24% greater than the actual distribution factors that resulted from field-testing.

Fu et al. (1996) conducted live load tests on four steel I-girder bridges of which three were tangent bridges and one was skewed. Comparison of the field test results to the LRFD distribution factors showed the code to be 13% to 34% conservative for the tangent bridges and 13% unconservative for the skewed bridge.

Additional field-testing of seventeen steel I-girder bridges was conducted by Eom and Nowak (2001). The bridges used in the study had span lengths ranging from 32 to 140 ft. and girder spacings from 4 ft. to 9 ft. - 4 in. The majority of the bridges were not skewed, but some moderately skewed bridges (10 to 30 degrees) were also included. Actual distribution factors obtained from the field tests were lower than those given by the specifications in all cases. It was found that the Standard Specifications were very

conservative for short spans with small girder spacings, and even more conservative for other situations. Also, the LRFD distribution factors were found to be more accurate than those from the Standard Specifications, although were still considered to be too conservative.

2.9 Factors Influence Live Load Distribution.

The procedures used to calculate live load distribution factors involve several different factors ranging from girder spacing to girder stiffness. The following paragraphs give a description of the different factors that were studied in order to determine the most important factors to be included in the new specifications.

2.9.1 Girder spacing

Girder spacing has been considered to be the most influential parameter affecting live load distribution since early work by Newmark (1938). Newmark and Siess (1942) originally developed simple, empirical equations expressing distribution factors as a function of girder spacing, span length, and girder stiffness. Later, (Newmark, 1949) the effect of the other two parameters was neglected and the distribution factors were expressed as a linear function of girder spacing only. These relationships are still incorporated in the Standard Specifications with minimal changes since their adoption.

Even though girder spacing is influential, it has been shown through analytical and field studies that the S/D factor consistently overestimates the actual live load

distribution factors. Also, sensitivity studies presented in NCHRP Report 12-26 (Nutt et al., 1988) and analytical studies by Tarhini and Frederick (1992) show that while girder spacing significantly effects live load distribution characteristics, the relationship is not linear as implied by the *S/D* method, and thus does not correlate well with the AASHTO Standard Specifications.

2.9.2 Span length

Nutt et al. (1988) determined that a non-linear relationship existed between span length and girder distribution factors. This relationship was most significant for moment in interior girders (moment and shear, as well as interior and exterior girders were evaluated in this study).

Tarhini and Frederick (1992) also observed a non-linear (quadratic) relationship between span length and the girder distribution factor. In this study, the quadratic increase in the distribution factor with increasing span length is due to the potentiality for an increased number of vehicles present on a longer bridge.

2.9.3 Girder stiffness

Newmark and Siess (1942) expressed the amount of live load distributed to an individual bridge girder in terms of the relative stiffness of the girder compared to the stiffness of the slab, expressed by the dimensionless parameter *H* (see AASHTO

Standard Specifications section). Results demonstrated that the relative stiffness (as defined by the parameter H) had a small effect on live load distribution.

Tarhini & Frederick (1992) also found girder stiffness to have a small, but negligible effect on live load distribution. For example, they studied the effects of relatively large changes in the moment of inertia of the cross section such as doubling the cross-sectional area of the girder and altering the thickness of the slab. These changes resulted in approximately a 5% difference compared to the original design, which the authors considered to be insignificant.

Nutt et al. (1988) defined girder stiffness by the parameter K_g

$$K_g = I + Ae^2 \quad (\text{Eqn. 2.2})$$

where A and I are the area and moment of inertia of the girder cross section, respectively, and e is the distance between the centers of gravity of the slab and beam. In order to confirm that this was an acceptable means of quantifying girder stiffness, individual values of moment of inertia, area and eccentricity were varied, while maintaining a constant value of $I + Ae^2$. It was observed that varying individual parameters was relatively inconsequential and that there was only a 1.5% difference obtained due to varying these individual parameters if $I + Ae^2$ was held constant. By defining girder stiffness in this manner, Nutt et al. (1988) found there was a significant relationship between girder stiffness and live load distribution. The effects of varying torsional stiffness were also evaluated in this study with results showing this parameter has only a relatively small impact on girder distribution factors (3% difference).

2.9.4 Deck Thickness

Conflicting information exists regarding the effect of the thickness of concrete decks on live load distribution. Newmark (1949) states that deck thickness will affect wheel load distribution, as deck thickness will have a direct influence on the relative stiffness. Although, in research by Tarhini & Frederick (1992), bridges having a slab thickness ranging from 5.5 to 11.5 in. were analyzed and it was found that these changes had a negligible effect on live load distribution.

Nutt et al. (1998) also considered the effect of this parameter to be small (10% difference between bridges with 6 and 9 in. slabs). Nonetheless, they did include this parameter in the recommended distribution factor equations contained in NCHRP Report 12-26.

2.9.5 Girder location

Girder location, i.e. interior vs. exterior, was found to have an influence on live-load distribution factors by Walker (1987). Specifically, results demonstrated that the S/D factors overestimate actual distribution to a lesser extent in exterior girders.

Zokaie (2000) states that edge girders are more sensitive to truck placement than interior girders. Therefore, either the lever rule or a correction factor could be used.

The width of deck overhang may be one contributing factor to the difference in distribution between interior and exterior girders. Specifically, deck overhang has been

shown to have a linear effect on live-load distribution to the exterior girder, while deck overhang is considered to have a negligible effect on interior girders (Nutt et al., 1988).

2.9.6 Continuity conditions

Nutt et al. (1988) also examined the difference in distribution factors between simple span and two-span continuous bridges. The results showed that the distribution factors obtained for the two-span bridges were 1 to 11% higher than the distribution factors that resulted for the corresponding simple-span bridges.

Later research by Zokaie (2000) states that there is a 5% difference between positive moments and 10% difference between negative moments for continuous versus simple span bridges. However, it is assumed that moment redistribution will cancel this effect and no correction factor is recommended (or included) for use in the LRFD Specifications.

2.9.7 Skew

Nutt et al. (1988) observed that skew did affect live load distribution. Specifically, increasing skew tends to decrease the wheel load distribution for moment and increase the shear force distributed to the obtuse corner of the bridge. In addition, they found this to be a non-linear effect and also state that this effect will be greater for increasing skew.

2.9.8 Cross Frame Characteristics

Walker (1987) has investigated the effect of diaphragms with the following results. For a load applied near the curb, the difference between the two types of models (with and without diaphragms) was negligible. Although, for a load transversely centered, the effect of cross frames is more pronounced.

Field studies by Kim & Nowak (1997), indicated that relatively widely spaced diaphragms lead to more uniform girder distribution factors between girders, although no information is provided regarding a relationship between increasing or decreasing distribution with cross frame spacing.

Nutt et al. (1988) state that cross bracing can have an important role in live load distribution. However, they give two reasons for not considering this parameter in their sensitivity studies: (1) the effect of interior cross frames decreases as the number or loaded lanes increases, and (2) the effect of these members is difficult to predict, as many field studies have shown diaphragms to be less effective than predicted in design.

2.9.9 Secondary Stiffening Elements

Research reported by Mabsout et al. (1997) indicates a distinct relationship between the presence of sidewalks and railings and girder distribution factors. Results for various combinations of sidewalk and/or railing on one or both sides of the bridge are compared with distribution factors obtained from current LFD and LRFD Specifications. In summary, depending on the combination and location of stiffening elements added

(sidewalk and/or railing, one or both sides of the bridge), the researchers found that the current LRFD girder distribution factors are 9 to 30% higher than those obtained in the finite element studies.

Nutt et al. (1988) point out that while secondary stiffening elements do affect live load distribution, considering these members (such as curbs and parapets) in design may be unconservative. For example, if the bridge were widened subsequent to its original design, the curbs and parapets would be removed. Therefore, the enhanced distribution as a result of these elements would be lost, and girders designed to take advantage of this behavior may become overstressed.

2.9.10 Composite Behavior

Based on analytical results, Tarhini & Frederick (1992) found the effect of composite vs. noncomposite construction to have a negligible effect on wheel load distribution in I-girder bridges. The difference in girder distribution factors for composite vs. non-composite bridges was 6 percent for a short span bridge (35 ft.) and 1.5 percent for a relatively long span bridge (119 ft.).

CHAPTER 3

DEVELOPMENT OF CURRENT AASHTO LOAD DISTRIBUTION FACTOR EQUATIONS

3.1 Introduction

The current distribution factors contained in the AASHTO LRFD Specification for slab-on-girder bridges are a result of the NCHRP Project 12-26, conducted by Imbsen & Associates (Nutt et al., 1988). This study focused on the development of new distribution factors and was initiated by a desire for more accurate distribution factors. Another goal of the project was to reduce the inconsistencies that exist in the Standard Specifications.

3.2 Method of Analysis Selection

An initial phase of this project was to select an appropriate method of analysis to be used in this study. Analytical models of fifteen previously field-tested bridges using five different modeling techniques were used to aid in the process. This group of bridges was comprised of concrete T-beam, concrete I-girder, steel I-girder, and continuous slab bridges. In addition one prestressed concrete box girder bridge was also evaluated. The bridges tested consisted of simply supported, single span bridges, and also two- and three-span continuous bridges. Straight and curved girders were included along with right and skewed bridges. Span lengths of these bridges ranged from 10 ft. (in case of a scale model) to 100 ft. Models were created of the bridges using grillage, equivalent

orthotropic plate, concentrically stiffened plate, eccentrically stiffened plate, and folded plate models. An evaluation of the results from the analytical models were compared to the field-testing results, which led the researchers to select the eccentrically stiffened plate and grillage models for use in the subsequent sensitivity studies.

3.3 Sensitivity Studies

Sensitivity studies were conducted in order to assess the effect of various parameters on live load distribution. The sensitivity studies were conducted using an “average” reinforced concrete T-beam bridge where only one parameter at a time was varied. Although these studies consisted of T-beam bridges, the authors state that the study reveals the parameters to which all types of beam-and-slab bridges are sensitive, and only the numerical values will change. The effects of the following variables were investigated in the sensitivity study: girder spacing, span length, girder stiffness, slab thickness, number of girders, number of design lanes, width of deck overhang, skew, truck configuration, support conditions, and end diaphragms. However, the effects of secondary stiffening elements (such as curbs and parapets), interior diaphragms, and horizontal curvature were not considered in this study. After analyzing the sensitivity of the distribution factors to the parameters listed above, it was determined that some of these variables did not have a significant effect, and therefore the parameters selected to use were girder spacing, span length, girder stiffness, and slab thickness only.

3.4 Parametric Study

A large database of 364 existing bridges from 10 different states was used to determine representative values for the parametric study with the values given in Table 3.1. The database of bridges is further explained in the following sections, along with the description of the parametric study used. Analyses were performed using all possible combinations of these parametric values, and all bridges analyzed had 6 girders, 2 design lanes, a deck overhang of 54 in., and no interior or end diaphragms with a HS20 truck used as the design vehicle.

3.4.1 Database of State DOT Bridges

This database used to develop the parametric study consists of 364 existing bridges comprised of 84 prestressed concrete T-beam, 104 concrete I-girder, and 176 steel I-girder bridges. These bridges are from several different geographic regions represented by ten states: Arizona, California, Florida, Maine, Minnesota, New York, Ohio, Oklahoma, Oregon, and Washington. The following data is provided for each bridge in the database; span length, total width, roadway width, skew, number of girders, girder spacing, girder depth, slab thickness, overhang, eccentricity between slab and girder, moment of inertia, cross-sectional area, and date constructed, and can be found in Table 3.2. Table 3.3 also provides the minimum, maximum, and average values of the database, along with histograms of different parameters, are also provided. Histograms of the data provided in the database can be found in Figs. 3.1 through 3.13.

3.4.2 Parametric Study Bridges

The database of bridges describe above was used to determine a range of parameters for a parametric study described in detail in the previous paragraphs with the given values shown in Table 3.1. In summary, the dimensions of the bridges in the parametric study ranged from a girder spacing of 3.5 to 16 ft., a span length of 20 to 200 ft., a girder stiffness from 10,000 to 7,000,000 in.⁴, and a slab thickness of 4.4 to 12 in. Table 3.4 shows the distribution factors obtained from this parametric study along with sequence number, slab thickness, girder inertia, span length, and girder spacing. These values were then used in the development of a new empirical formula for wheel load distribution.

3.5 Proposed Equations

The results from the parametric study were used to derive new empirical equations for wheel load distribution for interior girders. For the distribution of moment with two or more design lanes, four empirical equations with increasing complexity and accuracy were developed. The most accurate of these four equations was modified slightly and adopted into the LRFD Specifications, as shown below

$$DF = 0.15 + \left(\frac{S}{3}\right)^{0.6} \left(\frac{S}{L}\right)^{0.2} \left(\frac{I + Ae^2}{Lt_s^3}\right)^{0.1} \quad (\text{two lanes loaded}) \quad (\text{Eqn. 3.1})$$

where S = girder spacing
 L = span length
 I = transformed moment of inertia of the girder
 A = transformed area of the girder
 e = distance between the centroid of the slab and the centroid of the girder
 t_s = slab thickness.

It should be noted that this equation is altered by a factor of two in the LRFD

Specifications to present the distribution factors in terms of lines of wheels instead of trucks. Although this equation was selected for use because of its enhanced accuracy, the equation does have a negative attribute over the other three proposed equations for two or more design lanes. The equation contains the parameters I , A , and e , which are typically not known prior to design, creating a somewhat iterative procedure that is viewed negatively by bridge engineers.

Equations were also developed for moment with one design lane, end shear with two or more design lanes, end shear with one design lane, and distribution factors for concrete box girders as part of this project. Furthermore, correction factors for skewed supports, continuous spans, and interior shear were also developed. These equations are considered valid for bridges having girder spacing, span length, stiffness, and slab thickness that are within the range of these parameters used in the parametric study. Table 3.5 shows a partial reprint of one of the AASHTO LRFD Specifications load distribution factor tables, which resulted from the NCHRP 12-26 effort; this is for moment in interior beams.

3.6 Determination of Accuracy of Proposed Equations

Nutt et al. (1988) evaluated the accuracy of these equations using two distinct methods. For the first method of evaluation, a database of 30 representative beam-and-slab bridges from different states was compiled. The database included T-beam bridges, prestressed concrete I-girder bridges, and steel I-girder bridges that were selected to represent a wide range of bridge parameters. Specifically, the bridges had span lengths of 30 to 200 ft., girder spacings of 6 to 13.5 ft., girders with moments of inertia from 1,300 to 460,000 in.⁴, and slab thicknesses from 6 to 12 in. Models that represented these bridges as an eccentrically stiffened plate were created and the resulting distribution factor was determined in a method similar to the parametric study values.

These distribution factors resulting from the analytical models are compared to the empirical equation for two lanes loaded, as shown in Fig. 3.14, where the solid line represents a perfect correlation between the two distribution factors. As shown, the equation well represents the results of the computer analysis and is slightly conservative in most cases, which is desired. Although, there are a few instances where the equation is very unconservative, and the specific details of these bridges is not provided. The standard deviation of the ratio of the distribution factor obtained from the two methods was 0.038 and the authors attribute the differences to the effects of some parameters that are not included in the empirical expression (i.e., torsional inertia, roadway width, etc.) and simplifications made in deriving the expression.

In order to evaluate the proposed equations with a larger database of bridges, a multidimensional space interpolation (MSI) approach was used. This database consisted

of 304 bridges including T-beam, concrete I-girders, and steel I-girders with the geometric properties given in Table 3.2. The MSI approach is based on simple interpolation techniques that are then extended for the number of variables in a given equation (in this case four variables). This method was shown by the authors to be only slightly less accurate than the analytical results using an eccentrically stiffened plate, while offering the advantage of being less computationally demanding.

The positive correlation between the results from the MSI method and Equation 1 is shown in Fig. 3.15. This figure also shows that there is a relatively low amount of scatter between the two distribution factors, although the scatter does tend to increase with increasing distribution factor. It can also be observed from Fig. 3.15 that when for cases where there is some error between the two methods, the equations tend to err on the conservative side. To summarize, the average ratio of distribution factors from Equation 1 to the distribution factor obtained in the MSI approach was 1.029 with a standard deviation of 0.034.

Table 3.1 Parametric values used in development of LRFD distribution factors for beam-and-slab bridges

Parameter	Parametric Values				
Girder Spacing (ft)	3.5	5.0	7.5	10.0	16.0
Span Length (ft)	20		64	130	200
$I + Ae^2$ (1000 in ⁴)	10	50	560	3000	7000
Slab Thickness (in)	4.4		7.25		12

Table 3.2. NCHRP 12-26 database of bridges

State	Length ft	Width (out-to-out) ft	Skew	No. of Girders	Girder Spacing ft	Girder Depth ft	Slab Thick. in	Overhang ft	Roadway Width ft	Date	Eccentricity in	Moment of Inertia in ⁴	Area in ²
Bridge Database from Appendix B of the NCHRP Report 12-26 for Steel I-girder Bridges													
Arizona	67.00	34.00	20.00	4	8.83	2.92	7.00	3.75	30.00	1961	21.69	11282	5.35
Arizona	73.00	34.00	20.00	4	8.83	2.92	7.00	3.75	30.00	1961	21.69	11282	5.35
Arizona	77.00	34.00	20.00	4	8.83	2.92	7.00	3.75	30.00	1961	21.69	11282	5.35
Arizona	86.00	34.00	20.00	4	8.83	2.92	7.00	3.75	30.00	1961	21.69	11282	5.35
Arizona	53.00	35.00	30.00	4	9.33	2.75	7.00	2.25	30.00	1958	20.05	6699	3.83
Arizona	67.00	35.00	30.00	4	9.33	2.75	7.00	2.25	30.00	1958	20.05	6699	3.83
Arizona	46.00	35.17	9.77	4	8.83	3.00	7.50	4.25	30.00	1959	21.75	9739	4.71
Arizona	79.00	35.17	9.77	4	8.83	3.00	7.50	4.25	30.00	1959	21.75	9739	4.71
Arizona	44.73	35.17	20.00	4	7.00	1.33	9.00	-	22.00	1934	-	-	-
Arizona	30.00	34.00	0.00	5	7.50	2.00	7.75	2.00	32.00	1937	15.92	2364	2.47
Arizona	40.00	34.00	0.00	5	7.50	2.00	7.75	2.00	32.00	1937	15.92	2364	2.47
California	61.19	48.50	30.00	8	6.50	3.66	6.25	3.00	36.00	1953	-	-	-
California	47.00	36.00	60.54	7	5.17	2.50	9.00	2.50	34.00	1936	19.41	4461	3.18
California	113.17	34.00	0.00	4	8.50	5.21	7.13	4.25	28.00	1967	39.78	27833	6.15
California	121.68	33.00	46.96	4	9.33	6.00	7.25	2.50	28.00	1959	-	-	-
California	58.00	33.33	0.00	4	9.33	4.10	7.00	2.83	28.00	1955	-	-	-
California	50.00	33.50	30.00	5	7.50	3.75	6.50	3.38	28.00	1955	21.49	12103	5.71
California	130.10	33.33	64.20	5	8.33	5.42	6.38	2.50	28.00	1955	36.02	51110	8.08
California	92.50	44.00	63.47	6	7.31	4.56	6.75	2.83	40.00	1956	-	-	-
California	80.66	27.50	0.00	5	5.25	3.51	6.00	3.50	24.00	1949	21.00	9739	4.71
California	105.20	33.66	12.57	4	9.20	4.83	7.25	3.00	28.00	1958	-	-	-
California	187.00	128.00	66.10	15	8.50	6.00	7.25	3.50	122.00	1962	35.56	120145	13.95
California	70.50	75.00	40.99	9	8.66	3.79	6.88	2.83	69.33	1956	29.12	11500	4.78
California	130.00	41.00	0.00	3	15.50	7.92	9.63	5.00	39.00	1971	51.87	188585	13.00
California	155.00	41.00	0.00	3	15.50	7.92	9.63	5.00	39.00	1971	51.87	188585	13.00

Table 3.2 cont'd

State	Length ft	Width (out-to-out) ft	Skew	No. of Girders	Girder Spacing ft	Girder Depth ft	Slab Thick. in	Overhang ft	Roadway Width ft	Date	Eccentricity in	Moment of Inertia in ⁴	Area in ²
California	71.00	33.92	20.39	3	11.50	4.70	8.50	5.10	26.00	1947	-	-	-
California	35.00	33.92	20.39	3	11.50	4.70	8.50	5.10	26.00	1947	-	-	-
California	68.00	26.33	0.00	4	6.66	3.75	6.75	3.33	21.00	1954	21.32	14988	6.77
California	60.00	35.92	2.17	4	9.50	3.58	7.13	5.10	26.00	1958	21.69	17234	7.66
California	116.00	33.66	0.00	4	9.00	6.50	7.00	3.33	28.00	1960	42.25	68862	8.25
California	140.00	33.33	40.00	3	12.00	8.00	7.75	4.66	28.00	1959	48.38	230515	15.20
California	51.25	57.66	0.00	9	6.50	3.25	7.00	2.83	52.00	1957	20.29	5367	3.63
California	51.25	33.66	0.00	5	6.50	3.25	6.50	2.83	28.00	1957	20.29	5367	3.63
California	100.00	36.17	0.00	4	10.00	5.70	7.25	3.08	28.00	1951	-	-	-
California	75.25	43.92	0.00	6	7.75	5.00	6.63	2.17	37.00	1955	35.34	17101	4.15
California	91.25	43.92	0.00	6	7.75	5.00	6.63	2.17	37.00	1955	36.13	24195	5.28
California	65.50	33.33	46.78	4	8.75	3.64	6.88	3.52	28.00	1958	25.77	10061	5.16
California	48.77	33.33	46.78	4	8.75	3.64	6.88	3.52	28.00	1958	24.01	6925	3.86
California	151.13	33.33	0.00	3	12.00	8.33	7.75	4.66	28.00	1958	51.38	287125	16.50
California	75.00	33.33	0.00	3	12.00	8.33	7.75	4.66	28.00	1958	47.06	215965	6.35
California	55.00	37.92	15.52	4	10.00	3.66	7.13	3.96	28.00	1958	21.51	14988	6.77
Florida	142.00	84.75	0.00	10	9.25	5.50	7.50	2.00	79.25	1975	37.55	59869	7.29
Florida	205.00	84.75	0.00	10	9.25	5.50	7.50	2.00	79.25	1975	43.93	75951	8.94
Florida	180.00	46.75	22.92	6	8.20	4.67	7.00	2.11	44.00	1980	41.25	43570	7.35
Florida	43.00	30.67	11.55	10	3.00	2.50	10.00	1.00	28.00	1966	20.06	8826	5.59
Florida	49.00	30.67	11.55	10	3.00	2.50	10.00	1.00	28.00	1966	20.06	8826	5.59
Maine	20.00	23.00	0.00	5	5.00	1.50	6.50	1.08	22.00	1940	11.50	801	1.47
Maine	45.00	25.00	20.00	5	5.25	2.25	6.50	1.50	22.00	1940	16.79	3604	3.01
Maine	75.00	25.00	20.00	5	5.25	3.33	6.50	1.50	22.00	1940	-	-	-
Maine	50.00	35.00	0.00	5	7.92	2.75	7.50	1.17	30.00	1960	22.61	8641	4.28
Maine	60.00	25.00	0.00	5	5.00	3.00	7.00	2.00	22.00	1935	21.42	9012	4.42

Table 3.2 cont'd

State	Length ft	Width (out-to-out) ft	Skew	No. of Girders	Girder Spacing ft	Girder Depth ft	Slab Thick. in	Overhang ft	Roadway Width ft	Date	Eccentricity in	Moment of Inertia in ⁴	Area in ²
Maine	75.00	37.50	0.00	5	8.25	3.00	6.00	2.00	28.00	1956	25.60	16856	7.40
Maine	76.00	33.00	45.00	5	7.25	3.00	6.50	1.33	28.00	1961	25.02	15903	7.02
Maine	90.00	36.67	0.00	5	8.00	3.00	9.00	1.42	32.00	1979	27.33	18554	8.06
Maine	96.52	27.75	10.00	5	5.75	3.00	6.50	2.00	24.00	1956	26.66	17780	7.81
Maine	95.00	42.67	30.00	6	7.33	3.50	7.50	2.50	38.83	1970	28.38	20700	5.74
Maine	110.00	31.67	0.00	4	8.50	4.00	8.50	2.33	28.00	1971	32.94	29835	6.92
Maine	75.00	29.00	0.00	5	6.00	2.77	5.75	2.00	24.00	1963	19.38	11048	5.88
Maine	20.50	26.00	0.00	12	2.17	1.00	7.50	0.50	22.00	1957	9.80	234	0.91
Maine	44.00	42.58	13.50	6	7.97	1.25	7.50	1.42	39.00	1965	17.29	3604	3.00
Maine	70.00	42.67	0.00	6	7.50	3.00	8.50	1.92	39.00	1977	22.03	7796	3.97
Maine	100.00	33.67	0.00	5	7.00	3.00	8.00	1.92	29.83	1973	23.71	10460	4.90
Maine	201.00	67.17	10.00	8	8.67	9.50	8.50	2.33	54.00	1977	38.82	41776	7.16
Maine	161.00	67.17	10.00	8	8.67	9.50	8.50	2.33	55.00	1977	40.56	44936	7.69
Minnesota	40.00	28.33	30.00	13	2.29	1.50	10.00	0.00	26.33	1938	11.27	890	1.62
Minnesota	56.25	33.33	0.00	7	5.33	2.50	7.25	0.17	30.00	1920	18.78	5753	3.88
Minnesota	28.00	22.00	0.00	9	2.58	1.25	6.50	0.25	19.00	1926	11.25	516	1.12
Minnesota	54.25	30.67	45.00	12	2.62	2.17	7.25	0.33	27.00	1931	15.56	2096	2.24
Minnesota	43.00	30.33	0.00	7	4.83	2.25	7.00	0.33	27.00	1935	17.04	3267	3
Minnesota	51.00	33.17	0.00	7	5.25	2.50	6.50	0.33	30.00	1940	18.15	4461	3.18
Minnesota	50.00	34.50	0.00	5	7.00	2.75	6.00	2.58	30.00	1950	19.55	6699	3.83
Minnesota	68.00	34.00	0.00	5	7.00	3.00	6.00	2.54	30.00	1955	20.92	9012	4.42
Minnesota	65.00	34.50	0.00	5	7.00	3.00	6.00	2.58	30.00	1950	20.92	9012	4.42
Minnesota	121.50	64.25	0.00	8	8.08	3.67	9.00	3.33	46.83	1978	26.5	41824	10.98
Minnesota	47.50	50.33	60.00	6	8.83	2.50	9.00	2.58	46.50	1977	19.32	3989	2.91
Minnesota	65.00	50.33	60.00	6	8.83	2.50	9.00	2.58	46.50	1977	19.32	3989	2.91
Minnesota	98.00	45.08	0.00	5	9.83	4.83	8.25	2.67	36.00	1973	35.81	29122	5.35

Table 3.2 cont'd

	Length ft	Width (out-to-out) ft	Skew	No. of Girders	Girder Spacing ft	Girder Depth ft	Slab Thick. in	Overhang ft	Roadway Width ft	Date	Eccentricity in	Moment of Inertia in ⁴	Area
Minnesota	125.00	49.00	0.00	5	9.83	4.83	8.25	2.67	36.00	1973	34.73	27508	5.15
Minnesota	69.83	60.83	56.87	7	8.92	3.50	6.50	3.00	52.00	1964	26.50	11639.00	3.65
Minnesota	109.50	60.83	56.87	7	8.92	3.50	6.50	3.00	52.00	1964	29.62	13704.00	4.25
Minnesota	69.83	60.83	56.87	7	8.92	3.50	6.50	3.00	52.00	1964	26.50	11639.00	3.65
Minnesota	89.00	35.17	0.00	4	9.33	3.00	6.75	3.00	30	1962	25.13	10629.00	4.28
New York	105.00	47.71	0.00	6	8.67	3.00	12.01	1.69	36.00	1955	29.56	15587	6.91
New York	130.00	47.71	0.00	6	8.67	3.00	12.01	1.69	36.00	1955	32.80	19181	8.66
New York	100.73	47.00	0.00	8	6.60	1.50	7.00	2.00	33.00	1961	35.35	43005	8.13
New York	44.52	80.00	8.29	13	6.58	2.00	7.00	0.00	50.00	1945	15.88	5110	4.70
New York	96.52	57.83	27.93	8	7.40	1.33	7.50	2.00	55.00	1968	31.73	25933	6.98
New York	116.49	59.00	51.83	8	7.75	1.67	7.50	2.00	50.50	1968	32.16	56282	10.30
New York	110.02	81.00	51.83	11	7.60	1.67	7.50	2.00	74.50	1968	32.88	44028	8.55
New York	87.30	31.33	0.00	5	7.00	3.00	8.50	1.21	28.00	1970	24.53	17871	7.77
New York	71.72	57.00	10.64	7	8.57	3.00	7.00	2.00	50.00	1962	26.22	17002	7.46
New York	57.00	56.00	46.83	8	7.33	2.75	7.50	1.89	48.00	1967	22.90	8369	4.53
New York	86.33	56.00	46.83	8	7.33	2.75	7.50	1.89	48.00	1967	24.52	18518	9.18
New York	76.83	56.00	46.83	8	7.33	2.75	7.50	1.89	48.00	1967	24.06	14860	7.58
New York	31.92	33.54	28.00	5	7.61	2.75	7.00	2.42	27.00	1960	20.05	6699	3.83
New York	58.58	33.54	17.00	5	7.61	2.75	7.00	2.42	27.00	1960	23.87	10949	5.65
New York	62.97	34.25	52.10	6	5.57	3.00	6.50	2.50	26.00	19--	21.28	16092	7.20
New York	57.39	34.25	38.89	6	5.57	2.75	6.50	2.50	26.00	19--	21.28	8773	4.68
New York	37.40	34.25	33.86	6	5.57	2.50	6.50	2.50	26.00	19--	18.16	4461	3.18
New York	51.90	70.00	6.43	12	5.55	3.00	7.50	0.67	50.00	19--	21.83	10470	5.00
New York	83.60	63.00	13.00	8	8.23	4.00	7.50	2.83	40.00	1950	34.25	33754	5.25
New York	45.00	32.87	35.17	5	7.00	2.75	7.00	2.08	28.00	19--	20.16	7442	4.15
New York	92.75	32.87	35.17	5	7.00	3.00	7.00	2.08	28.00	19--	25.48	20035	8.67

Table 3.2 cont'd

State	Length ft	Width (out-to-out) ft	Skew	No. of Girders	Girder Spacing ft	Girder Depth ft	Slab Thick. in	Overhang ft	Roadway Width ft	Date	Eccentricity in	Moment of Inertia in ⁴	Area in ²
New York	50.50	32.87	35.17	5	7.00	2.75	7.00	2.08	28.00	19--	20.16	7442	4.15
New York	39.08	53.50	2.06	8	6.83	2.50	7.00	2.25	36.00	1955	18.41	4461	3.18
New York	84.58	53.50	2.06	8	6.83	3.00	7.00	2.25	36.00	1955	23.44	14988	6.77
New York	48.75	71.00	16.35	8	9.50	3.00	7.50	2.67	60.00	1955	26.38	10967	5.29
New York	80.25	71.00	16.35	8	9.50	3.00	7.50	2.67	60.00	1955	26.72	21353	9.27
New York	41.25	47.77	7.16	6	8.79	2.75	7.25	2.00	36.00	1957	21.77	7721	4.23
New York	75.67	47.77	7.16	6	8.79	3.00	7.25	2.00	36.00	1957	25.71	20252	8.70
Ohio	30.07	35.67	8.42	5	7.25	2	7.5	2.83	32.5	1953	15.25	2987	2.94
Ohio	38.92	35.67	8.42	5	7.25	2.50	7.50	2.83	32.50	1953	18.83	5347	3.65
Ohio	137.00	57.50	61.55	5	12.75	7.38	8.19	2.17	48.00	1962	48.97	223500	13.83
Ohio	55.00	44.00	12.00	6	7.87	2.75	8.25	1.89	36.00	1985	20.68	6699	3.83
Ohio	39.00	28.50	0.00	5	5.75	2.25	6.75	2.50	24.00	1941	16.83	3267	2.77
Ohio	162.00	56.00	58.93	6	10.17	11.71	9.00	2.00	51.00	1968	66.88	409716	14.00
Ohio	43.00	28.00	0.00	4	7.50	2.50	8.00	2.75	28.00	1985	18.82	3989	2.91
Ohio	12.00	30.00	17.50	11	3.00	0.83	4.42	0.42	30.00	19--	0.00	157	0.85
Ohio	75.00	75.00	56.84	12	6.75	3.00	7.75	0.67	67.00	1957	22.13	18819	8.23
Ohio	63.00	44.45	8.31	6	7.95	3.00	8.75	2.00	39.74	1964	22.41	16092	7.20
Ohio	42.50	37.67	0.00	12	3.21	2.00	4.42	0.83	36.00	1960	0.00	2096	2.24
Ohio	52.00	72.00	20.06	9	8.56	3.00	8.00	1.25	68.50	1968	21.92	9012	4.42
Ohio	72.00	72.00	20.06	9	8.56	3.00	8.00	1.25	68.50	1968	22.08	10470	5.00
Ohio	27.00	29.50	0.00	5	5.75	1.75	7.25	2.75	24.00	1953	14.13	1327	1.82
Ohio	65.54	29.50	0.00	5	5.75	1.75	7.25	2.75	24.00	1953	20.18	6699	3.83
Ohio	63.50	34.33	24.59	4	9.00	3.00	7.75	3.17	24.00	1964	21.80	9012	4.42
Ohio	45.00	34.33	24.59	4	9.00	3.00	7.75	3.17	24.00	1964	21.80	9012	4.42
Ohio	44.00	40.00	25.00	5	8.87	2.75	7.50	2.00	40.00	1955	20.41	7442	4.15
Ohio	55.00	40.00	25.00	5	8.87	2.75	7.50	2.00	40.00	1955	20.41	7442	4.15

Table 3.2 cont'd

State	Length ft	Width (out-to-out) ft	Skew	No. of Girders	Girder Spacing ft	Girder Depth ft	Slab Thick. in	Overhang ft	Roadway Width ft	Date	Eccentricity in	Moment of Inertia in ⁴	Area in ²
Ohio	62.56	63.50	2.50	8	8.83	3.00	8.75	1.58	56.75	1972	22.32	14988	6.77
Ohio	65.56	59.50	2.50	8	8.83	3.00	8.75	1.58	56.75	1972	22.49	12103	5.71
Ohio	64.00	30.00	2.50	4	8.83	3.00	8.75	1.58	26.50	19--	22.32	14988	6.77
Ohio	74.50	58.00	0.00	7	8.33	3.00	8.50	3.50	50.00	1965	22.19	14988	6.77
Ohio	66.25	58.00	0.00	7	8.33	3.00	8.50	3.50	50.00	1965	22.25	9739	4.71
Ohio	80.00	58.00	0.00	7	8.33	3.00	8.50	3.50	50.00	1965	22.49	12103	5.71
Ohio	93.12	58.00	0.00	7	8.33	3.00	8.50	3.50	50.00	1965	22.28	16092	7.30
Ohio	56.00	58.00	0.00	7	8.33	3.00	8.50	3.50	50.00	1965	22.25	9739	4.71
Ohio	70.00	44.00	30.00	6	7.87	3.00	7.75	1.79	44.00	1963	21.66	7796	3.97
Ohio	56.00	44.00	30.00	6	7.87	3.00	7.75	1.79	44.00	1963	21.66	7796	3.97
Ohio	80.00	55.17	10.26	7	8.25	3.00	9.00	2.83	49.83	1959	22.53	16092	7.20
Ohio	48.00	55.17	10.26	7	8.25	3.00	9.00	2.83	49.83	1959	22.50	9739	4.71
Ohio	80.00	43.17	10.26	7	8.25	3.00	9.00	2.83	37.83	1959	22.44	14988	6.77
Ohio	48.00	43.17	10.26	7	8.25	3.00	9.00	2.83	37.83	1959	22.42	9012	4.42
Oklahoma	36.00	22.50	0.00	5	5.25	2.17	8.75	0.50	20.00	1928	17.38	3000	2.70
Oklahoma	34.75	22.50	0.00	5	5.25	2.17	8.75	0.50	20.00	1928	17.38	3000	2.70
Oklahoma	50.00	24.33	0.00	5	5.17	2.75	6.50	1.58	22.00	1938	20.55	6699	3.83
Oklahoma	30.00	27.00	0.00	6	4.50	1.75	6.00	2.00	24.00	1935	14.38	1327	1.82
Oklahoma	34.35	24.33	45.00	5	5.17	2.25	6.50	1.58	22.00	1931	17.35	2825	2.47
Oklahoma	36.00	24.33	45.00	5	5.17	2.25	6.50	1.58	22.00	1931	17.35	2825	2.47
Oklahoma	31.67	28.00	30.00	6	4.92	2.00	7.50	1.21	26.00	1947	15.80	2364	2.47
Oklahoma	40.00	28.00	30.00	6	4.92	2.25	7.50	1.21	26.00	1947	17.21	3267	2.77
Oklahoma	61.00	29.00	0.00	6	4.92	2.75	7.50	1.21	24.00	1936	20.41	7442	4.15
Oklahoma	41.25	31.00	0.00	5	6.58	2.50	7.50	1.83	28.00	1956	20.30	6699	3.83
Oklahoma	59.83	31.00	0.00	5	6.58	3.17	7.50	1.83	28.00	1956	21.83	10470	5.00
Oklahoma	32.67	27.00	45.00	6	4.50	1.75	7.50	2.00	24.00	1935	15.80	2364	2.47

Table 3.2 cont'd

State	Length ft	Width (out-to-out) ft	Skew	No. of Girders	Girder Spacing ft	Girder Depth ft	Slab Thick. in	Overhang ft	Roadway Width ft	Date	Eccentricity in	Moment of Inertia in ⁴	Area in ²
Oklahoma	58.92	27.00	45.00	6	4.50	3.00	7.50	2.00	24.00	1935	21.83	10470	5.00
Oklahoma	37.17	22.50	0.00	5	5.25	2.17	8.75	0.33	20.00	1927	16.43	2364	2.47
Oklahoma	59.58	28.50	0.00	-	-	-	-	-	26.00	1953	-	-	-
Oklahoma	31.46	28.50	0.00	-	-	-	-	-	26.00	1953	-	-	-
Oklahoma	38.75	31.00	0.00	5	6.58	2.50	7.50	1.83	28.00	1956	23.66	4461	3.18
Oklahoma	44.00	26.33	30.00	6	4.92	2.25	7.50	1.21	24.00	1935	17.29	3604	3.00
Oklahoma	45.71	26.33	30.00	6	4.92	2.25	7.50	1.21	24.00	1935	17.21	3267	2.77
Oklahoma	31.25	26.50	0.00	5	5.67	2.00	8.00	1.29	24.00	1932	15.19	2096	2.24
Oklahoma	30.00	26.50	0.00	5	5.67	2.00	8.00	1.29	24.00	1932	-	-	-
Oklahoma	26.00	43.00	0.00	9	5.25	-	5.00	2.50	40.00	1955	-	-	-
Oklahoma	72.00	31.00	35.83	5	6.58	2.75	6.00	1.83	28.00	1954	19.55	6699	3.83
Oklahoma	81.50	31.00	35.83	5	6.58	2.75	6.00	1.83	28.00	1954	19.55	6699	3.83
Oklahoma	125.00	41.00	0.00	4	11.00	5.00	10.00	3.25	38.00	1983	40.99	51463	8.25
Oklahoma	160.00	41.00	0.00	4	11.00	5.00	10.00	3.25	38.00	1983	40.99	51463	8.25
Oregon	140.00	59.00	0.00	6	13.50	8.81	6.50	2.00	58.00	1951	55.75	203546	10.93
Oregon	113.00	76.00	0.00	6	9.00	4.00	7.00	6.00	70.00	1962	34.64	27429	6.13
Oregon	142.00	76.00	0.00	6	9.00	4.00	7.00	6.00	70.00	1962	34.64	27429	6.13
Oregon	64.00	34.83	30.00	4	11.00	4.50	7.50	0.90	32.00	1969	35.24	39977	5.80
Oregon	152.50	34.83	30.00	4	11.00	4.50	7.50	0.90	32.00	1969	37.79	45716	6.45
Oregon	53.00	34.83	30.00	4	11.00	4.50	7.50	0.90	32.00	1969	35.24	39977	5.80
Oregon	52.50	56.00	0.00	-	2.00	1.50	5.00	1.50	40.00	1960	10.95	1322	2.36
Bridge Database from Appendix B of the NCHRP Report 12-26 for Concrete T-beam Bridges													
Arizona	68.00	32.00	0.00	4	8.00	5.17	6.75	4.12	29.75	1973	34.38	417074	130.20
Arizona	71.00	32.00	0.00	4	8.00	5.17	6.75	4.12	29.75	1973	34.38	417074	130.20
California	31.21	16.00	33.75	3	7.35	2.33	9.00	0.58	14.66	1926	13.56	8437	30.80
California	31.00	30.10	27.50	6	5.75	2.33	6.50	0.00	24.00	1945	14.00	14079	26.55

Table 3.2 cont'd

State	Length ft	Width (out-to-out) ft	Skew	No. of Girders	Girder Spacing ft	Girder Depth ft	Slab Thick. in	Overhang ft	Roadway Width ft	Date	Eccentricity in	Moment of Inertia in ⁴	Area in ²
California	31.00	30.10	27.50	6	5.75	2.33	6.50	0.00	24.00	1945	14.00	14079	26.55
California	31.00	27.17	0.00	4	7.60	3.00	9.00	1.63	24.00	1929	18.00	24600	40.50
California	30.00	53.00	4.00	7	7.92	3.50	6.25	2.57	51.00	1966	21.00	53300	50.00
California	29.17	39.00	0.00	5	8.33	3.50	6.50	2.25	37.00	1966	21.00	53300	50.00
California	30.00	39.00	0.00	5	8.33	3.50	6.50	2.25	37.00	1966	21.00	53300	50.00
California	55.00	53.00	4.00	7	7.92	3.50	6.25	2.57	51.00	1966	21.00	53300	50.00
California	60.00	92.00	45.00	12	7.83	4.00	6.25	2.17	90.00	1967	24.00	78837	54.28
California	60.00	66.00	45.00	9	7.66	4.00	6.37	2.17	64.00	1957	24.00	78837	54.28
California	34.00	45.00	29.30	7	-	3.50	-	-	41.00	1965	-	-	-
California	71.00	33.17	0.00	4	8.50	5.00	6.62	3.23	28.00	1953	30.00	205300	86.47
California	59.00	73.00	29.00	6	13.08	2.75	8.50	0.00	64.00	1937	16.50	31860	63.70
California	39.00	41.00	5.00	5	8.25	2.50	6.50	3.50	39.00	1965	15.00	14060	30.50
California	38.00	40.50	0.00	5	9.00	3.50	7.00	2.21	39.00	1966	21.00	46450	45.50
California	53.00	33.75	24.36	4	8.00	4.75	6.50	3.75	28.00	1971	28.50	150250	70.70
California	72.00	33.75	24.36	4	8.00	4.75	6.50	3.75	28.00	1971	28.50	150250	70.70
California	43.00	33.75	33.21	6	6.25	3.50	7.25	0.71	32.00	1932	21.00	52454	52.13
California	43.00	23.75	33.21	4	6.25	3.50	7.25	1.75	22.00	1932	21.00	52454	52.13
California	33.00	33.00	22.00	3	12.75	5.00	9.00	2.88	30.00	1935	27.00	159470	94.50
California	31.50	31.50	30.00	6	5.83	2.25	-	-	28.00	1956	-	-	-
California	30.66	30.66	0.00	4	8.00	2.33	8.00	2.38	26.00	1938	14.00	10000	30.00
California	30.66	30.66	0.00	4	8.00	2.33	8.00	2.38	26.00	1938	14.00	10000	30.00
California	39.66	39.66	12.37	7	6.00	3.33	6.00	1.83	37.66	1966	20.00	39304	40.80
California	39.66	39.66	12.37	7	6.00	3.33	6.00	1.83	37.66	1966	20.00	39304	40.80
California	42.17	42.17	24.87	7	6.83	4.75	6.37	0.00	40.00	1954	28.50	151416	70.80
California	58.00	58.00	0.00	8	7.50	2.50	6.25	3.00	52.00	1961	15.00	15629	33.25
California	68.66	68.66	0.00	10	7.00	4.63	6.25	2.83	64.00	1963	27.76	99550	49.25

Table 3.2 cont'd

State	Length ft	Width (out-to-out) ft	Skew	No. of Girders	Girder Spacing ft	Girder Depth ft	Slab Thick. in	Overhang ft	Roadway Width ft	Date	Eccentricity in	Moment of Inertia in ⁴	Area in ²
California	45.83	45.83	10.05	6	8.00	5.17	6.50	2.66	41.00	1962	31.75	156700	61.00
Florida	25.00	33.42	0.00	5	7.17	2.00	7.00	2.00	26.00	1960	-	-	-
Maine	22.00	24.25	0.00	4	7.50	1.83	7.50	0.00	22.00	1981	14.75	15972	39.60
Maine	23.00	23.00	0.00	5	5.33	2.17	8.00	0.00	20.00	1925	16.50	18250	41.40
Maine	25.17	25.17	0.00	5	5.85	2.42	8.25	0.25	22.00	1954	17.63	31165	51.30
Maine	22.25	22.25	15.00	5	5.21	3.33	8.00	0.00	20.00	1926	24.00	85333	64.00
Maine	46.82	37.50	32.77	7	5.61	5.42	6.50	0.17	34.00	1952	15.75	31250	60.00
Maine	62.44	37.50	32.77	7	5.61	5.42	6.50	0.17	34.00	1952	15.75	31250	60.00
Minnesota	60.00	34.50	45.00	6	6.50	3.08	5.75	0.00	30.00	1952	21.88	100600	83.60
Minnesota	58.00	34.71	0.00	6	6.56	3.08	5.75	0.00	30.00	1947	21.88	100600	83.60
Minnesota	65.00	50.17	0.00	8	6.27	2.50	6.00	2.88	46.83	1979	13.55	74443	69.36
Minnesota	68.25	42.00	0.00	7	6.00	3.08	6.75	2.50	46.83	1983	16.92	567348	68.63
New York	39.00	34.33	0.00	4	8.33	2.96	9.00	4.66	22.00	1934	22.25	82021	78.10
Ohio	60.00	31.17	0.00	6	4.87	3.92	6.50	2.50	24.00	1979	26.75	177364	96.35
Ohio	40.00	32.25	0.00	7	4.96	2.21	6.50	0.54	29.00	1977	16.50	25588	43.73
Oklahoma	50.00	41.67	0.00	6	7.00	2.04	5.00	1.25	40.00	1984	14.35	62160	62.20
Oklahoma	50.00	42.00	0.00	6	7.00	2.87	5.00	1.00	40.00	1979	-	-	-
Oklahoma	31.25	33.00	0.00	6	5.87	-	7.50	-	28.00	1942	15.75	11000	33.00
Oklahoma	40.00	33.00	0.00	6	5.87	-	7.50	-	28.00	1942	24.00	91341	66.83
Oregon	70.00	41.42	43.78	5	9.00	4.25	7.50	1.92	40.00	1962	25.50	89170	56.55
Oregon	56.00	41.42	43.78	5	9.00	4.25	7.50	1.92	40.00	1962	25.50	89170	56.55
Oregon	27.00	41.42	43.78	5	9.00	4.25	7.50	1.92	40.00	1962	25.50	89170	56.55
Oregon	48.50	34.83	41.90	4	9.00	4.75	7.00	3.29	30.00	1961	28.50	151000	72.50
Oregon	62.00	34.83	41.90	4	9.00	4.75	7.00	3.29	30.00	1961	28.50	151000	72.50
Oregon	78.00	34.83	41.90	4	9.00	4.75	7.00	3.29	30.00	1961	28.50	151000	72.50
Oregon	56.00	34.83	41.90	4	9.00	4.75	7.00	3.29	30.00	1961	28.50	151000	72.50

Table 3.2 cont'd

State	Length ft	Width (out-to-out) ft	Skew	No. of Girders	Girder Spacing ft	Girder Depth ft	Slab Thick. in	Overhang ft	Roadway Width ft	Date	Eccentricity in	Moment of Inertia in ⁴	Area in ²
Oregon	56.00	38.50	0.00	4	9.33	4.00	7.00	5.25	30.00	1948	24.00	97600	69.70
Oregon	70.00	38.50	0.00	4	9.33	4.00	7.00	5.25	30.00	1948	24.00	97600	69.70
Oregon	50.00	38.50	0.00	4	9.33	4.00	7.00	5.25	30.00	1948	21.00	53600	52.50
Oregon	37.00	38.50	0.00	4	9.33	4.00	7.00	5.25	30.00	1948	21.00	53600	52.50
Oregon	49.00	28.00	-	4	-	3.80	6.50	1.75	26.00	1951	18.50	39000	50.30
Oregon	65.00	28.00	-	4	-	3.80	6.50	1.75	26.00	1951	18.50	39000	50.30
Oregon	35.00	28.75	0.00	4	7.33	1.92	7.00	3.50	26.00	1939	15.00	14190	32.20
Oregon	50.00	28.75	0.00	4	7.33	1.92	7.00	3.50	26.00	1939	15.00	14190	32.20
Oregon	47.00	45.50	50.68	4	7.75	2.52	7.75	3.37	42.00	1979	19.00	55360	72.60
Oregon	63.00	45.50	50.61	4	7.75	2.52	7.75	3.37	42.00	1979	19.00	55360	72.60
Oregon	54.00	45.50	52.98	4	7.75	2.52	7.75	3.37	42.00	1979	19.00	55360	72.60
Oregon	35.00	35.17	0.00	9	4.75	2.50	6.00	0.00	30.00	1954	18.00	29250	39.00
Oregon	24.00	59.00	0.00	-	-	-	6.50	2.00	58.00	1951	-	-	-
Washington	26.00	10.25	0.00	8	-	1.17	6.50	1.33	9.50	1974	-	-	-
Washington	20.00	10.25	0.00	8	-	1.17	6.50	1.33	9.50	1974	-	-	-
Washington	41.44	33.17	0.00	4	10.00	2.50	10.00	-	24.00	1926	-	-	-
Washington	72.00	28.50	45.00	2	16.00	3.75	8.63	6.33	24.00	1934	27.74	164000	94.00
Washington	50.00	28.50	45.00	2	16.00	2.75	8.63	6.33	24.00	1934	21.66	65216	70.00
Washington	93.00	28.50	45.00	2	16.00	3.75	8.63	6.33	24.00	1934	27.74	164000	94.00
Washington	45.00	26.71	0.00	4	7.17	2.75	6.50	3.79	24.00	1939	17.25	30200	40.20
Washington	22.50	39.38	0.00	5	8.54	2.75	6.50	2.50	36.00	1946	16.75	27000	44.55
Washington	32.00	39.33	45.00	17	2.42	1.63	5.50	0.17	36.00	1950	9.75	2972	18.00
Washington	24.00	39.33	45.00	17	2.42	1.63	5.50	0.17	36.00	1950	9.75	2972	18.00
Washington	25.00	17.42	0.00	3	6.75	2.33	8.00	1.42	16.00	1930	16.00	13824	28.80
Washington	12.00	37.75	0.00	5	7.50	2.54	6.50	1.75	34.00	1948	15.25	19000	39.60
Washington	45.00	37.75	0.00	5	7.50	2.54	6.50	1.75	34.00	1948	15.25	19000	39.60

Table 3.2 cont'd

State	Length ft	Width (out-to-out) ft	Skew	No. of Girders	Girder Spacing ft	Girder Depth ft	Slab Thick. in	Overhang ft	Roadway Width ft	Date	Eccentricity in	Moment of Inertia in ⁴	Area in ²
Washington	40.00	22.83	0.00	2	12.00	4.08	11.00	3.00	20.00	1926	-	-	-
Washington	56.00	22.83	0.00	2	12.00	4.08	11.00	3.00	20.00	1926	-	-	-
Bridge Database from Appendix B of the NCHRP Report 12-26 for Prestressed I-girder Bridges													
Arizona	84.50	47.17	14.08	7	6.83	4.50	7.00	2.25	40.00	1970	32.70	260730	78.90
Arizona	45.00	47.17	14.08	7	6.83	4.50	7.00	2.25	40.00	1970	32.70	260730	78.90
Arizona	89.67	95.17	29.12	11	8.58	4.50	8.50	3.42	92.00	1983	33.52	260730	78.90
Arizona	77.00	40.58	20.00	6	7.00	3.75	7.00	2.21	38.00	1972	28.23	125390	56.00
Arizona	78.50	35.17	20.00	6	5.58	3.75	6.50	2.71	30.00	1962	27.98	125390	56.00
California	79.17	34.00	8.00	5	7.10	5.25	6.00	2.75	28.00	1961	32.27	260730	78.90
California	113.00	43.00	0.00	7	6.42	6.33	6.87	2.50	40.00	1984	37.84	318000	64.20
California	96.00	58.00	0.00	8	7.50	5.66	6.25	2.75	52.00	1962	34.53	248000	60.00
California	70.50	58.00	0.00	8	7.50	5.66	6.25	2.75	52.00	1962	34.53	248000	60.00
California	84.00	68.66	0.00	10	7.00	4.63	6.25	2.83	66.00	1964	31.43	187800	55.80
California	61.63	74.00	0.00	10	7.66	3.66	6.25	2.50	73.00	1968	22.03	63300	43.20
California	27.00	74.00	0.00	10	7.66	3.66	6.25	2.50	73.00	1968	22.03	63300	43.20
California	80.00	45.83	10.50	6	8.00	5.14	6.25	3.16	41.00	1964	31.43	187800	55.80
California	101.00	45.75	7.00	7	6.90	5.25	7.00	2.50	38.00	1981	31.80	187800	55.80
California	84.00	190.00	0.00	19	9.10	5.38	7.13	3.64	188.00	1972	35.00	187800	55.80
California	72.50	37.00	5.28	5	7.75	4.66	6.25	3.00	28.00	1967	28.33	137300	51.60
California	62.25	37.00	5.28	5	7.75	4.66	6.25	3.00	28.00	1967	28.33	137300	51.60
California	52.00	53.00	47.70	6	8.83	5.25	6.50	4.42	51.00	1970	31.55	187800	55.80
California	76.25	53.00	47.70	6	8.83	5.25	6.50	4.42	51.00	1970	31.55	187800	55.80
California	84.24	53.00	47.70	6	8.83	5.25	6.50	4.42	51.00	1970	31.55	187800	55.80
California	47.50	43.50	11.04	5	8.75	5.33	7.75	4.25	40.00	1981	32.18	187800	55.80
California	74.80	43.50	11.04	5	8.75	5.33	7.75	4.25	40.00	1981	32.18	187800	55.80
California	91.50	43.50	11.04	5	8.75	5.33	7.75	4.25	40.00	1981	32.18	187800	55.80

Table 3.2 cont'd

State	Length ft	Width (out-to-out) ft	Skew	No. of Girders	Girder Spacing ft	Girder Depth ft	Slab Thick. in	Overhang ft	Roadway Width ft	Date	Eccentricity in	Moment of Inertia in ⁴	Area in ²
California	58.43	41.00	40.00	5	8.25	5.17	6.25	4.00	39.00	1970	31.43	187800	55.80
California	94.33	41.00	40.00	5	8.25	5.17	6.25	4.00	39.00	1970	31.43	187800	55.80
California	94.33	57.00	47.20	7	8.00	5.17	6.25	4.00	55.00	1970	31.43	187800	55.80
California	109.75	66.00	19.15	10	6.64	5.58	6.00	3.08	48.00	1969	34.40	248600	60.00
California	79.00	66.00	19.15	8	8.47	5.58	6.38	3.08	48.00	1969	34.59	248600	60.00
California	90.00	52.00	14.10	8	6.58	4.42	6.00	2.96	40.00	1971	27.73	125390	56.00
California	67.50	46.00	0.00	7	6.83	4.66	6.00	2.50	32.00	1963	28.20	137300	51.60
California	97.21	82.00	9.18	10	8.25	6.25	6.25	3.87	80.00	1971	37.53	318000	64.20
California	67.75	68.66	12.88	12	6.00	3.63	6.00	1.33	66.00	1963	21.90	63300	43.20
Florida	40.00	31.17	0.00	4	9.70	3.00	7.00	6.00	28.00	1957	23.67	50980	36.90
Florida	60.00	31.17	0.00	6	5.83	3.00	7.00	6.00	28.00	1957	23.67	50980	36.90
Florida	82.00	46.75	0.00	5	9.69	4.50	7.50	3.17	44.00	1976	33.02	260730	78.90
Florida	32.50	31.00	0.00	4	6.75	3.75	7.00	1.25	26.00	1960	28.23	125390	56.00
Florida	72.00	31.00	0.00	4	6.75	3.75	7.00	1.25	26.00	1960	28.23	125390	56.00
Florida	37.50	43.00	10.11	6	7.83	3.75	7.00	1.25	38.00	1960	28.23	125390	56.00
Florida	64.50	43.00	10.11	6	7.83	3.75	7.00	1.25	38.00	1960	28.23	125390	56.00
Florida	75.58	43.00	2.57	6	7.42	3.75	7.00	1.17	38.00	1960	28.23	125390	56.00
Florida	63.58	31.50	3.50	5	5.50	3.75	7.00	1.25	26.00	1960	28.23	125390	56.00
Florida	38.92	31.00	3.50	4	6.75	3.75	7.00	1.25	26.00	1960	28.23	125390	56.00
Florida	79.00	42.50	0.00	9	4.75	3.75	7.00	1.17	38.00	1960	28.23	125390	56.00
Florida	79.00	31.50	0.00	6	5.42	3.75	7.00	1.17	26.00	1960	28.23	125390	56.00
Florida	47.50	31.50	0.00	4	9.03	3.75	7.00	1.17	26.00	1960	28.23	125390	56.00
Florida	65.25	84.75	0.00	10	8.77	3.75	7.50	2.21	79.25	1975	33.02	260730	78.90
Florida	87.00	84.75	0.00	10	8.77	3.75	7.50	2.21	79.25	1975	33.02	260730	78.90
Florida	46.00	70.75	39.26	9	8.12	3.00	7.00	2.00	68.00	1980	23.67	50980	36.90
Florida	113.75	70.75	39.26	15	4.50	4.50	7.00	2.00	68.00	1980	32.77	260730	78.90

Table 3.2 cont'd

State	Length ft	Width (out-to-out) ft	Skew	No. of Girders	Girder Spacing ft	Girder Depth ft	Slab Thick. in	Overhang ft	Roadway Width ft	Date	Eccentricity in	Moment of Inertia in ⁴	Area in ²
Florida	113.67	82.75	39.26	15	6.33	4.50	7.00	2.00	80.00	1980	32.77	260730	78.90
Florida	46.00	82.75	39.26	11	7.67	3.00	7.00	2.00	80.00	1980	23.67	50980	36.90
Florida	74.00	26.00	18.13	4	7.33	3.75	7.00	1.33	24.00	1962	28.23	125390	56.00
Florida	65.00	26.00	18.13	4	7.33	3.75	7.00	1.33	24.00	1962	28.23	125390	56.00
Florida	41.75	54.25	0.00	6	9.80	3.00	7.00	2.12	52.00	1970	23.67	50980	36.90
Florida	61.50	54.25	0.00	10	5.44	3.00	7.00	2.12	52.00	1970	28.23	125390	56.00
Florida	45.50	54.25	0.00	7	8.17	3.00	7.00	2.12	46.00	1970	23.67	50980	36.90
Florida	91.50	54.25	0.00	7	8.17	4.50	7.00	1.79	46.00	1970	32.77	260730	78.90
Florida	40.00	54.25	0.00	6	9.80	3.00	7.00	1.79	46.00	1970	23.67	50980	36.90
Florida	50.75	62.25	39.23	8	8.14	3.00	7.00	1.79	60.00	1969	23.67	50980	36.90
Florida	95.00	62.25	39.23	8	8.14	4.50	7.00	1.79	60.00	1969	32.77	260730	78.90
Florida	71.00	67.67	7.12	10	7.33	3.75	7.00	0.33	64.00	1964	24.73	125390	56.00
Florida	70.08	32.00	7.20	5	7.00	3.75	7.00	1.33	30.00	1964	24.73	125390	56.00
Florida	36.75	35.33	4.28	4	10.00	3.00	7.00	1.83	33.00	1971	23.67	50980	36.90
Florida	99.50	35.33	4.28	6	6.00	4.50	7.00	1.83	33.00	1971	29.27	260730	78.90
Florida	36.00	52.00	9.22	6	8.96	3.00	7.25	1.50	50.00	1962	23.67	50980	36.90
Florida	40.50	42.00	8.77	5	9.50	3.00	7.25	1.50	40.00	1961	20.17	50980	36.90
Florida	35.00	52.00	18.15	6	9.60	3.00	7.25	1.25	50.00	1962	20.17	50980	36.90
Florida	66.50	52.00	18.15	7	8.00	4.50	0.00	1.25	50.00	1962	24.78	125390	56.00
Florida	95.07	89.50	0.00	14	6.51	4.50	7.50	2.00	81.50	1973	29.27	260730	78.90
Florida	101.68	89.50	0.00	14	6.51	4.50	7.50	2.00	81.50	1973	29.27	260730	78.90
Florida	129.00	89.50	0.00	12	7.77	6.00	7.50	2.00	81.50	1973	35.62	733320	108.50
Florida	47.00	46.75	0.00	6	8.20	3.00	7.00	2.37	44.00	1978	20.17	50980	36.90
Florida	82.00	46.75	0.00	5	9.69	4.50	7.50	2.33	44.00	1978	29.27	260730	78.90
Florida	64.00	47.62	0.00	6	9.25	3.75	7.50	2.00	40.00	1976	24.73	125390	56.00
Minnesota	96.02	42.00	19.27	6	6.83	4.50	6.00	3.42	36.00	1977	32.27	260730	78.90

Table 3.2 cont'd

State	Length ft	Width (out-to-out) ft	Skew	No. of Girders	Girder Spacing ft	Girder Depth ft	Slab Thick. in	Overhang ft	Roadway Width ft	Date	Eccentricity in	Moment of Inertia in ⁴	Area in ²
Minnesota	81.00	50.83	0.00	8	6.50	3.75	9.00	1.92	47.00	1976	29.23	125390	56.00
Minnesota	74.50	47.17	0.00	5	10.25	3.75	8.00	2.54	44.00	1972	28.73	125390	56.00
Minnesota	97.00	50.75	0.00	6	8.75	5.25	8.00	3.00	46.92	1975	-	-	-
Minnesota	96.00	50.75	30.00	7	7.33	4.50	8.00	2.42	46.50	1975	33.27	260730	78.90
New York	63.00	33.33	9.00	8	3.67	3.00	5.25	1.00	28.00	1957	16.46	79145	54.03
Ohio	47.00	66.00	0.00	9	7.50	3.00	7.50	2.42	52.00	1967	26.65	59077	47.10
Oklahoma	50.00	49.42	0.00	5	10.50	3.75	8.50	3.21	46.75	1970	29.98	125390	56.00
Oregon	22.81	64.33	0.00	18	3.21	1.75	5.00	0.00	55.83	1962	11.30	40134	51.10
Oregon	30.75	64.33	0.00	18	3.21	1.75	5.00	0.00	55.83	1962	11.30	40134	51.10
Oregon	18.75	30.75	0.00	7	4.21	1.46	5.25	0.00	26.00	1975	5.83	9599	41.90
Oregon	60.00	34.00	35.42	4	9.33	3.75	6.25	3.00	30.00	1964	27.86	125390	56.00
Oregon	58.00	34.00	35.42	4	9.33	3.75	6.25	3.00	30.00	1964	27.86	125390	56.00
Oregon	92.00	29.50	0.00	4	8.00	4.50	7.50	2.50	26.00	1970	33.00	260730	78.90
Oregon	47.55	76.39	35.07	10	8.00	3.00	7.00	-	-	1964	23.67	50980	36.90
Oregon	42.24	76.39	34.52	10	8.00	3.00	7.00	-	-	1964	23.67	50980	36.90
Washington	136.20	53.73	0.00	8	6.75	6.13	7.00	3.25	52.00	1978	39.09	455967	62.63
Washington	56.00	35.00	15.65	6	5.92	4.00	6.25	3.92	30.00	1961	-	-	-
Washington	48.00	35.00	15.65	6	5.92	4.00	6.25	3.92	30.00	1961	-	-	-
Washington	60.00	69.00	28.63	13	5.35	-	-	-	66.00	1964	-	-	-
Washington	70.00	69.00	28.63	13	5.35	-	-	-	66.00	1964	-	-	-
Washington	113.00	52.00	45.00	8	6.83	4.83	6.50	1.71	50.50	1966	31.10	249044	54.65
Washington	66.75	35.00	0.00	6	5.44	3.67	-	-	28.00	1967	-	-	-
Washington	41.00	35.00	0.00	6	5.44	3.67	-	-	28.00	1967	-	-	-
Washington	48.00	42.17	22.00	6	7.25	6.13	7.00	3.00	40.00	1971	39.09	455967	62.63
Washington	118.00	42.17	22.00	6	7.25	6.13	7.00	3.00	40.00	1971	39.09	455967	62.63
Washington	90.00	42.17	22.00	6	7.25	6.13	7.00	3.00	40.00	1971	39.09	455967	62.63

Table 3.2 cont'd

State	Length ft	Width (out-to-out) ft	Skew	No. of Girders	Girder Spacing ft	Girder Depth ft	Slab Thick. in	Overhang ft	Roadway Width ft	Date	Eccentricity in	Moment of Inertia in ⁴	Area in ²
Washington	38.96	124.03	0.00	-	-	-	-	-	118.03	1963	-	-	-
Washington	35.75	95.45	0.00	-	-	-	-	-	91.45	1963	-	-	-
Washington	43.92	112.75	0.00	-	-	-	-	-	108.75	1963	-	-	-

Table 3.3 Parameter ranges for NCHRP 12-26 bridge database

Parameter	Minimum	Maximum	Average
Girder Spacing (ft)	2.2	16	7.6
Span Length (ft)	12	205	67.4
I (in ⁴)	1138	2,970,000	164,296
Slab Thickness (in)	4.4	12.0	7.2

Table 3.4. NCHRP 12-26 parametric study database

Seq No.	Slab Thickness (in)	Girder Stiffness (in ⁴)	Span Length (ft)	Girder Spacing (ft)	Distribution Factor
1	4.40	10000	20	3.50	0.675
2	4.40	10000	20	5.00	0.844
3	4.40	10000	20	7.50	1.150
4	4.40	10000	20	10.00	1.410
5	4.40	10000	20	16.00	1.704
6	4.40	10000	64	3.50	0.636
7	4.40	10000	64	5.00	0.668
8	4.40	10000	64	7.50	0.751
9	4.40	10000	64	10.00	0.871
10	4.40	10000	64	16.00	1.113
11	4.40	10000	130	3.50	0.631
12	4.40	10000	130	5.00	0.654
13	4.40	10000	130	7.50	0.701
14	4.40	10000	130	10.00	0.753
15	4.40	10000	130	16.00	0.861
16	4.40	10000	200	3.50	0.628
17	4.40	10000	200	5.00	0.652
18	4.40	10000	200	7.50	0.692
19	4.40	10000	200	10.00	0.732
20	4.40	10000	200	16.00	0.808
21	4.40	50000	20	3.50	0.837
22	4.40	50000	20	5.00	1.106
23	4.40	50000	20	7.50	1.588
24	4.40	50000	20	10.00	1.919
25	4.40	50000	20	16.00	2.605
26	4.40	50000	64	3.50	0.690
27	4.40	50000	64	5.00	0.851
28	4.40	50000	64	7.50	1.134
29	4.40	50000	64	10.00	1.399
30	4.40	50000	64	16.00	1.885
31	4.40	50000	130	3.50	0.674
32	4.40	50000	130	5.00	0.740
33	4.40	50000	130	7.50	0.889
34	4.40	50000	130	10.00	1.070
35	4.40	50000	130	16.00	1.338
36	4.40	50000	200	3.50	0.672
37	4.40	50000	200	5.00	0.714
38	4.40	50000	200	7.50	0.806
39	4.40	50000	200	10.00	0.926
40	4.40	50000	200	16.00	1.131
41	4.40	560000	20	3.50	0.960
42	4.40	560000	20	5.00	1.183
43	4.40	560000	20	7.50	1.655

Table 3.4 cont'd

Seq No.	Slab Thickness (in)	Girder Stiffness (in ⁴)	Span Length (ft)	Girder Spacing (ft)	Distribution Factor
44	4.40	560000	20	10.00	1.989
45	4.40	560000	20	16.00	2.731
46	4.40	560000	64	3.50	0.714
47	4.40	560000	64	5.00	0.991
48	4.40	560000	64	7.50	1.445
49	4.40	560000	64	10.00	1.812
50	4.40	560000	64	16.00	2.543
51	4.40	560000	130	3.50	0.698
52	4.40	560000	130	5.00	0.884
53	4.40	560000	130	7.50	1.170
54	4.40	560000	130	10.00	1.425
55	4.40	560000	130	16.00	1.926
56	4.40	560000	200	3.50	0.686
57	4.40	560000	200	5.00	0.813
58	4.40	560000	200	7.50	1.039
59	4.40	560000	200	10.00	1.253
60	4.40	560000	200	16.00	1.566
61	4.40	3000000	20	3.50	0.991
62	4.40	3000000	20	5.00	1.197
63	4.40	3000000	20	7.50	1.665
64	4.40	3000000	20	10.00	1.998
65	4.40	3000000	20	16.00	2.745
66	4.40	3000000	64	3.50	0.808
67	4.40	3000000	64	5.00	1.101
68	4.40	3000000	64	7.50	1.601
69	4.40	3000000	64	10.00	1.955
70	4.40	3000000	64	16.00	2.704
71	4.40	3000000	130	3.50	0.717
72	4.40	3000000	130	5.00	0.971
73	4.40	3000000	130	7.50	1.376
74	4.40	3000000	130	10.00	1.724
75	4.40	3000000	130	16.00	2.424
76	4.40	3000000	200	3.50	0.712
77	4.40	3000000	200	5.00	0.929
78	4.40	3000000	200	7.50	1.219
79	4.40	3000000	200	10.00	1.470
80	4.40	3000000	200	16.00	2.006
81	4.40	7000000	20	3.50	0.996
82	4.40	7000000	20	5.00	1.198
83	4.40	7000000	20	7.50	1.666
84	4.40	7000000	20	10.00	1.999
85	4.40	7000000	20	16.00	2.748
86	4.40	7000000	64	3.50	0.866

Table 3.4 cont'd

Seq No.	Slab Thickness (in)	Girder Stiffness (in ⁴)	Span Length (ft)	Girder Spacing (ft)	Distribution Factor
87	4.40	7000000	64	5.00	1.138
88	4.40	7000000	64	7.50	1.634
89	4.40	7000000	64	10.00	1.979
90	4.40	7000000	64	16.00	2.728
91	4.40	7000000	130	3.50	0.731
92	4.40	7000000	130	5.00	1.036
93	4.40	7000000	130	7.50	1.477
94	4.40	7000000	130	10.00	1.847
95	4.40	7000000	130	16.00	2.597
96	4.40	7000000	200	3.50	0.719
97	4.40	7000000	200	5.00	0.962
98	4.40	7000000	200	7.50	1.305
99	4.40	7000000	200	10.00	1.614
100	4.40	7000000	200	16.00	2.259
101	7.25	10000	20	3.50	0.621
102	7.25	10000	20	5.00	0.784
103	7.25	10000	20	7.50	1.078
104	7.25	10000	20	10.00	1.318
105	7.25	10000	20	16.00	1.584
106	7.25	10000	64	3.50	0.585
107	7.25	10000	64	5.00	0.644
108	7.25	10000	64	7.50	0.749
109	7.25	10000	64	10.00	0.876
110	7.25	10000	64	16.00	1.119
111	7.25	10000	130	3.50	0.579
112	7.25	10000	130	5.00	0.527
113	7.25	10000	130	7.50	0.695
114	7.25	10000	130	10.00	0.762
115	7.25	10000	130	16.00	0.890
116	7.25	10000	200	3.50	0.578
117	7.25	10000	200	5.00	0.624
118	7.25	10000	200	7.50	0.685
119	7.25	10000	200	10.00	0.738
120	7.25	10000	200	16.00	0.829
121	7.25	50000	20	3.50	0.761
122	7.25	50000	20	5.00	1.017
123	7.25	50000	20	7.50	1.453
124	7.25	50000	20	10.00	1.762
125	7.25	50000	20	16.00	2.320
126	7.25	50000	64	3.50	0.681
127	7.25	50000	64	5.00	0.808
128	7.25	50000	64	7.50	1.027
129	7.25	50000	64	10.00	1.232

Table 3.4 cont'd

Seq No.	Slab Thickness (in)	Girder Stiffness (in ⁴)	Span Length (ft)	Girder Spacing (ft)	Distribution Factor
130	7.25	50000	64	16.00	1.535
131	7.25	50000	130	3.50	0.669
132	7.25	50000	130	5.00	0.726
133	7.25	50000	130	7.50	0.840
134	7.25	50000	130	10.00	0.972
135	7.25	50000	130	16.00	1.169
136	7.25	50000	200	3.50	0.667
137	7.25	50000	200	5.00	0.706
138	7.25	50000	200	7.50	0.781
139	7.25	50000	200	10.00	0.870
140	7.25	50000	200	16.00	1.014
141	7.25	560000	20	3.50	0.898
142	7.25	560000	20	5.00	1.150
143	7.25	560000	20	7.50	1.630
144	7.25	560000	20	10.00	1.962
145	7.25	560000	20	16.00	2.681
146	7.25	560000	64	3.50	0.713
147	7.25	560000	64	5.00	0.948
148	7.25	560000	64	7.50	1.293
149	7.25	560000	64	10.00	1.599
150	7.25	560000	64	16.00	2.220
151	7.25	560000	130	3.50	0.697
152	7.25	560000	130	5.00	0.858
153	7.25	560000	130	7.50	1.087
154	7.25	560000	130	10.00	1.232
155	7.25	560000	130	16.00	1.580
156	7.25	560000	200	3.50	0.685
157	7.25	560000	200	5.00	0.796
158	7.25	560000	200	7.50	0.982
159	7.25	560000	200	10.00	1.157
160	7.25	560000	200	16.00	1.367
161	7.25	3000000	20	3.50	0.970
162	7.25	3000000	20	5.00	1.188
163	7.25	3000000	20	7.50	1.659
164	7.25	3000000	20	10.00	1.992
165	7.25	3000000	20	16.00	2.736
166	7.25	3000000	64	3.50	0.734
167	7.25	3000000	64	5.00	1.047
168	7.25	3000000	64	7.50	1.503
169	7.25	3000000	64	10.00	1.863
170	7.25	3000000	64	16.00	2.595
171	7.25	3000000	130	3.50	0.721
172	7.25	3000000	130	5.00	0.952

Table 3.4 cont'd

Seq No.	Slab Thickness (in)	Girder Stiffness (in ⁴)	Span Length (ft)	Girder Spacing (ft)	Distribution Factor
173	7.25	3000000	130	7.50	1.238
174	7.25	3000000	130	10.00	1.489
175	7.25	3000000	130	16.00	2.046
176	7.25	3000000	200	3.50	0.712
177	7.25	3000000	200	5.00	0.909
178	7.25	3000000	200	7.50	1.147
179	7.25	3000000	200	10.00	1.336
180	7.25	3000000	200	16.00	1.643
181	7.25	7000000	20	3.50	0.985
182	7.25	7000000	20	5.00	1.194
183	7.25	7000000	20	7.50	1.663
184	7.25	7000000	20	10.00	1.996
185	7.25	7000000	20	16.00	2.743
186	7.25	7000000	64	3.50	0.775
187	7.25	7000000	64	5.00	1.085
188	7.25	7000000	64	7.50	1.574
189	7.25	7000000	64	10.00	1.935
190	7.25	7000000	64	16.00	2.675
191	7.25	7000000	130	3.50	0.723
192	7.25	7000000	130	5.00	0.974
193	7.25	7000000	130	7.50	1.323
194	7.25	7000000	130	10.00	1.644
195	7.25	7000000	130	16.00	2.297
196	7.25	7000000	200	3.50	0.722
197	7.25	7000000	200	5.00	0.944
198	7.25	7000000	200	7.50	1.202
199	7.25	7000000	200	10.00	1.414
200	7.25	7000000	200	16.00	1.853
201	12.00	10000	20	3.50	0.591
202	12.00	10000	20	5.00	0.774
203	12.00	10000	20	7.50	1.073
204	12.00	10000	20	10.00	1.310
205	12.00	10000	20	16.00	1.571
206	12.00	10000	64	3.50	0.549
207	12.00	10000	64	5.00	0.622
208	12.00	10000	64	7.50	0.781
209	12.00	10000	64	10.00	0.903
210	12.00	10000	64	16.00	1.151
211	12.00	10000	130	3.50	0.544
212	12.00	10000	130	5.00	0.612
213	12.00	10000	130	7.50	0.697
214	12.00	10000	130	10.00	0.778
215	12.00	10000	130	16.00	0.922

Table 3.4 cont'd

Seq No.	Slab Thickness (in)	Girder Stiffness (in ⁴)	Span Length (ft)	Girder Spacing (ft)	Distribution Factor
216	12.00	10000	200	3.50	0.543
217	12.00	10000	200	5.00	0.610
218	12.00	10000	200	7.50	0.686
219	12.00	10000	200	10.00	0.747
220	12.00	10000	200	16.00	0.850
221	12.00	50000	20	3.50	0.711
222	12.00	50000	20	5.00	0.927
223	12.00	50000	20	7.50	1.288
224	12.00	50000	20	10.00	1.543
225	12.00	50000	20	16.00	1.901
226	12.00	50000	64	3.50	0.659
227	12.00	50000	64	5.00	0.755
228	12.00	50000	64	7.50	0.922
229	12.00	50000	64	10.00	1.092
230	12.00	50000	64	16.00	1.326
231	12.00	50000	130	3.50	0.651
232	12.00	50000	130	5.00	0.699
233	12.00	50000	130	7.50	0.783
234	12.00	50000	130	10.00	0.879
235	12.00	50000	130	16.00	1.033
236	12.00	50000	200	3.50	0.651
237	12.00	50000	200	5.00	0.688
238	12.00	50000	200	7.50	0.745
239	12.00	50000	200	10.00	0.809
240	12.00	50000	200	16.00	0.917
241	12.00	560000	20	3.50	0.814
242	12.00	560000	20	5.00	1.090
243	12.00	560000	20	7.50	1.553
244	12.00	560000	20	10.00	1.874
245	12.00	560000	20	16.00	2.515
246	12.00	560000	64	3.50	0.708
247	12.00	560000	64	5.00	0.908
248	12.00	560000	64	7.50	1.163
249	12.00	560000	64	10.00	1.376
250	12.00	560000	64	16.00	1.774
251	12.00	560000	130	3.50	0.688
252	12.00	560000	130	5.00	0.811
253	12.00	560000	130	7.50	0.990
254	12.00	560000	130	10.00	1.150
255	12.00	560000	130	16.00	1.346
256	12.00	560000	200	3.50	0.680
257	12.00	560000	200	5.00	0.762
258	12.00	560000	200	7.50	0.894

Table 3.4 cont'd

Seq No.	Slab Thickness (in)	Girder Stiffness (in ⁴)	Span Length (ft)	Girder Spacing (ft)	Distribution Factor
259	12.00	560000	200	10.00	1.028
260	12.00	560000	200	16.00	1.191
261	12.00	3000000	20	3.50	0.918
262	12.00	3000000	20	5.00	1.161
263	12.00	3000000	20	7.50	1.640
264	12.00	3000000	20	10.00	1.971
265	12.00	3000000	20	16.00	2.696
266	12.00	3000000	64	3.50	0.721
267	12.00	3000000	64	5.00	0.972
268	12.00	3000000	64	7.50	1.340
269	12.00	3000000	64	10.00	1.664
270	12.00	3000000	64	16.00	2.303
271	12.00	3000000	130	3.50	0.718
272	12.00	3000000	130	5.00	0.919
273	12.00	3000000	130	7.50	1.148
274	12.00	3000000	130	10.00	1.328
275	12.00	3000000	130	16.00	1.637
276	12.00	3000000	200	3.50	0.703
277	12.00	3000000	200	5.00	0.867
278	12.00	3000000	200	7.50	1.070
279	12.00	3000000	200	10.00	1.232
280	12.00	3000000	200	16.00	1.420
281	12.00	7000000	20	3.50	0.953
282	12.00	7000000	20	5.00	1.180
283	12.00	7000000	20	7.50	1.654
284	12.00	7000000	20	10.00	1.986
285	12.00	7000000	20	16.00	2.725
286	12.00	7000000	64	3.50	0.714
287	12.00	7000000	64	5.00	1.023
288	12.00	7000000	64	7.50	1.448
289	12.00	7000000	64	10.00	1.803
290	12.00	7000000	64	16.00	2.501
291	12.00	7000000	130	3.50	0.726
292	12.00	7000000	130	5.00	0.951
293	12.00	7000000	130	7.50	1.203
294	12.00	7000000	130	10.00	1.413
295	12.00	7000000	130	16.00	1.863
296	12.00	7000000	200	3.50	0.716
297	12.00	7000000	200	5.00	0.913
298	12.00	7000000	200	7.50	1.133
299	12.00	7000000	200	10.00	1.301
300	12.00	7000000	200	16.00	1.537

Table 3.5. Representative AASHTO LRFD distribution factors (partial reprint from AASHTO Table 4.6.2.2b-1) (AASHTO, 2002)

Types of Beams	Applicable Cross-Section from Table 4.6.2.2.1-1	Distribution Factors	Range of Applicability
Concrete Deck, Filled Grid, or Partially Filled Grid on Steel or Concrete Beams, T- and Double T-Sections	a, e, k and also l, j if sufficiently connected to act as a unit	<p>One Design Lane Loaded:</p> $0.06 + \left(\frac{S}{14}\right)^{0.4} \left(\frac{S}{L}\right)^{0.3} \left(\frac{K_g}{12.0Lt_s^3}\right)^{0.1}$ <p>Two or More Design Lanes Loaded:</p> $0.075 + \left(\frac{S}{9.5}\right)^{0.6} \left(\frac{S}{L}\right)^{0.2} \left(\frac{K_g}{12.0Lt_s^3}\right)^{0.1}$	$3.5 \leq S \leq 160$ $4.5 \leq t_s \leq 12.0$ $20 \leq L \leq 240$ $N_b \geq 4$
		<p>use lesser of the values obtained from the equation above with $N_b = 3$ or the lever rule</p>	<p>$N_b = 3$</p>

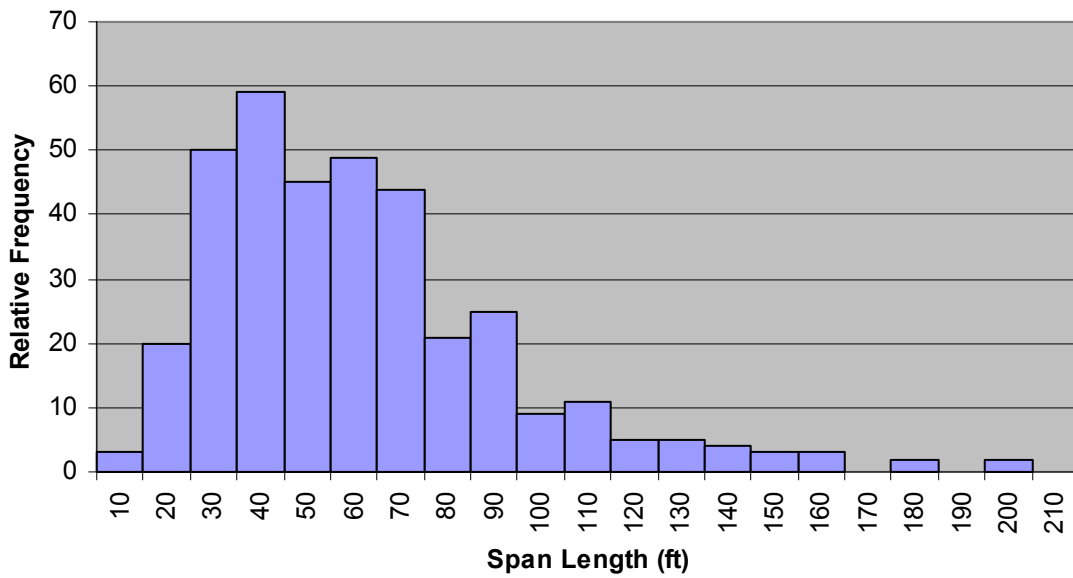


Figure 3.1. Histogram of relative frequency for span length

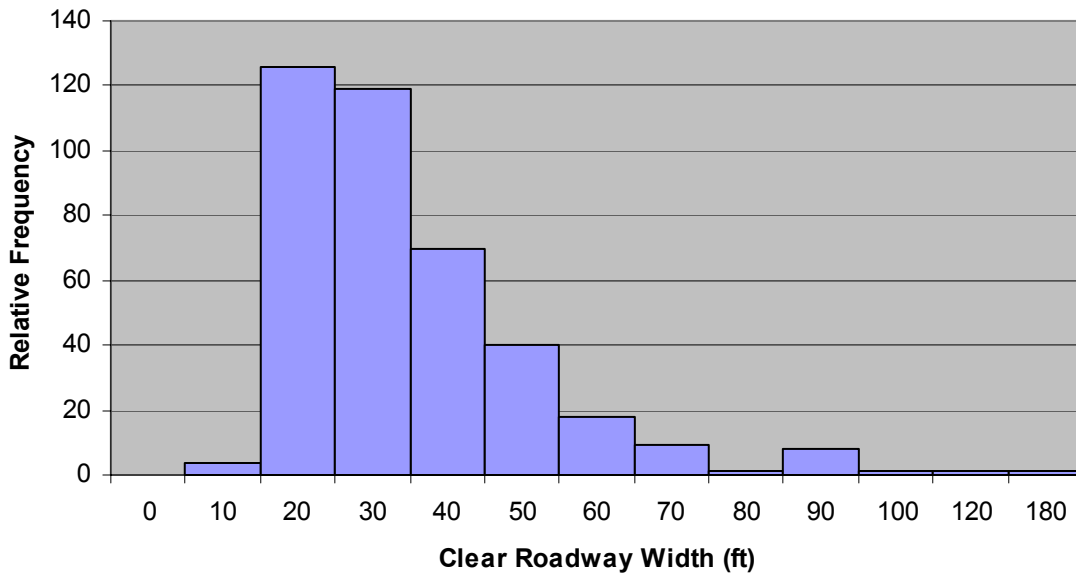


Figure 3.2. Histogram of relative frequency for clear roadway width

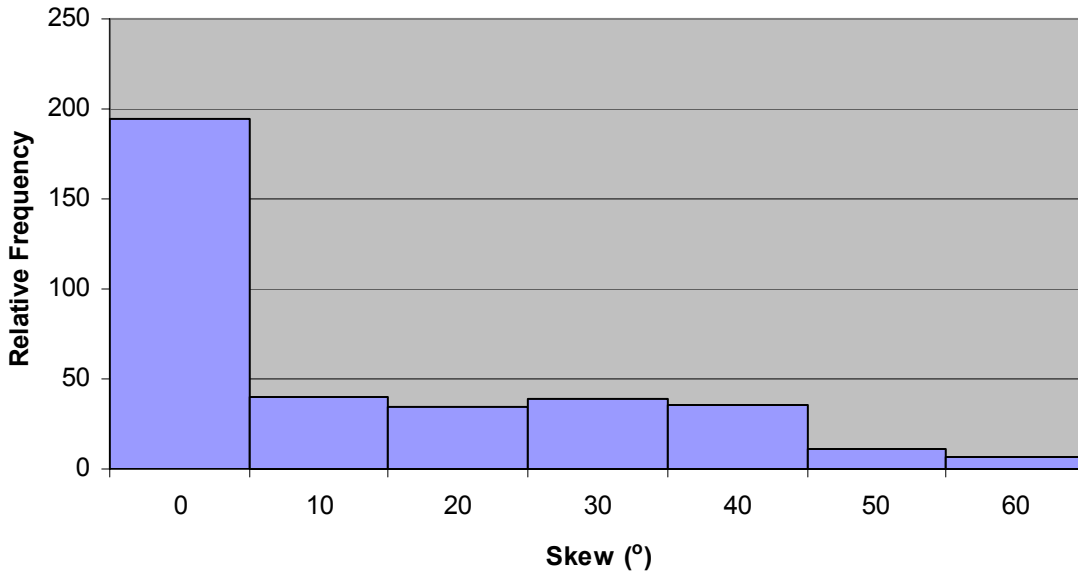


Figure 3.3. Histogram of relative frequency for skew

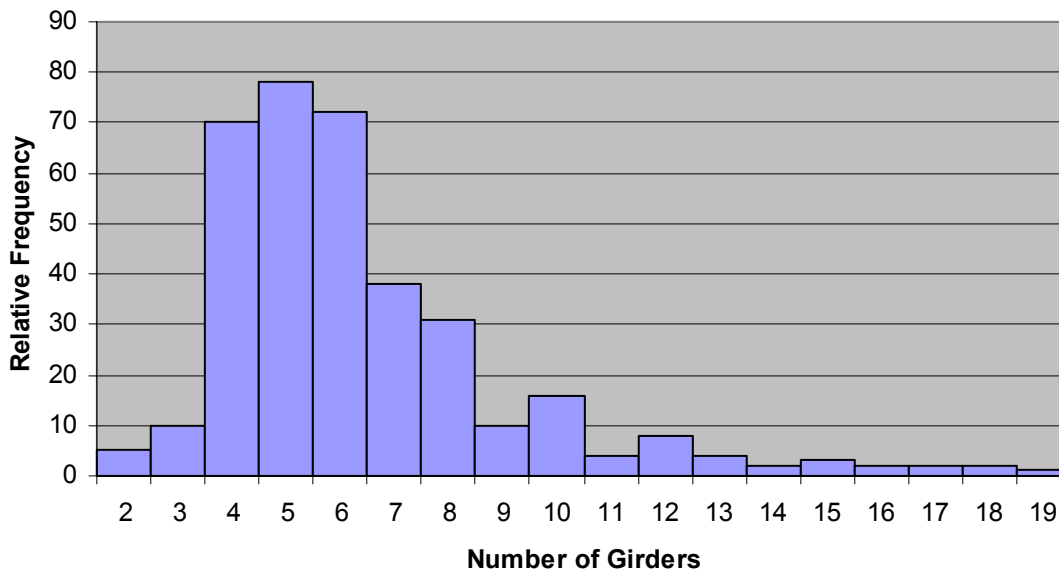


Figure 3.4. Histogram of relative frequency for number of girders



Figure 3.5. Histogram of relative frequency for girder spacing

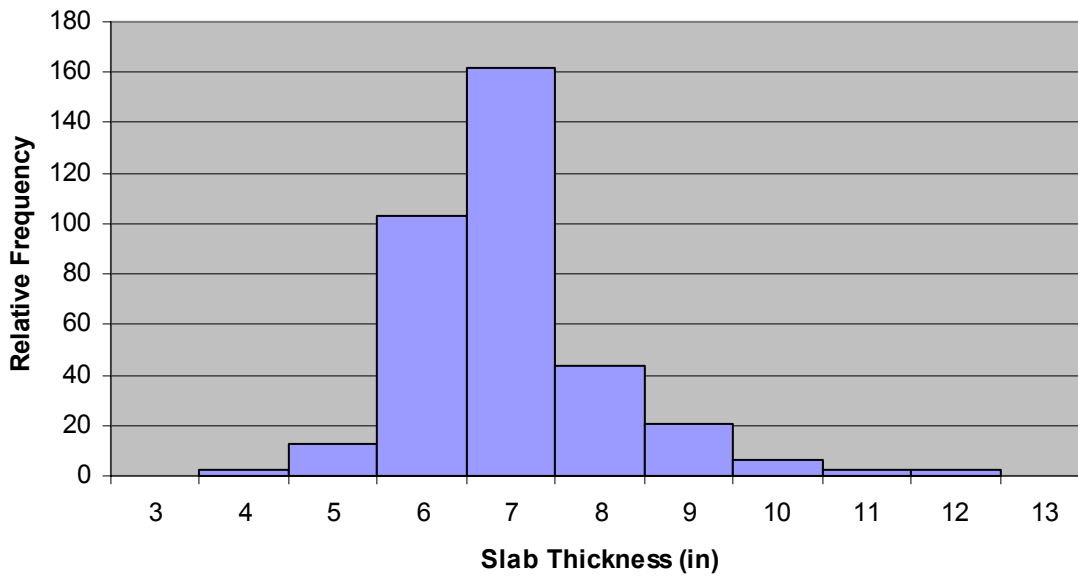


Figure 3.6. Histogram of relative frequency for slab thickness

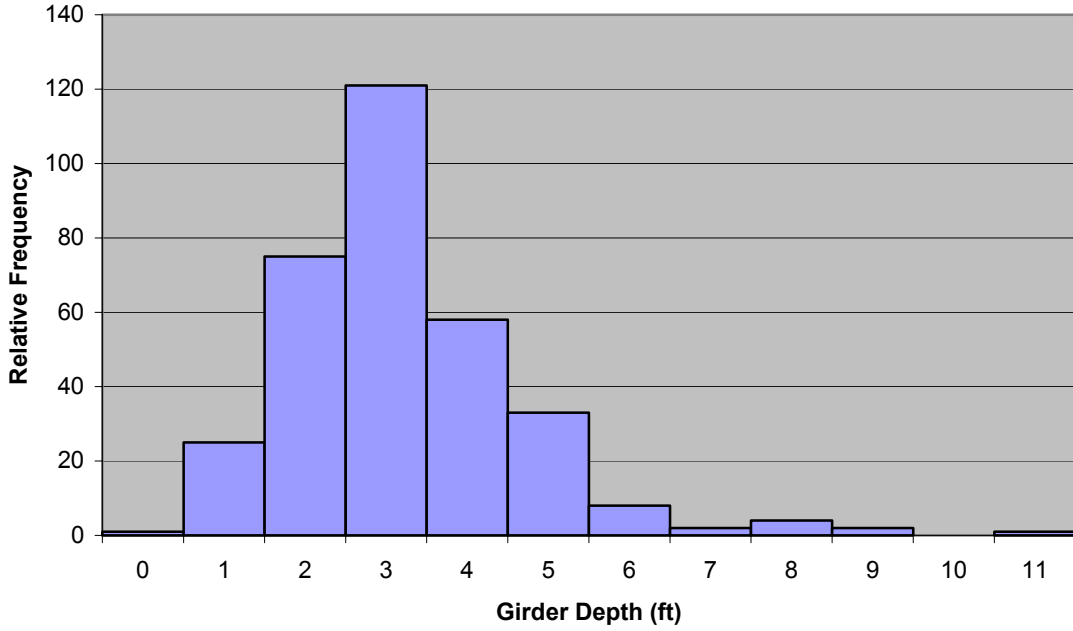


Figure 3.7. Histogram of relative frequency for girder depth

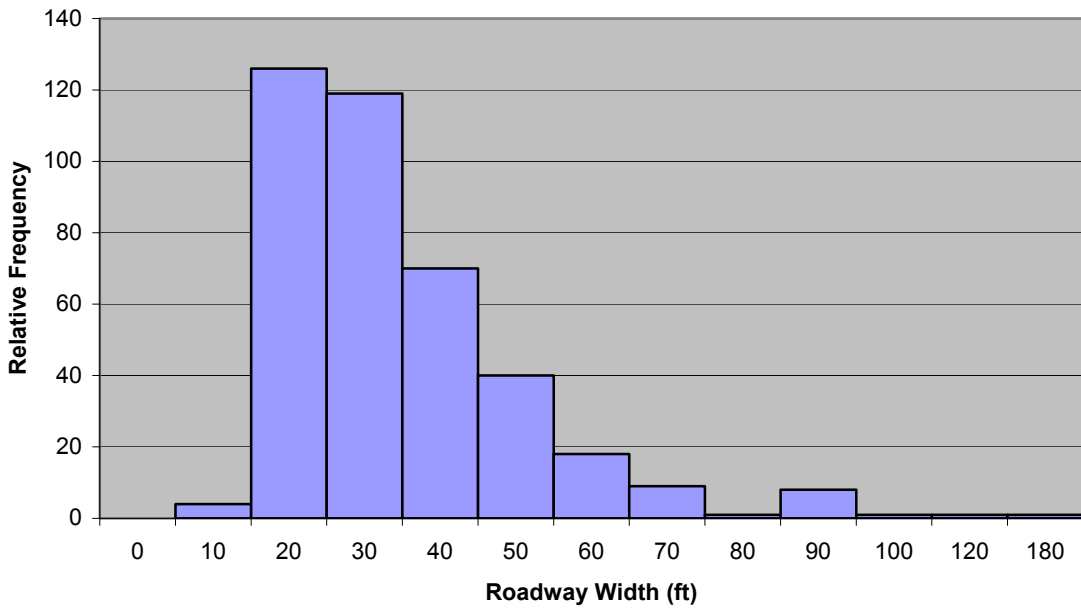


Figure 3.8. Histogram of relative frequency for roadway width (out-to-out)

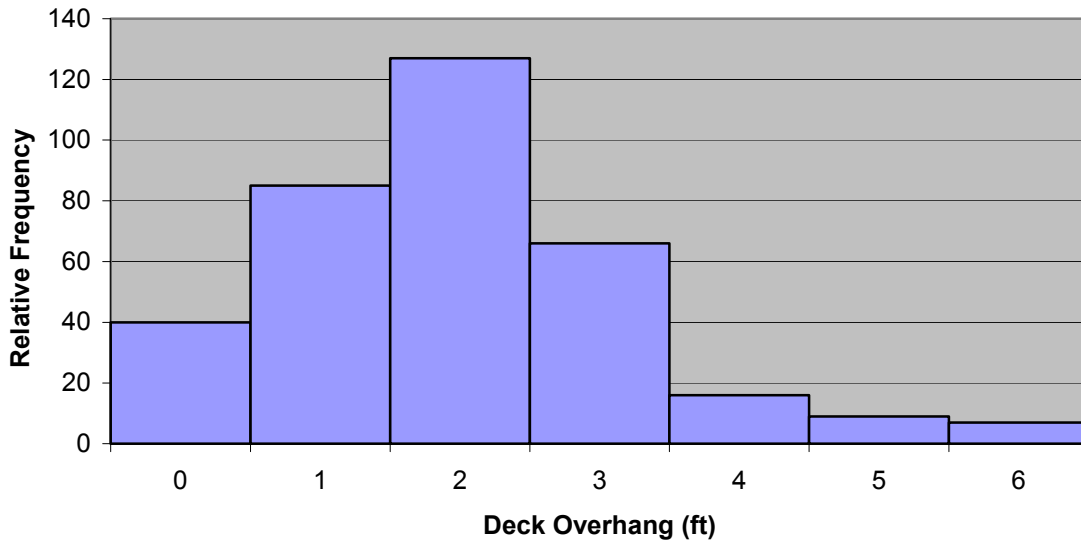


Figure 3.9. Histogram of relative frequency for deck overhang

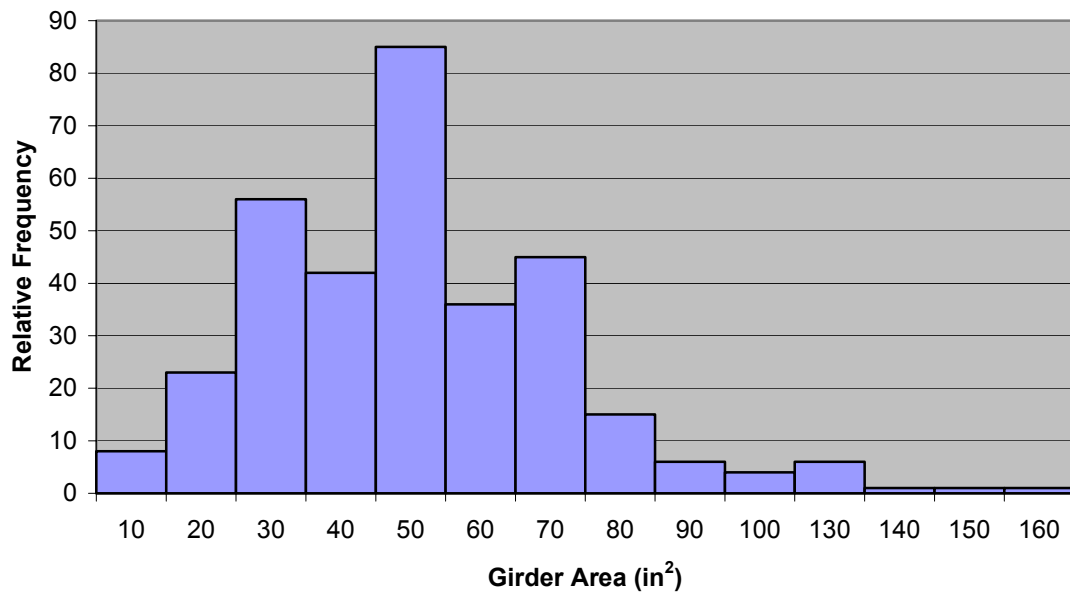


Figure 3.10. Histogram of relative frequency for girder area

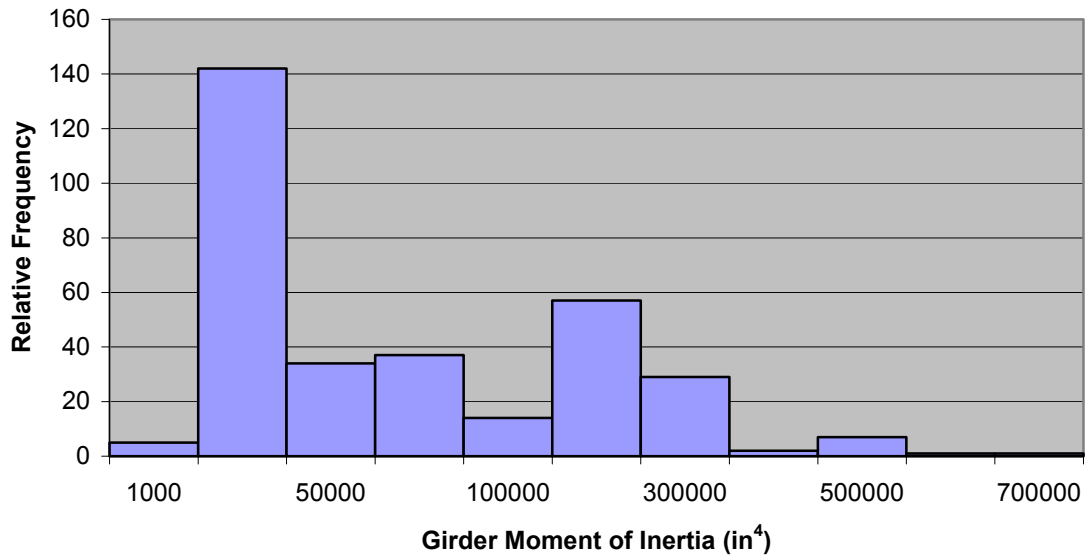


Figure 3.11. Histogram of relative frequency for girder moment of inertia

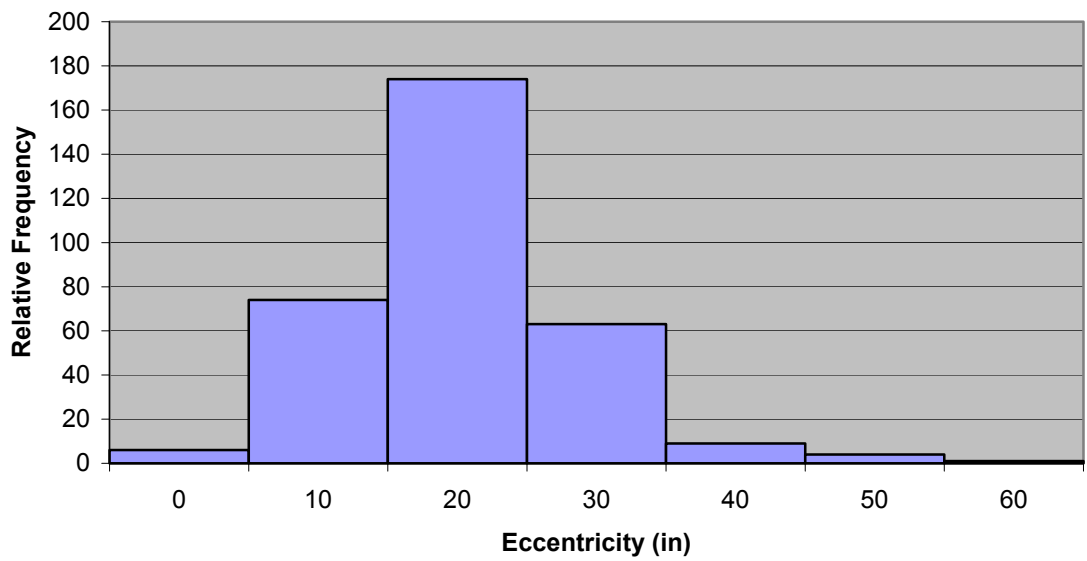


Figure 3.12. Histogram of relative frequency for eccentricity

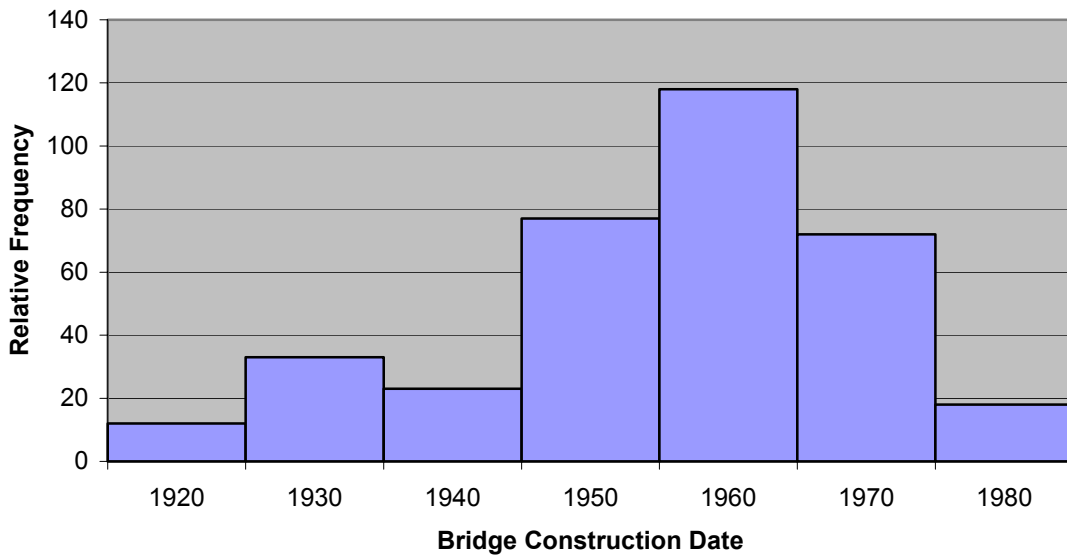


Figure 3.13. Histogram of relative frequency for bridge construction date

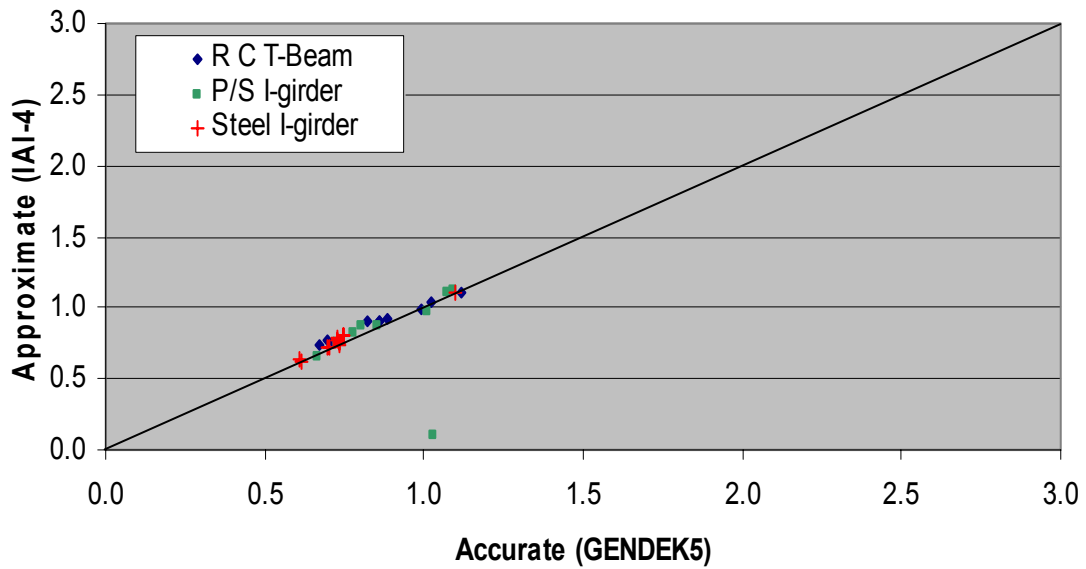


Figure 3.14. Comparison of proposed distribution factors vs. analytical results

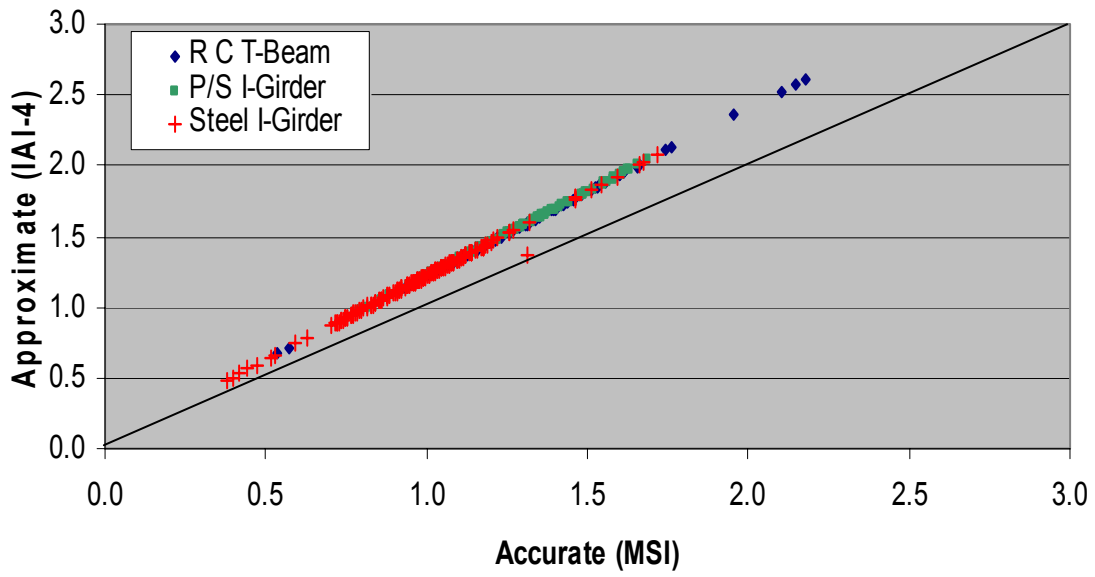


Figure 3.15. Comparison of proposed distribution factors vs. MSI results

CHAPTER 4

COMPUTATION OF DISTRIBUTION FACTORS FOR SLAB-ON-STEEL GIRDER BRIDGES

4.1 Introduction

Literature gathered from previous research has provided many different procedures for computing live load distribution factors, which range from using bottom flange strains and stress to the summation of moments of each member of the system. This chapter presents several procedures developed and presented in archival literature for computing live load distribution factors. Analytical studies are also conducted to compare these procedures and example calculations are provided. The FEA tools used in the analytical studies are subsequently presented in Chapter 5. The bridge used for comparisons and examples is a Federal Highway Administration (FHWA) test bridge discussed by Moore et al. (1990). Finally, the results for each procedure are then presented in comparison to the current specifications.

4.2 Barker Method

Barker et al. (1999) used two different methods to compute live load distribution factors using elastic moments and bottom flange stresses. The first method for computing load distribution factors, based on elastic moments, is shown in Eqn. 4.1. This was developed by Bakht (1988) for research done for the Ministry of Transportation of Ontario. The second method, shown in Eqn. 4.2, used the bottom flange stress at

midspan of the girders along with the section moduli to compute load distribution factors.

Barker Method One:

$$Distribution\ Factor = \frac{2 \cdot M_i^{girder}}{\sum_{i=1}^n M_i^{girder}} \quad (Eqn. 4.1)$$

where M_i^{girder} = elastic moment of the girder

Barker Method Two:

$$Distribution\ Factor = \frac{2 \cdot (\sigma_i^{girder} * S_i^{ADIM})}{(\sigma_i^{girder} \cdot S_i^{ADIM}) + \sum (\sigma_i \cdot S_i)} \quad (Eqn. 4.2)$$

where σ_i^{girder} = measured stress at bottom flange
 S_i = analytical section modulus with design dimensions
 S^{ADIM} = analytical section modulus with measured dimensions

Barker uses three strain gauges, two placed in the web and one on the bottom flange, to fit a curve that represents a linear stress profile through a given cross section (Barker et al; 1999). The least squares method is used to fit the line to the experimental results and can be best described by the following equation.

$$\begin{bmatrix} \sum \sigma_i^2 & \sum \sigma_i \\ \sum \sigma_i & n \end{bmatrix} \cdot \begin{Bmatrix} a \\ b \end{Bmatrix} = \begin{Bmatrix} \sum d_i \sigma_i \\ \sum d_i \end{Bmatrix} \quad (Eqn. 4.3)$$

where σ_i = experimentally determined stress (ksi)
 d_i = depth from the bottom of bottom flange (in)
 a = slope of best fit line
 b = neutral axis (in)

Figure 4.1 shows the representative location of the strain gauges, as well as the location of the neutral axis, b . Solving Eqn. 4.3 gives the following equation for a distance from

the bottom flange (depth vs. stress value) to any given stress in the girder from the slope, a , and neutral axis, b , calculated in Eqn 4.3.

$$d_i = a \cdot \sigma_a + b \quad (\text{Eqn. 4.4})$$

σ_a = stress after compensating for axial stresses at the neutral axis

The elastic moment, M_i (Eqn. 4.8) can be calculated from breaking the load carrying mechanism into three parts: the steel girder bending about its own neutral axis (M_L), the reinforced concrete slab bending about its own neutral axis (M_u), and a couple, Na , that is a function of the amount of composite action between the concrete area and steel section (Na) (Barker, 1999). These representative equations are provided below in Eqns. 4.5 to 4.7, while Fig. 4.2 presents a graphical explanation of how the experimental stresses are transformed in the three components described above (Barker, 1999).

$$M_L = (\sigma_{bf} - \sigma_a) \cdot S_{stl} \quad (\text{Eqn. 4.5})$$

$$M_u = M_L \cdot \left(\frac{E_C \cdot I_C}{E_S \cdot I_S} \right) \quad (\text{Eqn. 4.6})$$

$$Na = (\sigma_a + A_{stl}) \cdot a \quad (\text{Eqn. 4.7})$$

$$M_i = M_L + M_u + Na \quad (\text{Eqn. 4.8})$$

σ_{bf} = bottom flange stress after compensating for axial stresses
 S_{stl} = section modulus of the steel alone
 E_c = modulus of elasticity for concrete
 E_s = modulus of elasticity for steel
 I_c = Moment of Inertia of the concrete alone
 I_s = Moment of Inertia of the steel section alone
 A_{stl} = Area of the steel section

After the elastic moments for each girder are computed, the load distribution factor can be calculated from Eqn. 4.1. The equation is multiplied by 2 times the number of lines of wheels used in the loading to present the distribution factors in terms of the number of trucks.

Equation 4.2 involves the use of bottom flange stresses along with the short-term section modulus using both the actual and design dimensions of each girder in the system. The section modulus is computed from the following

$$S_i = \frac{I_b}{b} \quad (\text{Eqn. 4.9})$$

where I_i = moment of inertia
 b = distance from neutral axis of the section to extreme fiber.

The moment of inertia for the cross sections can be obtained from information already available from previous data reduction of the experimental results, with the axial corrected depth vs. stress curve, and the flexural stress equation $\sigma = \frac{Mc}{I}$ (Barker, 1999).

The equation for moment of inertia is presented as

$$I_i = -M_i \cdot a \quad (\text{Eqn. 4.10})$$

where M_i = elastic moment
 a = slope of the depth vs. stress curve.

From Eqn. 4.2, for the girder of interest, the bottom flange stress is multiplied by the actual dimensioned section modulus, S_{ADIM} . This value is then divided by the summation of the same stress and actual dimensioned section modulus along with the remaining stresses for the adjacent girder multiplied by their respective design dimensioned section modulus, S_i . The distribution factors are changed from line of wheels to trucks by multiplying by a factor of 2 times the number of lines of wheels used in the loading.

4.3 Stallings Method

Stallings and Yoo (1991) performed a series of experimental field tests on three short span steel I-girder bridges with one and two lanes loaded to help evaluate the load capacity of the bridges and to assess the behavior of these bridges. One aspect investigated in this study was the computation of load distribution and the comparison to code specified equations. Equation 4.11, written in terms of bottom flange strain, was developed to compute the load distribution factor from recorded data taken in the experimental testing of the three bridges.

$$Distribution\ Factor = \frac{(n \cdot \varepsilon_i)}{\left(\sum_{i=1}^k \varepsilon_i \cdot w_i \right)} \quad (Eqn. 4.11)$$

n = number of wheel lines applied during loading

ε_i = strain at the midspan of the bottom flange of the i^{th} girder

w_i = ratio of the girder section modulus of the i^{th} girder to girder section modulus of a typical interior girder

The load distribution factor was computed from Eqn. 4.11 by multiplying the number of wheel lines applied during the loading with the bottom flange strain recorded from the girder of interest. This was then divided by the summation of bottom flange strain recorded the ratio of steel section moduli for each girder.

4.4 Bakht Method

Bakht presents a procedure similar to the AASHTO Standard Specification equation of $\frac{S}{D_{df}}$, where S is the girder spacing and D_{df} is the design factor associated with the type of bridge superstructure. The design factor, D_{df} , can be computed using Bakht's procedure from bottom flange strains recorded at the location of maximum moment due to the applied loading. The procedure described below was utilized in the development of the live load distribution factors adopted in Ontario Highway Bridge Design Code (OHBDC, 1991).

The design factors defined in the OHBDC were developed using an orthotropic plate procedure determining a design factor, D_{df} , based on the intensity of the transverse distribution of moments. The OHBDC equation for load distribution factors was developed from the parameters of girder spacing and span length. Additionally, the OHBDC incorporated a correction factor that was used to account for the number of lanes loaded, design lane width, and type of bridge superstructure.

The load distribution factor was calculated in this procedure from:

$$Distribution\ Factor = \frac{S}{D_{df}} \quad (Eqn. 4.12)$$

where S is the girder spacing (in units of length) and D_{df} is the design factor (in consistent units of length). The design factor is computed from Eqn. 4.13 by multiplying the girder spacing divided by number of lines of wheels applied during the loading with the summation of bottom flange stains recorded from experimental testing divided by the

recorded bottom flange strain of the girder of interest.

$$D_{df} = \left(\frac{S}{n} \right) \cdot \left(\frac{\sum \varepsilon_i}{\varepsilon_{\max}} \right) \quad (\text{Eqn. 4.13})$$

- D_{df} = design factor, ft
- S = girder spacing, ft
- n = number of lines of wheels applied during loading
- ε_{\max} = maximum strain created due to loading (at the loaded girder)
- ε_i = strain at the i^{th} girder

The calculation for the load distribution factor presented in Eqn. 4.12 can be completed upon the computation of the design factor provided in Eqn. 4.13.

4.5 Mabsout Method

Mabsout (1997) calculated live load distribution factors for a system of girders from the moment computed from a finite element analysis of the 3D bridge at a critical section divided by the moment computed from a line of wheels of an HS20 truck applied to a single girder, as analyzed in a typical 2D line girder analysis, as shown in Eqn. 4.14.

$$\text{Distribution Factor} = \frac{M^{FEA}}{M^{TRUCK}} \quad (\text{Eqn. 4.14})$$

The FEA moments for a proposed critical effective section, consisting of elements from the deck, and girder web and flanges, was used to compute the total moment of the section, M^{FEA} . The deck was assumed to have an effective width of $\frac{S}{2}$ on each adjacent side of the girder of interest. The moments were computed, using Eqn. 4.15, for every element included in the critical section.

$$M^{FEA} = \sum_{i=1}^n \sigma_i \cdot Area_i \cdot c_i \quad (\text{Eqn. 4.15})$$

where σ_i = stress obtained from the FEA output for i^{th} element
 $Area_i$ = area of the i^{th} element
 c_i = distance of the neutral axis to the i^{th} element

As shown in Eqn. 4.15, the FEA moment was computed for each element in the critical section by multiplying the stress in the element found in the FEA output data, σ , the area of the element, and the distance of the element from the neutral axis, c . The neutral axis was determined by locating the point of zero stress from the stress profile provided in the FEA output data. From the summation of these moments the total moment for the FEA model, M^{FEA} , was computed for the assumed effective section. The moment, M^{TRUCK} , is determined by calculating the maximum moment for a line girder subjected to a single line of wheels (see Fig. 4.7). Equation 4.14 is used to compute the load distribution factor for the FEA bridge model by dividing the previously calculated M^{FEA} with M^{TRUCK} .

4.6 Example Calculations

This section uses results from the analysis of an AISI-FHWA scale model laboratory bridge (Moore et al., 1990) to demonstrate the calculation of the live load distribution factors using the previously described methods.

The AISI-FHWA bridge consists of a 2-span continuous structure with equal 56 ft spans. The cross section of the 19 ft. – 2 ³/₈ in. wide bridge is comprised of a 4 in. concrete deck supported by 3 steel plate girders with 6 ft. – 9 ⁵/₈ in. spacing and 2 ft. – 9

$\frac{9}{16}$ in. overhangs. Figure 4.5 shows a cross-section for the AISI-FHWA bridge and Figs. 4.5 and 4.6 show the elevation and girder sizes respectively.

The loading case used to demonstrate the previously described distribution factor procedures consists of 3 simulated lanes (see Fig. 4.6) each comprised of two 16.6 kip wheel loads with an axle spacing of 2 ft. – $4\frac{13}{16}$ in. In the actual testing, the loading was performed by moving a single 16.6 kip load to each of the wheel load positions shown in Fig. 4.6 and superposition was used to assess the experimental distribution factors. In the FEA modeling, all wheel loads were applied simultaneously. The 3-lane loaded load pattern was applied at the 0.4L point with the stress/strain data from the 0.4L point used to determine the maximum positive bending distribution factor and at the 0.6L point with the stress/strain data from 5 ft. in of the 1.0L point used to determine the maximum negative bending distribution factor.

The analytical results used in these calculations were obtained using the commercial packages FEMap (1999) and ABAQUS v.6.3.1 (2002) to conduct a refined 3D analytical model of the example bridge. A detailed discussion of this FEA modeling along with extensive model validation studies using both experimental data along with the analytical results of others is presented subsequently in Chapter 5.

4.6.1 Barker Method 1 for Positive Moment Region

The elastic moment calculation requires an equation for the location of the neutral axis. The equation is derived from Eqn. 4.3 using the following matrix with all the data

needed to solve this matrix found in Table 4.1.

$$\begin{bmatrix} \sum \sigma_i^2 & \sum \sigma_i \\ \sum \sigma_i & n \end{bmatrix} \cdot \begin{Bmatrix} a \\ b \end{Bmatrix} = \begin{Bmatrix} \sum d_i \sigma_i \\ \sum d_i \end{Bmatrix} \quad (\text{Eqn. 4.3})$$

Solving this matrix gives the following equation

$$d_i = a \cdot \sigma_a + b \quad (\text{Eqn. 4.4})$$

$$d_i = 3.45875 \cdot \sigma_a + 4.6117.$$

By setting σ_a equal to zero, the neutral axis can be determined for the girder of interest.

$$y_1 = 4.6117 \text{ in}$$

The neutral axis location is now used to calculate a (the distance of from the bottom of the bottom flange to the neutral axis) along with the stress and the neutral axis and area of the steel section for use in Eqn. 4.7 to compute the N_a value. Equation 4.5 is computed for M_L using the stress obtained at the bottom flange minus the stress at the neutral axis multiplied by the steel section modulus from Eqn. 4.9. The moment caused by the reinforced concrete slab bending about its own neutral axis, M_u can be calculated by multiplying the corresponding M_L computed in Eqn. 4.5 by the ratio of the modulus of elasticity and moment of inertia for the concrete over steel as seen in Eqn. 4.7. The elastic moment, M_i , of each girder is then computed by the summation of M_L , M_u , and N_a .

Girder 1:

$$M_L = (18.254 - 0) \cdot 102 = 1861.9 \text{ in-kips} \quad (\text{Eqn. 4.5})$$

$$M_u = 1861.9 \cdot \left(\frac{4000 \cdot 256}{29000 \cdot 427.4} \right) = 153.8 \text{ in-kips} \quad (\text{Eqn. 4.6})$$

$$N_a = (0 \cdot 11.25) \cdot 4.6117 = 0 \text{ in-kips} \quad (\text{Eqn. 4.7})$$

$$M_i = 1861.9 + 153.8 + 0 = 2016 \text{ in-kips} \quad (\text{Eqn. 4.8})$$

Girder 2:

$$M_L = (25.1715 - 0) \cdot 102 = 2567.5 \text{ in-kips} \quad (\text{Eqn. 4.5})$$

$$M_u = 2567.5 \cdot \left(\frac{4000 \cdot 256}{29000 \cdot 427.4} \right) = 212.1 \text{ in-kips} \quad (\text{Eqn. 4.6})$$

$$N_a = (0 \cdot 11.25) \cdot 4.6117 = 0 \text{ in-kips} \quad (\text{Eqn. 4.7})$$

$$M_i = 2567.5 + 212.1 + 0 = 2780 \text{ in-kips} \quad (\text{Eqn. 4.8})$$

Girder 3:

$$M_L = (25.1715 - 9.8956) \cdot 102 = 1558.1 \text{ in-kips} \quad (\text{Eqn. 4.5})$$

$$M_u = 1558.1 \cdot \left(\frac{4000 \cdot 256}{29000 \cdot 427.4} \right) = 128.7 \text{ in-kips} \quad (\text{Eqn. 4.6})$$

$$N_a = (9.8956 \cdot 11.25) \cdot 4.6117 = 513.4 \text{ in-kips} \quad (\text{Eqn. 4.7})$$

$$M_i = 1558.1 + 128.7 + 513.4 = 2200 \text{ in-kips} \quad (\text{Eqn. 4.8})$$

The total girder moments for each respective girder may now be incorporated into Eqn.

4.3 to determine the maximum positive bending live load distribution factor

$$\text{Distribution Factor} = \frac{2780}{(2016 + 2780 + 2200)} \cdot 2 \cdot 3 \quad (\text{Eqn. 4.1}).$$

The distribution factor for the positive moment region using Barker Method 1 is

Distribution Factor = 2.384.

4.6.2 Barker Method 1 for Negative Moment Region

The computation of M_L , M_u , N_a , and y_1 is completed using the procedures described in Section 4.6.1 as shown below.

$$d_i = 3.45875 \cdot \sigma_a + 4.6117 \quad (\text{Eqn. 4.4})$$

$$y_1 = 4.6117 \text{ in}$$

Girder 1:

$$M_L = (8.95 - 0) \cdot 179 = 1602.1 \text{ in-kips} \quad (\text{Eqn. 4.5})$$

$$M_u = 1602.1 \cdot \left(\frac{4000 \cdot 256}{29000 \cdot 434.8} \right) = 130.1 \text{ in-kips} \quad (\text{Eqn. 4.6})$$

$$N_a = (0 \cdot 11.25) \cdot 4.6117 = 0 \text{ in-kips} \quad (\text{Eqn. 4.7})$$

$$M_i = 1602.1 + 130.1 + 0 = 1732 \text{ in-kips} \quad (\text{Eqn. 4.8})$$

Girder 2:

$$M_L = (13.338 - 0) \cdot 179 = 2387.5 \text{ in-kips} \quad (\text{Eqn. 4.5})$$

$$M_u = 2387.5 \cdot \left(\frac{4000 \cdot 256}{29000 \cdot 434.8} \right) = 193.9 \text{ in-kips} \quad (\text{Eqn. 4.6})$$

$$N_a = (0 \cdot 11.25) \cdot 4.6117 = 0 \text{ in-kips} \quad (\text{Eqn. 4.7})$$

$$M_i = 2387.5 + 193.9 + 0 = 2581 \text{ in-kips} \quad (\text{Eqn. 4.8})$$

Girder 3:

$$M_L = (8.95 - 0) \cdot 179 = 1602.1 \text{ in-kips} \quad (\text{Eqn. 4.5})$$

$$M_u = 1602.1 \cdot \left(\frac{4000 \cdot 256}{29000 \cdot 434.8} \right) = 130.1 \text{ in-kips} \quad (\text{Eqn. 4.6})$$

$$N_a = (0 \cdot 25.406) \cdot 4.6117 = 0 \text{ in-kips} \quad (\text{Eqn. 4.7})$$

$$M_i = 1602.1 + 130.1 + 0 = 1732 \text{ in-kips} \quad (\text{Eqn. 4.8})$$

The total girder moments for each respective girder may now be incorporated into Eqn. 4.3 to determine the maximum positive bending live load distribution factor

$$\text{Distribution Factor} = \frac{2581}{(1732 + 2581 + 1732)} \cdot 2 \cdot 3 \quad (\text{Eqn. 4.1}).$$

The distribution factor for the negative moment region using the Barker Method 1 is

Distribution Factor = 2.562.

4.6.3 Barker Method 2 for Positive Moment Region

The second procedure described in Section 4.2 was used to calculate the load distribution factor in this example for the positive moment region with the use of Eqn. 4.9 and 4.2. The section modulus of each section was computed in Eqn. 4.9 and stress values from Table 6.1 are applied to Eqn. 4.9 along with previously mentioned section moduli of each girder

$$\text{Distribution Factor} = \frac{2 \cdot (25.1715 \cdot 149)}{(25.1715 \cdot 149) + \sum ((18.2540 \cdot 150) \cdot 2)} \quad (\text{Eqn. 4.2}).$$

$$\text{Distribution Factor} = 0.813$$

This distribution factor must then be multiplied by the number of trucks applied during the loading, as seen on Fig. 4.4.

$$\text{Distribution Factor} = 3 \text{ trucks} \cdot 0.850$$

The distribution factor for the positive moment region using the Barker Method 2 is

Distribution Factor = 2.439.

4.6.4 Barker Method 2 for Negative Moment Region

The same procedure was followed as described in Section 4.6.3 for computation

of load distribution factors for the negative moment region using Equations 4.9 and 4.2.

$$\text{Distribution Factor} = \frac{2 \cdot (-13.338 \cdot 610)}{(-13.338 \cdot 610) + \sum ((-8.95 \cdot 615) \cdot 2)} \quad (\text{Eqn. 4.2})$$

$$\text{Distribution Factor} = 0.850$$

Again, the distribution factor computed must again be multiplied by the number of trucks applied during the loading.

$$\text{Distribution Factor} = 3 \text{ trucks} \cdot 0.850$$

The distribution factor for the negative moment region using Barker Method 2 is

Distribution Factor = 2.550.

4.6.5 Stallings Method for Positive Moment Region

The load distribution factor is computed using the Stallings procedure with the use of Eqn. 4.10 described in Section 4.3 using bottom-flange strains obtained for the girders and the results are found in Table 4.1. Figure 4.4 shows three lanes of trucks are applied for this loading case, creating six wheel lines this particular bridge. All exterior and interior girders have the same cross-section provided in Fig. 4.3, therefore, the ratio of the girder section modulus of the i^{th} girder to the section modulus of the interior girder is equal to one. The distribution factor can now be computed from Eqn. 4.11 as

demonstrated below

$$\text{Distribution Factor} = \frac{(6 \cdot 0.0009416)}{\left(\sum (0.0006632 + 0.0009416 + 0.0006632) \right)} \quad (\text{Eqn. 4.11}).$$

The distribution factor for the positive moment region using the Stallings Method is:

Distribution Factor = 2.491

4.6.6 Stallings Method for Negative Moment Region

Using the same procedures as described in Section 4.6.5 and Equation 4.11, the load distribution factor for the negative moment region using the Stalling procedure is

$$\text{Distribution Factor} = \frac{(6 \cdot 0.0001487)}{\left(\sum (0.0001004 + 0.0001487 + 0.0001000) \right)} \quad (\text{Eqn. 4.11}).$$

The distribution factor for the negative bending region using the Stallings Method is

Distribution Factor = 2.556.

4.6.7 Bakht Method for Positive Moment Region

Equation 4.13 given in Section 4.4 computes the design factor girder spacing, number of wheel lines applied during the loading, and bottom-flange strains, similar to the Stallings procedure described in Section 4.6.5. The first parameter, $\frac{S}{n}$, can be

computed by taking the girder spacing found in Fig 4.3 and dividing it by an the number of wheel lines applied for the loading. The summation of recorded strains for each girder is divided by the strain of the girder of interest, and this terms are then multiplied together to calculate the load distribution applied the structure, as shown below using Eqn. 4.13

$$D_{df} = \left(\frac{6.8021}{6} \right) \cdot \left(\frac{\sum (0.0006632 + 0.0009416 + 0.0006632)}{0.0009416} \right) \quad (\text{Eqn. 4.13})$$

$$D_{df} = 2.731 \text{ ft.}$$

The distribution factor is the calculated using the using Eqn. 4.11 where S is the girder spacing and the design value, D_{df} , was solved previously. Equation 4.12 yields

$$\text{Distribution Factor} = \frac{S}{D_{df}} \quad (\text{Eqn. 4.12})$$

$$\text{Distribution Factor} = \frac{6.8021 \text{ ft}}{2.731 \text{ ft}}$$

The distribution factor for the positive moment region using the Bakht Method is

Distribution Factor = 2.491.

4.6.8 Bakht Method for Negative Moment Region

The procedure for the negative moment region utilizing the Bakht procedure is identical to the described calculation described in Section 4.6.7, and using Eqns. 4.12 and 4.13

$$D_{df} = \left(\frac{6.8021}{6} \right) \cdot \left(\frac{\sum (0.0001004 + 0.0001487 + 0.0001000)}{0.001487} \right) \quad (\text{Eqn. 4.13})$$

$$D_{df} = 2.662.$$

This distribution factor Eqn. 4.12 yields

$$\text{Distribution Factor} = \frac{S}{D_{df}} \quad (\text{Eqn. 4.12})$$

$$\text{Distribution Factor} = \frac{6.8021 \text{ ft}}{2.662 \text{ ft}}$$

The distribution factor for the negative moment region using the Bakht Method is:

Distribution Factor = 2.556.

4.6.9 Mabsout Method for Positive Bending Region

The Mabsout Method computes the distribution factor by summing the moments of slab, flange, and web sections. Using Eqn. 4.15, the moment of each element is computed by multiplying the stress values obtained from FEA output by the area of the element and the distance from the neutral axis as shown in Table 4.2 for every element in the proposed effective section. The moments were summed to obtain the total moment on the section, M^{FEA} , caused by the applied loading. CONSYS (2000) was used to determine the maximum moment, M^{TRUCK} , applied to a girder by one line of wheels from the truck used. The calculated moments are

$$M^{FEA} = 8708 \text{ in-kips}$$

$$M^{TRUCK} = 4147 \text{ in-kips.}$$

The distribution factor is computed by inserting the calculated values into Eqn. 4.14

$$\text{Distribution Factor} = \frac{8708}{4147} \quad (\text{Eqn. 4.14}).$$

Mabsout Method provides a distribution factor for the positive moment region of

Distribution Factor = 2.100.

4.6.10 Mabsout Method for Negative Moment Section

The same procedure as described in Section 4.6.11 is used along with Eqn. 4.15 to determine the load distribution factor for the negative moment region.

$$M^{FEA} = 2948 \text{ in-kips}$$

$$M^{TRUCK} = 1278 \text{ in-kips}$$

Equation 4.13 yields the form

$$\text{Distribution Factor} = \frac{2948}{1278} \quad (\text{Eqn. 4.14}).$$

The distribution factor for the negative moment region using the Mabsout Method is

Distribution Factor = 2.308.

4.7 Comparisons

The previous sections in this chapter presented an overview of various methods developed to compute live load distribution factors from both experimental and analytical data. Further, example calculations were presented based on the controlled load testing

and subsequent analytical modeling of a large scale test conducted by the FHWA (Moore et al., 1990). Summary results for these comparisons are presented in Table 4.4. This table shows that the Barker methods 1 and 2, Stallings method, and the Bakht all predict relatively similar distribution factors while they are approximately 17% higher than the experimentally determined distribution factors. While the Mabsout method was found to produce a distribution factor that was within 7% of the experimental distribution factor, this procedure requires the use of an assumed effective section. As the Bakht procedure is relatively straightforward in its application, it is based on no assumed section properties, and has been used in the development and verification of the OHBDC distribution factors. This procedure will be employed in subsequent tasks in this study requiring the computation of live load distribution.

Table 4.1. Bottom-flange strains, stresses, and D values for AISI-FHWA bridge calculations

Positive Moment Data (0.4L)					
Girder	Strains (in/in)	Girder	Stresses (ksi)	Girder	d _i values (in)
1	0.0006632	1	18.2540	1	0.00
2	0.0009416	2	25.1715	2	0.00
3	0.0006632	3	18.2540	3	3.00
Negative Moment Data (1.0L)					
Girder	Strains (in/in)	Girder	Stresses (ksi)	Girder	d _i values (in)
1	0.0001004	1	-8.9500	1	0.00
2	0.0001487	2	-13.3380	2	0.00
3	0.0001000	3	-8.9500	3	2.00

Table 4.2. Mabsout method results showing the element stress, area, distance from neutral axis, and calculated moments for the positive moment region

	Stress (ksi)	Area (in ²)	c (in)	Moment (in-kips)
Slab Elements	-1.0314	23.05	-3.862	91.82
	-1.0492	24.00	-3.862	97.25
	-1.0756	24.00	-3.862	99.70
	-1.0984	24.00	-3.862	101.81
	-1.1493	24.00	-3.862	106.53
	-1.2247	23.19	-3.862	109.68
	-1.3166	23.19	-3.862	117.90
	-1.5204	22.50	-3.862	132.12
TF Elements	-0.7829	1.41	-1.737	1.91
	-1.2715	1.41	-1.737	3.11
Web Elements	0.6046	1.36	1.825	1.50
	6.7068	1.36	7.262	66.21
	12.5253	1.36	12.700	216.23
	18.3106	1.36	18.137	451.46
	24.2677	1.36	23.575	777.71
BF Elements	27.5948	4.50	25.857	3210.80
	26.8298	4.50	25.857	3121.80

Table 4.3. Mabsout method results showing the element stress, area, distance from neutral axis, and calculated moments for the positive moment region

	Stress (ksi)	Area (in²)	c (in)	Moment (in-kips)
Slab Elements	0.1793	23.05	3.649	15.08
	0.1780	24.00	3.649	15.59
	0.1795	24.00	3.649	15.72
	0.1843	24.00	3.649	16.14
	0.1934	24.00	3.649	16.94
	0.2080	23.19	3.649	17.60
	0.2336	23.19	3.649	19.77
	0.2720	22.50	3.649	22.33
	0.2264	23.19	3.649	19.16
	0.1921	23.19	3.649	16.26
	0.1686	24.00	3.649	14.76
	0.1501	24.00	3.649	13.15
	0.1356	24.00	3.649	11.88
	0.1238	24.00	3.649	10.85
	0.1143	23.05	3.649	9.62
TF Elements	0.4998	1.41	1.524	1.07
	0.5839	1.41	1.524	1.25
Web Elements	-0.4383	1.36	-1.467	0.87
	-1.9167	1.36	-6.904	17.99
	-3.8663	1.36	-12.342	64.87
	-5.4331	1.36	-17.779	131.31
	-8.6887	1.36	-23.217	274.22
BF Elements	-10.4254	4.50	-26.070	1223.04
	-8.5108	4.50	-26.070	998.44

Table 4.4. Results from example distribution factor calculations

Method of Analysis	0.4L Position	1.0L Position
FHWA Experimental Results	2.122	2.154
Barker Method 1	2.384	2.562
Barker Method 2	2.439	2.550
Stallings Method	2.491	2.556
Bakht Method	2.491	2.556
Mabsout Method	2.100	2.308

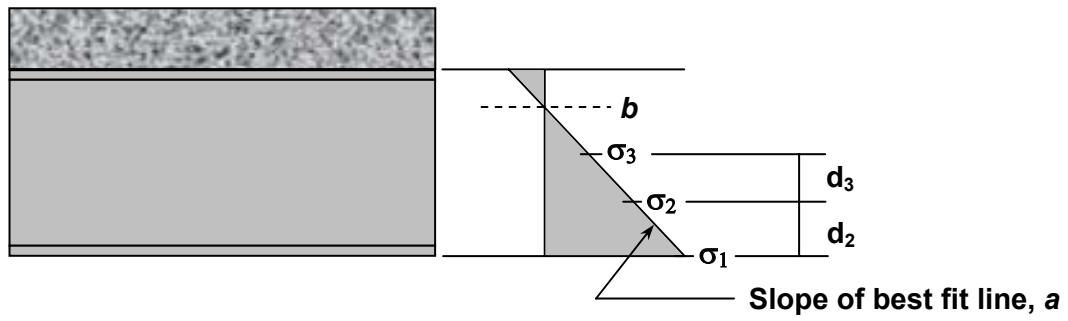


Figure 4.1. Diagram of variables found in Eqn. 4.3 for elastic moment calculation (Barker, 1999)

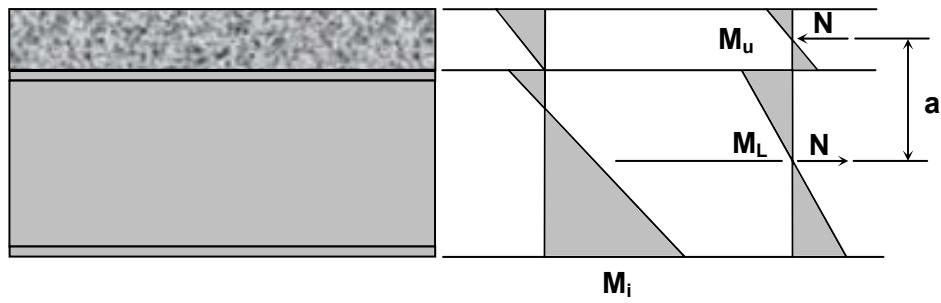


Figure 4.2. Diagram of the components used to compute elastic moment calculated in Eqns. 4.5 to 4.8 (Barker, 1999)

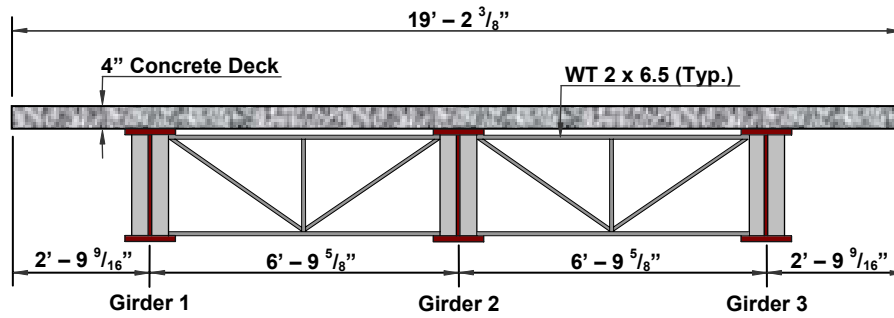


Figure 4.3. AISI- FHWA bridge cross-section

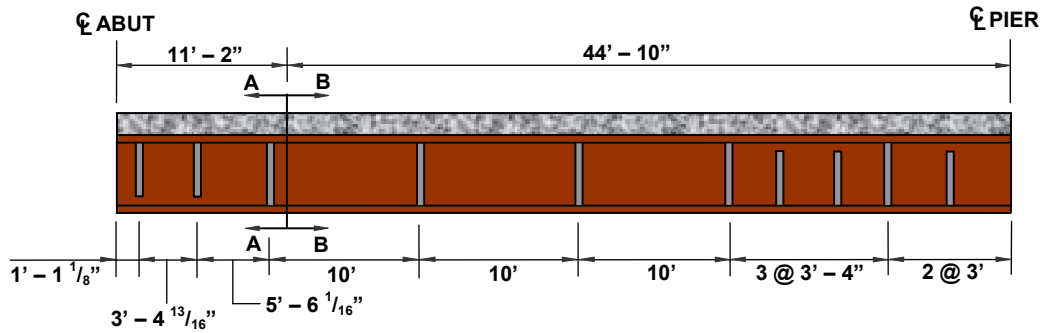


Figure 4.4. AISI-FHWA bridge plan view showing the location of flange transitions

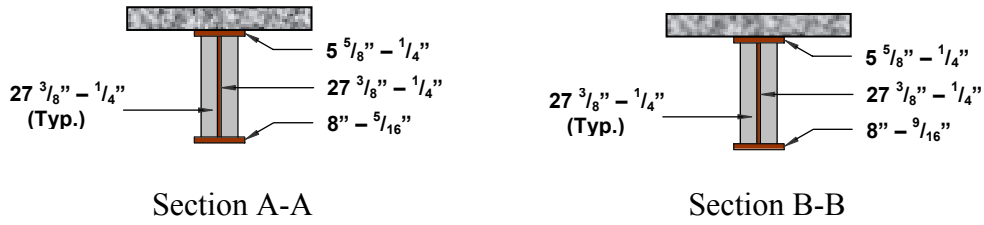


Figure 4.5. Cross section of girder profiles for the AISI-FHWA bridge

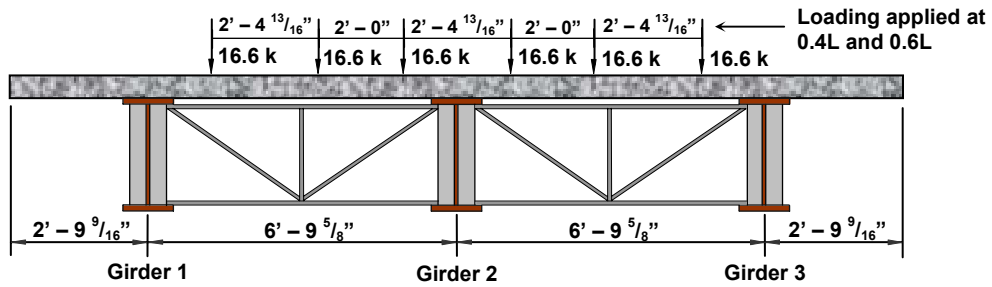


Figure 4.6. Transverse load positions for AISI-FHWA bridge

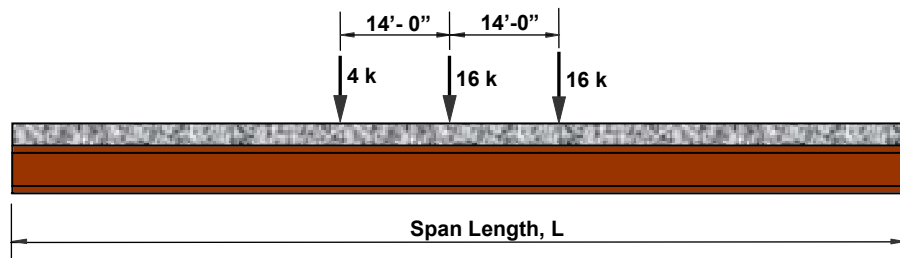


Figure 4.7. Hypothetical loading position of a line of wheels for the calculation of Mabsout M^{truck}

CHAPTER 5

MODELING OF COMPOSITE STEEL I-GIRDER BRIDGES: DESCRIPTION OF TOOLS AND VERIFICATION STUDIES

5.1 Introduction

The purpose of this chapter is to present a description of the FEA tools used in this study to perform elastic analyses of composite steel bridge superstructures for the purpose of determining live load distribution factors. Also presented in this chapter are several verification studies used in this work to assess the accuracy of the modeling tools employed in this study.

For this purpose, information was obtained through archival literature searches on four previously experimentally tested actual and scale model bridges. The bridges provided in this section represent a wide range of physical size, girder spacing, and span length. Bridges that were selected include a bridge tested by Newmark and Siess (1943), which was one of the test bridges used in the development of the original $\frac{S}{5.5}$ distribution factor. Also included is an AISI-FHWA test bridge subsequently analyzed by Tiedeman et al. (1993) which was used to demonstrate a variety of composite steel bridge performance characteristics including live load distribution. Additionally, there is a medium span length bridge tested by Bakht (1988) that was used to assess live load distribution in the OHBDC (1991) and a bridge tested by Stallings and Yoo (1991). The later was selected due to the completeness of information provided by the investigators and that they used this bridge to assess live load distribution in an actual bridge structure.

5.2 Description of FEA modeling tools

FEA modeling conducted in this study was performed using the commercial programs FEMap (1999), which is both a pre- and post-processor, and ABAQUS v.6.3-1 (2002) which serves as the analysis engine. These tools allow the investigator to construct a refined 3D model of the structure that may individually model girder flange and web plates as well as the reinforced concrete deck. Also, it may incorporate such items as parapets, diaphragms, and cross frame members, and may model the composite action between the reinforced concrete deck and the steel girders. Element selection in these studies include the use of 4-node reduced integration shell elements (ABAQUS S4R) for both the flanges and the web. Mesh discretization of the steel girder consisted of using 2 elements across the width of the flanges and 8 elements through the depth of the web. Steel cross frame members were modeled using a beam element, comprised of 5 elements per cross frame member. The reinforced concrete deck and any secondary stiffening elements, such as edge barriers, were modeled using a 20-node reduced integration solid element (ABAQUS C3D20R). Mesh discretization for the deck slab consisted of using approximately 1 element per square ft. The composite action between the steel girders and the slab was modeled using a multi point constraint (ABAQUS MPC Beam) spaced longitudinally approximately every foot. Figure 5.1 shows a typical FEA mesh for one of the bridges in this study. As all analyses were performed well within the elastic range for the bridges, typical elastic constitutive laws for both the steel and concrete were selected to represent the material response. For the parametric studies described in Chapter 6, all steel was assumed to be 50 ksi and the concrete was assumed

to be 4 ksi. Whereas, for the bridges modeled in this chapter, material properties reported by the specific investigators were incorporated in the respective models.

5.3 Verification Studies

5.3.1 Comparison with Newmark Bridges

Newmark and Siess (1943) performed extensive research on a laboratory bridge to assess load distribution and to calibrate the distribution factor used in the current AASHTO Standard Specification. In their research reports, Newmark and Siess (1943), they present both the experimentally determined deflections and live load distribution factors for several loading conditions.

The bridge was simply supported and had a span length of 15 feet. The cross-section consists of a 1.75 in. thick deck supported by 5 girders spaced at 1 ft. – 6 in., as shown in Fig. 5.2. Figure 5.3 shows an elevation of the bridge. Also shown in Figs. 5.1 and 5.2 is the loading used to assess deflections and live load distribution. The loading consisted of placing four 5-kip concentrated loads symmetrically about the centerline of the girder at 1 ft. – 6 in. on center.

Deflections were evaluated based on the information given by Newmark and Siess (1943) from the field testing results and compared to the FEA modeled bridge created for this study. The results are presented graphically in Fig. 5.4 which shows the deflection obtained on the bottom flange of each girder at the location of the load. A

summary of comparisons reveals only a 2.6% to 5.6% difference in deflection between the Newmark values and the WVU FEA.

Distribution factors were also evaluated from the data obtained from the FEA model and information provided by Newmark and Siess. Table 5.1 shows the distribution factors computed using the methods described in Chapter 4 for this particular bridge along with the experimental value calculated by Newmark and Siess and the AASHTO LRFD distribution factor. While the differences between the Barker procedures, Stallings procedure, and Bakht's procedure are approximately 22% lower than the experimental values and the value calculated using Mabsout's method is approximately 14% higher, due to the scale of the bridge it is felt that the values are well within reason and, coupled with subsequent comparisons, yield an acceptable level of accuracy for these methods. While there is only a 2% difference between the experimental distribution factor and that computed using the AASHTO LRFD equation, the geometry of this bridge fell well outside the range of applicability of the AASHTO LRFD equations and therefore no reasonable conclusions can be made as to the accuracy of this comparison.

5.3.2 Comparison with FHWA-AISI Model Bridge

In 1990, the Federal Highway Administration (FHWA) and the American Iron and Steel Institute (AISI) performed an extensive testing program on a two-span continuous plate girder bridge to assess a variety of steel bridge performance characteristics. Research done by Tiedeman et al. (1993) compared FEA model results

with actual bottom-flange stresses obtained in the testing of the FHWA-AISI Bridge. The research done in this report provides an opportunity to effectively compare stress values obtained using various FEA packages along with the experimentally obtained values.

A description of the superstructure geometry for the AISI-FHWA test bridge is provided in Section 4.6. Figures 4.1 through 4.3 show the cross section and elevation views presenting the dimensions for all members of the superstructure along with girder profiles for the respective girder transitions for this bridge. The loading cases evaluated by Tiedeman et al. (1993) consisted of simulated wheel loads being placed at the 0.44L point and the 0.65L point. These were done to maximize the negative and positive bending respectively. Points 0.44L and 0.66L were used as opposed to the theoretical points of 0.4L and 0.6L due to constraints with the physical loading apparatus. Loading for this set of tests consisted of applying a series of 7 kip concentrated loads spaced 2 ft.-4 ¹³/₁₆ in. apart via hydraulic actuators that were attached to the floor and pull a high tensile rod through the deck. The load pattern and transverse placement of loads is identical to the pattern used in the 16.6 kip wheel load tests conducted on this structure, described in 4.6 and shown in Fig. 4.4 for the maximum positive and negative bending locations. For both one lane and three lanes loaded, Tiedeman et al. measured the bottom flange stresses at the 0.4L and 5 feet in front of the 1.0L at the 0.4L and 1.0L point and compared these values with the results of their FEA. Tiedeman et al. used the ANSYS finite element program developed by Swanson Analysis System, Inc. to conduct their FEA modeling.

Figures 5.5 and 5.6 show the comparisons for the bottom flange stresses measured at the longitudinal points in Girder 2 between the experimental results, Tiedeman et al.'s FEA, and the WVU FEA for the one and three lane loaded cases respectively. Figures 5.7 and 5.8 show similar results for the 0.65L load cases also with one and three lanes loaded respectively. It can be seen that there is excellent agreement between the Tiedeman et al. and WVU FEA as well as between both analytical models and the experimental data.

5.3.3 Comparison with Bakht Medium Span Length Bridge

Bakht (1988) performed extensive research on the development of live load distribution factors for the Ontario Highway Bridge Design Code (1991), and the computation of design factors, D_{df} where Distribution Factor = $\frac{S}{D_{df}}$, used in the development of the live load distribution factor equation currently used in the OHBDC. Bakht performed experimental testing of a medium span length simply supported bridge to experimentally determine the D_{df} value and compare this with predictions in the OHBDC as well as to evaluate other design parameters. In this study, an analytical comparison is made with the experimentally determined deflections and D_{df} values for this bridge.

The simply supported bridge had a span length of 150 feet and consisted of an 8 in. deck placed on 5 girders spaced at 9.75 ft. with a 7.75 in. sidewalk and a 24 in. high parapet as shown in Fig. 5.9. Figure 5.10 shows the plan view of the Bakht Bridge giving the cross-frame dimensions (L 4x3x0.375) location along the span every 25 feet with the

location of flange transitions designated by A-A and B-B. The girder cross-sections can be seen in Fig. 5.11 and consist of a 16 in. x 1 in. top flange plate and an 18 in. x 1.5 in. bottom flange plate for section A-A while section B-B has a top flange plate of 18 in. x 1.25 in. and a bottom flange plate of 20 in. x 1.75 in., the web plate for both sections A-A and B-B is an 84 in. x 0.375 in. Three loading conditions are used in this testing involving a Kenworth and a Mack truck with the longitudinal loading positions and values shown in Fig. 5.12 and the horizontal loading positions shown in Fig. 5.13. It is important to note that load case 1 and load case 2 are loaded in the same position except the values of axle loads are different.

The design factor, D_{df} , was evaluated using the method described by Bakht (1988) from Eqn. 4.12 (given on page 68) by multiplying the factor of girder spacing divided by number of wheel lines applied during the loading with the factor of the sum of the bottom flange strains divided by the bottom flange strain of the girder of interest. The calculated distance factors for each load case and the distance factor determined by Bakht given in Table 5.2. To summarize, the Load Case 1 distance factor showed a 7.2% higher difference from the Bakht distance factor, the Load Case 2 D_{df} was 4.1% higher than the Bakht distance factor, and the Load Case 3 distance factor was 0.4% lower than the Bakht distance factor. The FEA results represent a very good correlation with the Bakht's values, showing Bakht's method of computing distribution factors to work successfully coupled with the analytical modeling used in these studies.

The FEA deflections were also compared with Bakht's recorded deflections. The deflection for the three load cases can be seen graphically on Fig. 5.14. These results well match trends observed in grillage modeling conducted by Bakht to assess bending

moments. Bakht (1988) explains the difference between the analytical and experimental results as attributable to bearing restraint.

5.2.5 Comparison with Stallings Bridges

Stallings and Yoo (1991) field-tested several bridges to compare ratings determined from FEA grid analyses to AASHTO computed ratings. Comprehensive bridge geometry, loading, and experimental results were presented by Stallings and Yoo for the Childersburg bridge. For this reason, this bridge was selected as a calibration tool for the FEA modeling as well as to compare the various methods for computing the distribution factors described in Chapter 4.

The bridge modeled in this study consisted of two simply supported approach spans for a steel truss with span lengths of 44 feet and 77 feet with a 6.75 in. deck placed on 4 girders spaced at 5.83 feet with a 10.5 in. sidewalk on each side of the deck as seen in Fig. 5.15. The steel girders were Bethlehem B beams taken from the 1930 Bethlehem steel manual with the cross-section of the girder profile for each bridge shown in Fig. 5.16. Two lanes of trucks were placed at the transverse loading position shown in Fig. 5.15 and the longitudinal placement shown in Fig. 5.17. Note that Fig. 5.17 also shows the weight of each wheel.

The load distribution factors for the two Stallings Bridges using the procedures described in Chapter 4 were computed and are presented in Table 5.3 along with the distribution factor obtained by Stallings and Yoo in the experimental testing. A summary of the results again provide very good correlation with the Barker, Bakht, and Stalling

procedures producing a reasonable difference between the analytical values and the distribution factors acquired from physical testing. The Mabsout procedure showed a larger difference with the largest error being approximately 16% conservative.

5.3 Conclusions

This chapter successfully compared FEA models with previous experimental tests, experimentally determined distribution factors providing an evaluation of the different distribution factor methods described in Chapter 4, and compared with previous FEA results. The Newmark and AISI-FHWA Bridges helped in the verification of proper modeling techniques and provided some additional information to use in the selection of a proper procedure for the calculation of load distribution factors to be used in further studies. Also Newmark Bridge showed excellent accuracy in the modeling of deflections and also the stress comparisons from the AISI-FHWA Bridge were accurately modeled and compared well with previous FEA studies of that bridge.

Further parametric studies, described in Chapter 6, require the accurate calculation of distribution factors. Therefore, it is important to select an accurate and robust method to calculate these factors from the FEA data. The Mabsout method requires the selection of a hypothetical effective section that may influence the results. The other methods described in this study all produce distribution factors that are very close to one another. Bakht's distribution factor method has been extensively correlated with the results of field test data and was used as the basis for the formulation of the live

load distribution factors in the OHBDC. For this reason, further parametric studies in this work will use the Bakht procedure to compare the live load distribution factor.

Table 5.1. Example distribution factors for Newmark bridge

Bridge	Exp. Results	Barker #1	Barker #2	Stallings	Bakht	Mabsout	AASHTO LRFD	AASHTO Standard
Newmark	0.587	0.461	0.456	0.456	0.456	0.671	0.6	0.273

Table 5.2. Design factors for Bakht medium span bridges

Load Case	Bakht Design Factor (ft)	FEA Design Factor (ft)
Load Case 1	12.70	11.84
Load Case 2	12.34	11.84
Load Case 3	7.55	7.51

Table 5.3. Distribution factors for Stallings’s bridges

Bridge	Experimental Results	Barker #1	Barker #2	Stallings	Bakht	Mabsout	AASHTO LRFD	AASHTO Standard
Stallings - 44	1.190	1.078	1.075	1.072	1.072	1.029	1.130	1.060
Stallings - 77	1.100	1.065	1.061	1.058	1.058	1.036	1.086	1.060

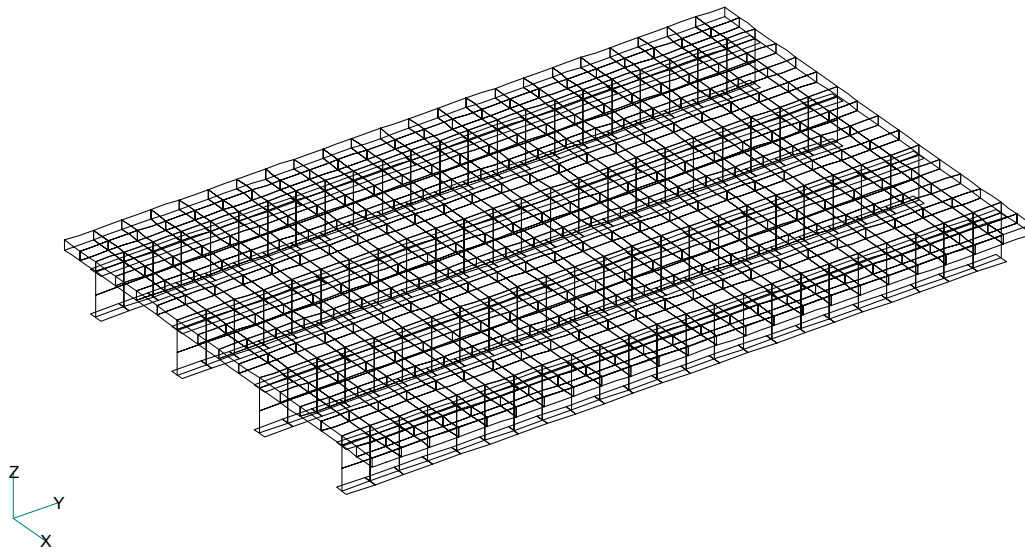


Figure 5.1. Typical FEA mesh discretization for WVU bridge model

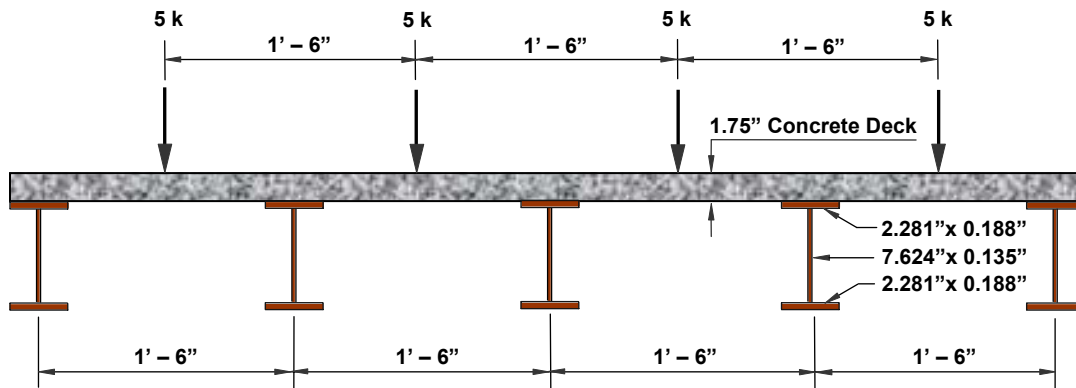


Figure 5.2. Newmark bridge cross-section with horizontal loading positions

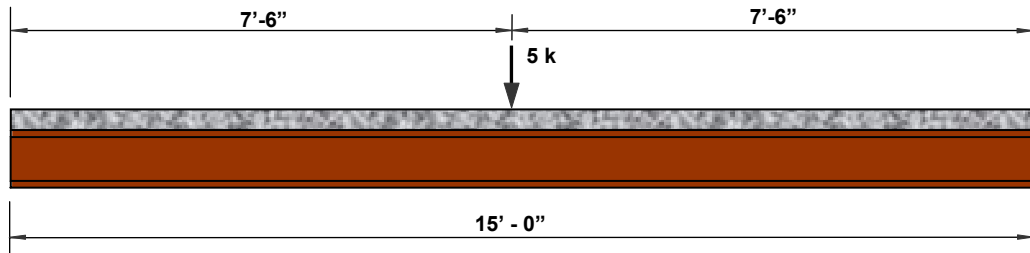


Figure 5.3. Plan view of the Newmark bridge showing longitudinal dimensions and loading

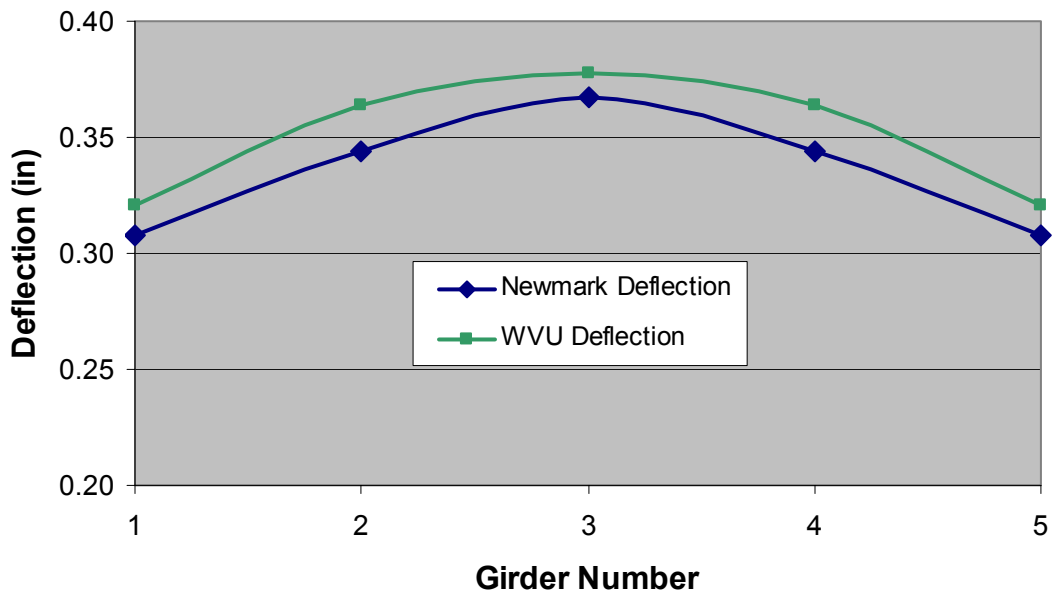


Figure 5.4. Comparison of deflection between Newmark experimental testing and WVU FEA for the Newmark bridge in Section 5.2.1

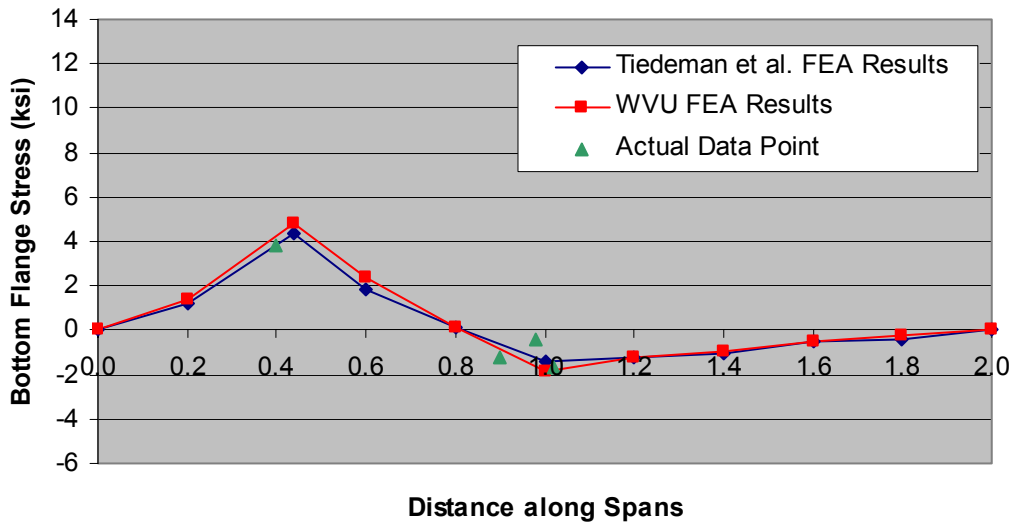


Figure 5.5. Bottom flange stress for 0.44L-1 lane-loaded comparing actual data, Tiedeman et al. FEA results, and WVU FEA results

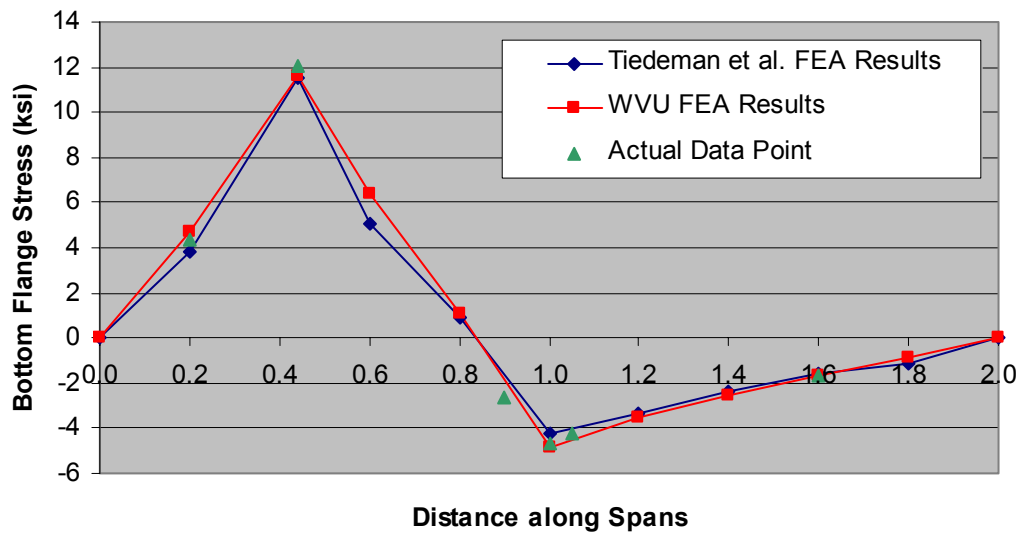


Figure 5.6. Bottom flange stress for 0.44L-3 lanes-loaded comparing actual data, Tiedeman et al. FEA results, and WVU FEA results

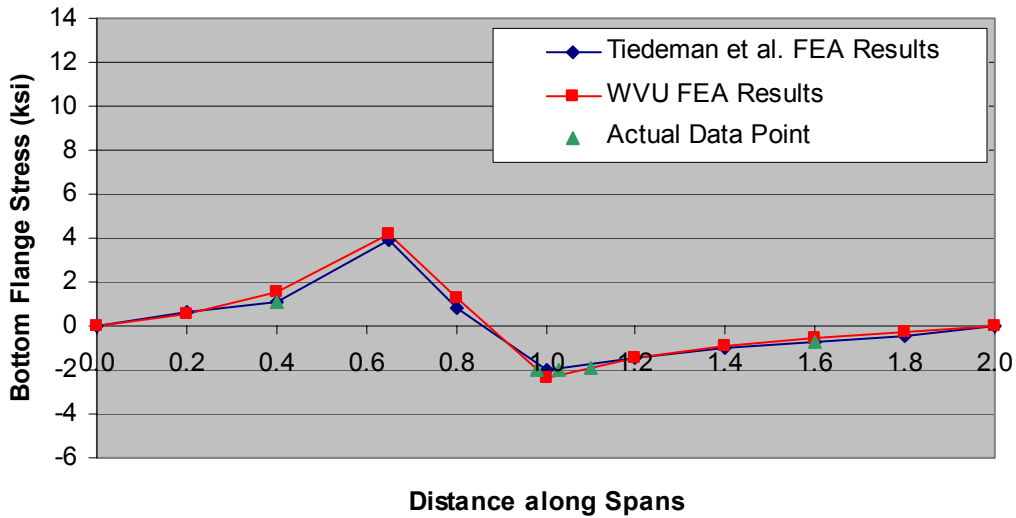


Figure 5.7. Bottom flange stress for 0.65L-1 lane-loaded comparing actual data, Tiedeman et al. FEA results, and WVU FEA results

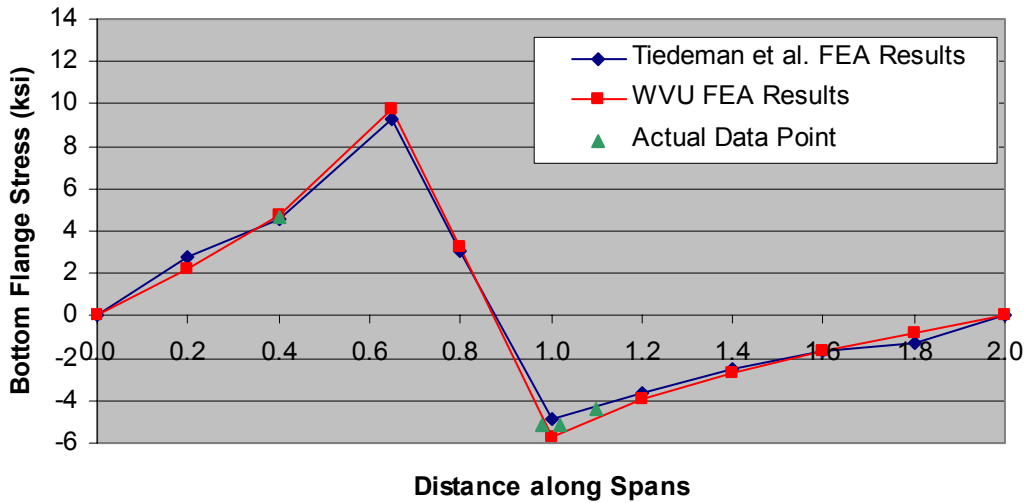


Figure 5.8. Bottom flange stress for 0.65L-3 lanes-loaded comparing actual data, Tiedeman et al. FEA results, and WVU FEA results

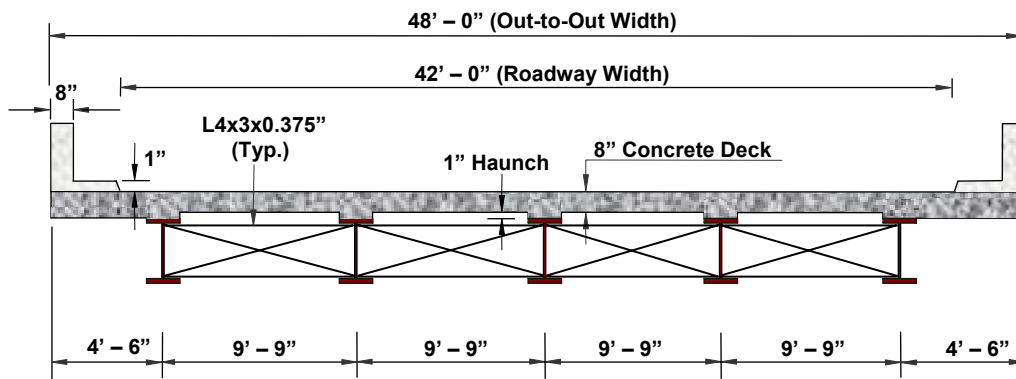


Figure 5.9. Cross-section view dimensions of Bakht medium span length bridge

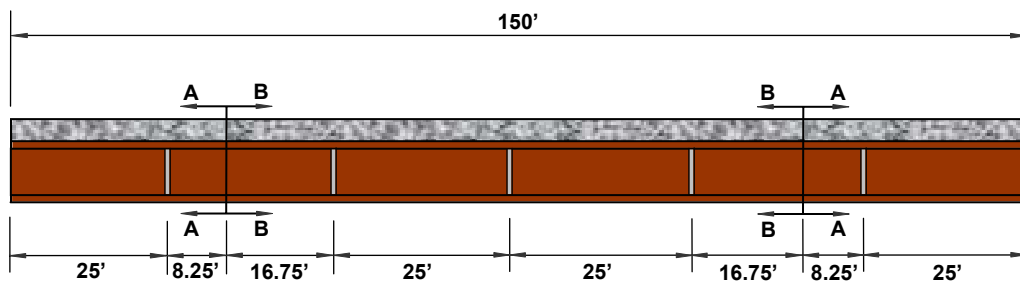


Figure 5.10. Plan view of Bakht bridge showing girder transitions and cross-frame locations

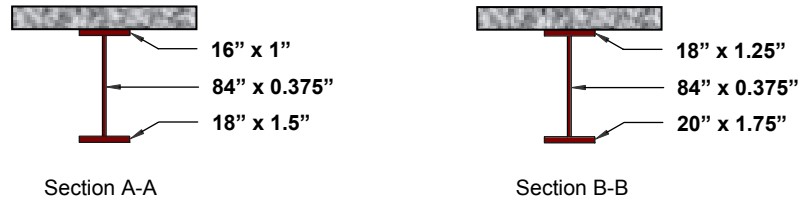


Figure 5.11. Cross-sections for Bakht medium span length bridge

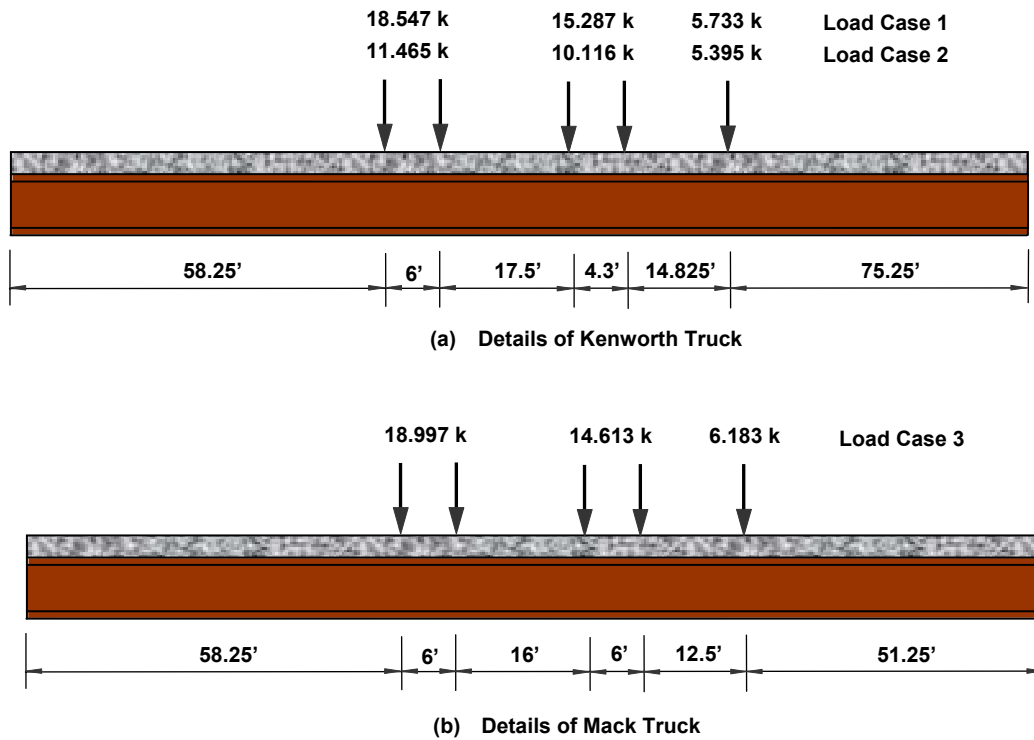
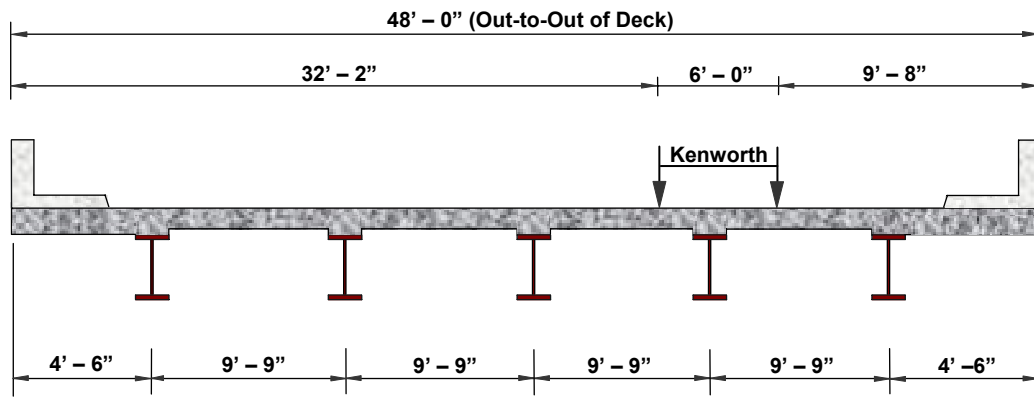
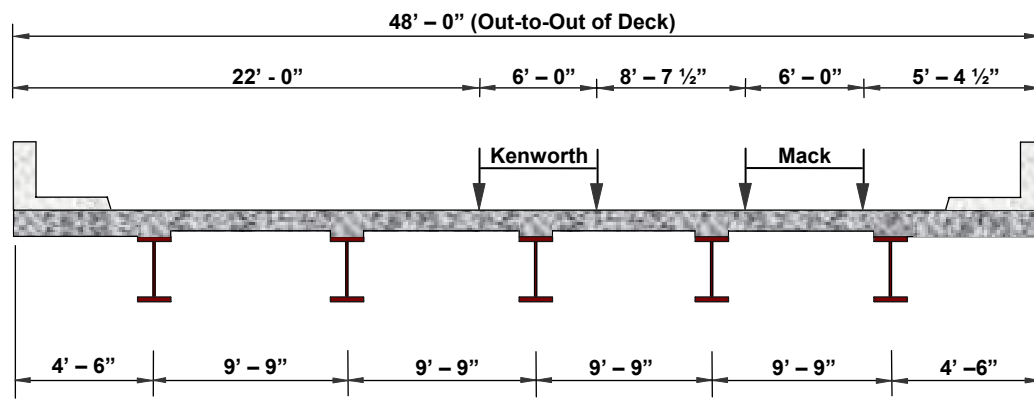


Figure 5.12. Plan view showing the location of longitudinal loading for each load case involving (a) Kenworth truck and (b) Mack truck



Load Case 1 and 2



Load Case 3

Figure 5.13. Plan view showing the location of transverse loading positions for each load case involving a (a) Kenworth and (b) Mack truck

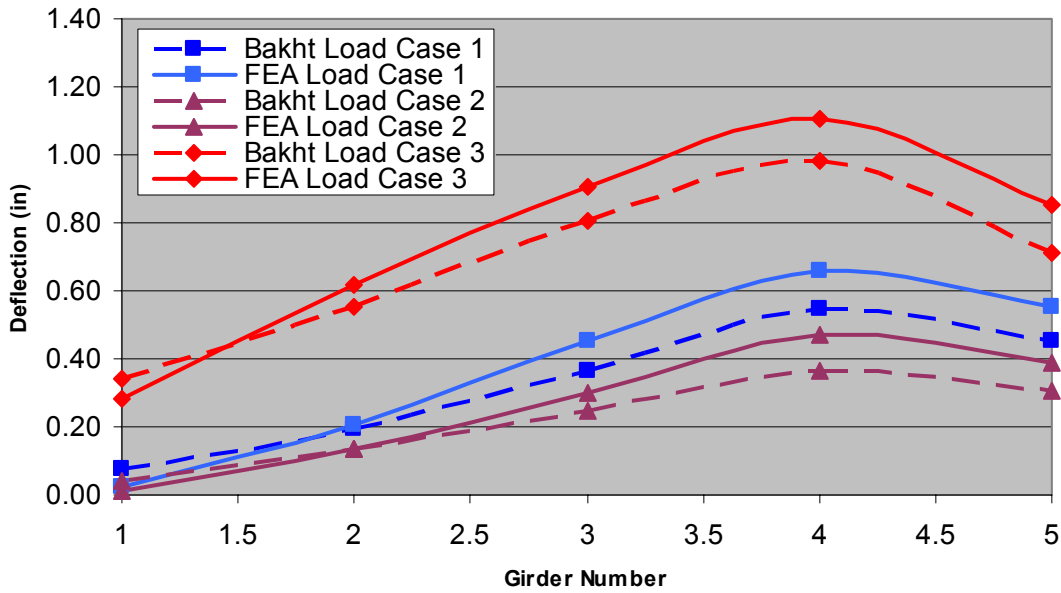


Figure 5.14. Comparison of deflection from the Bakht field-testing and WVU FEA model for the 3 load cases presented in Section 5.2.3

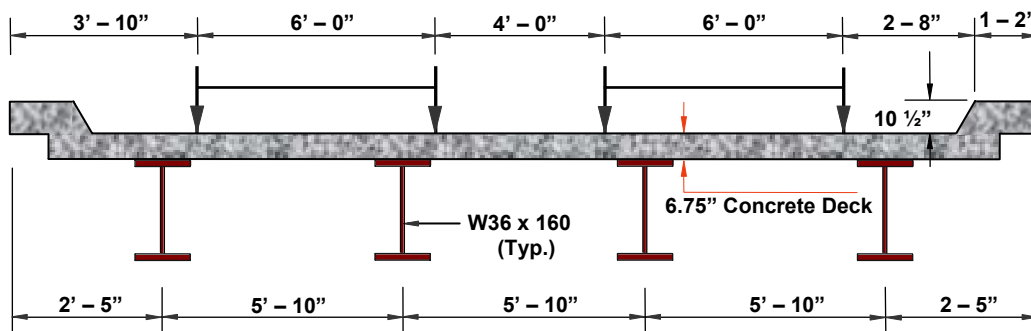


Figure 5.15. Stalling bridges cross-section and horizontal truck loading positions

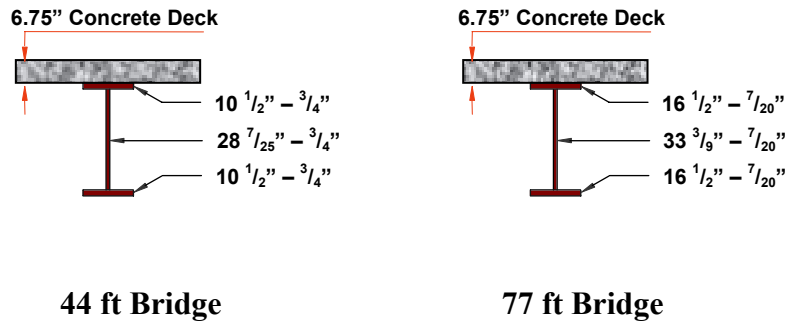


Figure 5.16. Cross-section for Stallings's bridges

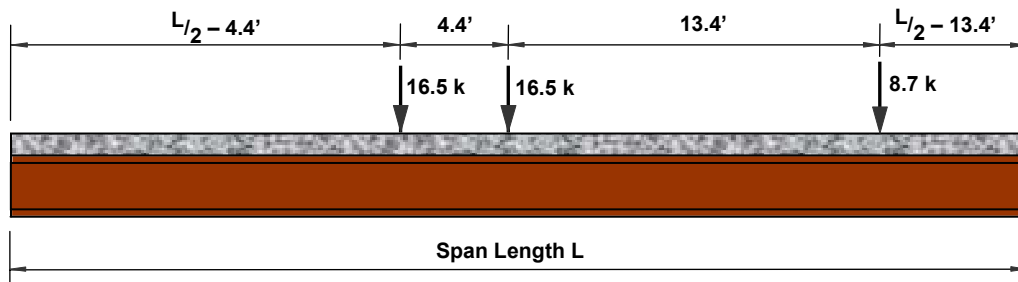


Figure 5.17. Plan view of Stalling bridges showing longitudinal dimensions and loading for two truck tests

CHAPTER 6

PARAMETRIC STUDIES

6.1 Introduction

The primary objective of this chapter is to develop a set of parametric studies for a discrete range of parameters for simply supported composite steel bridge superstructures to evaluate live load distribution in these structures. The goal is to use the analysis results to compute the live load distribution factors using Bakht's procedure (described in Section 4.4). The resulting distribution factors will subsequently be assessed to ascertain the relative importance of parameters selected in the study, they will be compared with current AASHTO Specifications, and a simplified model applicable to the range of parameters used in this study will be proposed. Results of the sensitivity studies, along with the development of the proposed distribution factor model will be presented subsequently in Chapter 7.

6.2 Range of Parameters

Three 4-girder cross sections with varying girder spacings were selected for the parametric studies. These sections, shown in Figs. 6.1, 6.2, and 6.3, and labeled cross-section 1, cross-section 2, and cross-section 3 respectively, are representative of typical bridges in the U.S. inventory. The primary parameters in this study include girder spacing, girder span length, steel yield strength, and cross section span-to-depth ratio.

- ***Girder spacing:*** As shown in Figs. 6.1, 6.2, and 6.3, three girder spacings were incorporated in these studies: 11 ft. – 6 in. (a relative wide girder spacing), 10 ft. – 4 in. (an intermediate spacing), and 8 ft. – 6 in. (a narrow girder spacing)
- ***Girder span length:*** All bridge models were simply supported and have span lengths ranging from 100 ft. to 300 ft. Cross-sections one and three had lengths of 100, 200, and 300 ft. whereas cross section 2 had span lengths of 100, 150, 200, and 250 ft.
- ***Steel yield strength:*** For each given variation of girder spacing, span length, and span to depth ratio cross section geometries were provided for both homogenous Gr. 50 ($F_y = 50$ ksi) design and Gr. 70 ($F_y = 70$ ksi) design.
- ***Span-to-depth ratio:*** Three span to depth ratios were used, $L/D = 20, 25,$ and 30 where $D =$ overall superstructure depth.

The bridge cross sections used in this study were initially taken from those incorporated in the AISI Short Span Steel Bridges (1995). Previous work with these cross sections (Clingenpeel, 2001; Barth et al., 2001) was conducted to assess optimized designs for these members. Commercial software based on AASHTO Standard Specifications (Simon v8.1, 1996) and the AASHTO LRFD Specifications (MDX, 1999) was used to perform line girder designs to produce least weight members for the range of parameters described above. These optimized sections served as the basis for the 3D FEA models conducted in this study. Table 6.1 presents the basic cross section geometry for each girder used in this work. Also Fig. 6.4 provides a hypothetical girder elevation as a reference to the parameters provided in Table 6.1.

For each hypothetical configuration a FEA model of the superstructure was constructed and two lanes of HS20 truck loading were placed to maximize the positive bending at 0.5L of one of the interior girders in the bridge. The transverse loading positions are also presented in Figs. 6.1, 6.2, and 6.3. Figure 6.5 shows the longitudinal load position used to maximize mid-span bending. After an elastic analysis was performed for the given loading, bottom flange stain data was used in conjunction with the Bakht procedure (described in Section 4.4) to compute the live load distribution factors.

Figure 6.6 shows the variation in girder stiffness as a function of span length for the bridges in the parametric study. This figure also plots stiffness versus span length for the bridges used in the NCHRP parametric study conducted to derive the AASHTO LRFD distribution factors, for a population of bridges in various state DOT inventories (discussed in Section 3.4.1), and for a small group of actual bridges from an inventory at WVU. In this figure stiffness is defined as the term, K_g (see AASHTO section 4.6.2.2.1) where

$$K_g = n \cdot (I + Ae^2) \quad (\text{Eqn. 6.1})$$

It is interesting to note that the range of stiffness values incorporated in the NCHRP parametric studies falls well outside the feasible stiffness values of actual bridges. This fact is, however, noted by the NCHRP investigators. Also of note is the fact that it is the inclusion of this stiffness parameter, K_g , in the distribution factor equation (see Eqn. 6.1 and AASHTO section 4.6.2.2.1) that leads to part of the deterrent to the use of the LRFD equations.

6.3 General Results

As previously stated, after performing each analysis, the mid-span bottom flange stresses were substituted in the expression

$$D_{df} = \left(\frac{S}{n} \right) \cdot \left(\frac{\sum \varepsilon_i}{\varepsilon_{\max}} \right) \quad (\text{Eqn. 4.12})$$

to determine the design factor, D_{df} . Given the calculated D_{df} value, the live load distribution factor for mid-span moment was then computed as

$$\text{Distance Factor} = \frac{S}{D_{df}} \quad (\text{Eqn. 6.2}).$$

Table 6.2 provides a summary of the resulting D_{df} values and corresponding distribution factors for each of the parametric variations. Also shown in this table are the respective distribution factors computed using the AASHTO LRFD (AASHTO, 2002) and AASHTO Standard Specifications (AASHTO, 1992) along with the percent difference between these values and the analytical distribution factor. The average percent difference between the AASHTO LRFD Specifications and the FEA results is 20% on the conservative side. Also the corresponding maximum and minimum percent difference is 33% and 8% respectively. For the AASHTO Standard Specifications, the average difference between the FEA results and the code predictions is 29% on the conservative side and the corresponding maximum and minimum values are 46% and 15% respectively.

6.3.1 Influence of girder spacing

Figure 6.7 shows the influence of girder spacing on the analytical D_{df} values from each of the three cross section girder spacings. It can be seen, as would be expected, that there is a fairly increasing linear relationship between girder and the D_{df} value. This is exactly the trend witnessed by Newmark and Siess and incorporated in the AASHTO Standard Specifications.

6.3.2 Girder span length

Figure 6.8 shows the influence of span length on the design factor, D_{df} , for each of the three cross sections. It can be seen that for each respective cross section, there is a small increase in the D_{df} values as a function of increased span length.

6.3.3 Steel yield strength

A comparison between yield strength may be made by assessing the results shown in Table 6.2. For example, in cross section 1 bridge 1L2S115F5LD20 is a 200 ft. span length bridge with $L/D = 20$ comprised of 50 ksi steel. The resulting distribution factor for this bridge was 0.606. The corresponding 70 ksi bridge 1L2S115F7LD20, yielded a distribution factor of 0.602. The difference between these value being 0.66%. This trend is similar for other yield stress comparisons with the average difference being 0.5%. It should however be expected that for the bridges assessed in this parametric study there

would be negligible difference in load distribution as a function of yield stress. For each respective member, the yield stress is changed while the L/D value is kept approximately the same. Therefore, these members will have similar stiffness values.

6.3.4 Span to depth ratio

For a typically proportioned bridge, the span to depth ratio has a direct relationship with the girder stiffness. Figure 6.9 shows a plot of the resulting analytical D_{df} values as a function of stiffness, as defined by K_g , for each of the load cross sections. While for very low stiffness values there is a small variation in the trend, over the wide range of stiffness values used in this study there is a very negligible change in the resulting D_{df} value.

6.4 Further Data Reduction

The results of the parametric studies coupled with sensitivity analyses presented in this chapter will subsequently be used in Chapter 7 to develop a simplified empirically based model for the distribution factor. This model will be used to predict maximum positive bending in simply supported spans within the range of parameters evaluated in this study.

Table 6.1. Key parameters for WVU parametric bridges

Span Length (ft)	Top Flange (A)			Top Flange (B)			Bottom Flange (A)			Bottom Flange (B)			Web		
	b _{tf} (in)	t _{tf} (in)	Length (ft)	b _{tf} (in)	t _{tf} (in)	Length (ft)	b _{bf} (in)	t _{bf} (in)	Length (ft)	b _{bf} (in)	t _{bf} (in)	Length (ft)	d (in)	t _w (in)	Length (ft)
Cross-Section 1	100	12	0.813	100			12	2.625	100				45	0.438	100
	100	12	1.438	100			15	2.938	100				33	0.500	100
	100	12	0.750	100			12	2.500	100				47	0.375	100
	100	12	1.125	100			14	3.000	100				33	0.438	100
	100	12	1.688	100			18	3.000	100				25	0.563	100
	200	27	1.188	200			27	1.313	200				108	0.688	200
	200	22	1.625	200			22	2.688	200				82	0.563	200
	200	27	2.875	200			28	3.000	200				65	0.625	200
	200	27	1.125	200			29	0.875	200				108	0.813	200
	200	21	1.250	200			22	2.313	200				62	0.625	200
	200	18	2.375	200			25	2.750	200				65	0.500	200
	300	42	1.625	300			42	0.938	300				168	1.125	300
	300	33	2.750	300			33	2.500	300				130	0.875	300
	300	38	3.000	300			42	3.000	300				105	0.688	300
	300	42	1.625	300			42	0.750	300				168	1.250	300
	300	33	1.563	300			33	1.938	300				131	1.000	300
	300	27	2.375	300			33	2.813	300				107	0.813	300

Table 6.1. cont'd

Span Length (ft)	Top Flange (A)			Top Flange (B)			Bottom Flange (A)			Bottom Flange (B)			Web			
	b _{tf} (in)	t _{tf} (in)	Length (ft)	b _{tf} (in)	t _{tf} (in)	Length (ft)	b _{bf} (in)	t _{bf} (in)	Length (ft)	b _{bf} (in)	t _{bf} (in)	Length (ft)	d (in)	t _w (in)	Length (ft)	
Cross Section 2	100	12	0.9375	100			12	1.812	100				48	0.375	100	
	100	12	1.000	100			16	1.938	100				35	0.375	100	
	100	14	1.750	100			18	2.312	100				27	0.313	100	
	100	12	0.750	100			12	1.500	100				48	0.500	100	
	100	12	0.875	100			12	2.375	100				35	0.375	100	
	100	12	1.250	100			16	2.312	100				27	0.375	100	
	150	18	0.938	150			18	0.875	150	18	1.563	90	79	0.563	150	
	150	16	0.813	30	16	1.375	90	16	1.562	30	16	2.625	90	60	0.563	150
	150	18	1.000	30	18	2.000	90	20	2.000	30	20	3.000	90	48	0.438	150
	150	16	0.750	150			16	0.750	150	16	1.250	90	79	0.625	150	
	150	14	0.750	30	14	1.500	90	14	1.500	30	14	2.313	90	60	0.563	150
	150	14	1.000	30	14	1.750	90	18	1.500	30	18	2.500	90	48	0.563	150
	200	28	1.062	200			28	0.750	200	28	1.063	120	109	0.688	200	
	200	22	0.938	40	22	1.625	120	22	1.250	40	22	2.500	120	83	0.688	200
	200	21	1.375	40	21	2.375	120	28	1.562	40	28	2.875	120	67	0.438	200
	200	26	1.062	200			26	0.750	200				109	0.750	200	
	200	20	1.062	200			20	1.000	200	20	2.125	120	84	0.625	200	
	200	14	1.062	40	14	1.813	120	20	1.688	40	20	2.875	120	67	0.438	200
	250	32	1.312	250			32	1.000	250				138	0.875	250	
	250	28	1.125	50	28	2.125	150	28	1.062	50	28	2.125	150	109	0.688	250
250	28	1.375	50	28	2.875	150	40	1.812	50	40	3.000	150	86	0.625	250	
250	30	1.000	50	30	1.188	150	30	0.750	50			137	0.875	250		
250	22	1.125	50	22	2.000	150	24	1.625	50	24	2.875	150	87	0.688	250	

Table 6.1. cont'd

Span Length (ft)	Top Flange (A)			Top Flange (B)			Bottom Flange (A)			Bottom Flange (B)			Web			
	b _{tf} (in)	t _{tf} (in)	Length (ft)	b _{tf} (in)	t _{tf} (in)	Length (ft)	B _{bf} (in)	t _{bf} (in)	Length (ft)	B _{bf} (in)	t _{bf} (in)	Length (ft)	d (in)	t _w (in)	Length (ft)	
Cross Section 3	100	14	0.750	100			14	1.313	100				49	0.375	100	
	100	14	1.063	100			14	2.750	100				37	0.438	100	
	100	18	1.188	100			18	2.813	100				29	0.438	100	
	100	14	0.750	100			14	1.625	100				49	0.313	100	
	100	16	0.750	100			16	2.063	100				37	0.375	100	
	100	20	0.938	100			20	2.063	100				29	0.375	100	
	200	28	0.875	40	28	1.063	120	28	0.750	40	28	1.750	120	109	0.688	200
	200	22	0.875	40	22	1.500	120	22	1.313	40	22	2.500	120	85	0.438	200
	200	26	1.125	40	26	1.750	120	26	1.688	40	26	2.875	120	69	0.313	200
	200	28	0.875	40	28	1.000	120	28	0.750	40	28	0.750	120	109	0.875	200
	200	20	0.813	40	20	0.938	120	20	0.875	40	20	1.625	120	85	0.688	200
	200	20	0.875	40	20	1.188	120	20	1.313	40	20	2.375	120	69	0.625	200
	300	44	1.313	60	44	1.500	180	44	0.750	60	44	1.125	180	169	1.063	300
	300	34	1.250	60	34	1.563	180	34	1.250	60	34	2.250	180	133	0.875	300
	300	38	1.500	60	38	2.125	180	38	1.625	60	38	2.875	180	109	0.688	300
	300	44	1.313	60	44	1.500	180	44	0.750	60	44	0.750	180	169	1.313	300
300	30	1.125	60	30	1.375	180	30	0.750	60	30	1.500	180	133	1.063	300	
300	36	1.375	60	36	1.625	180	36	1.000	60	36	1.750	180	109	0.875	300	

Table 6.2. Summary of FEA results for distribution factors calculated from WVU parametric study

	Bridge	FEA Design Factor, D_{df}	Resulting FEA DF	AASHTO LRFD DF	Percent Difference between AASHTO LRFD DF and FEA DF	AASHTO Standard DF	Percent Difference between AASHTO Standard DF and FEA DF
Cross-Section 1	1L1S115F5LD20	17.628	0.652	0.787	21	0.864	33
	1L1S115F5LD25	17.844	0.644	0.772	20	0.864	34
	1L1S115F7LD20	17.764	0.647	0.788	22	0.864	34
	1L1S115F7LD25	17.816	0.645	0.767	19	0.864	34
	1L1S115F7LD30	17.968	0.640	0.755	18	0.864	35
	1L2S115F5LD20	18.962	0.606	0.785	30	0.864	43
	1L2S115F5LD25	18.990	0.606	0.765	26	0.864	43
	1L2S115F5LD30	19.210	0.599	0.758	27	0.864	44
	1L2S115F7LD20	19.088	0.602	0.778	29	0.864	44
	1L2S115F7LD25	19.104	0.602	0.720	20	0.864	44
	1L2S115F7LD30	19.164	0.600	0.743	24	0.864	44
	1L3S115F5LD20	19.026	0.604	0.797	32	0.864	43
	1L3S115F5LD25	19.370	0.594	0.775	30	0.864	45
	1L3S115F5LD30	19.388	0.593	0.763	29	0.864	46
	1L3S115F7LD20	19.158	0.600	0.796	33	0.864	44
	1L3S115F7LD25	19.394	0.593	0.767	29	0.864	46
	1L3S115F7LD30	19.434	0.592	0.750	27	0.864	46

Table 6.2. cont'd

	Bridge	FEA Design Factor, D_{df}	FEA DF	AASHTO LRFD DF	Percent Difference between AASHTO LRFD DF and FEA DF	AASHTO Standard DF	Percent Difference between AASHTO Standard DF and FEA DF	
Cross-Section 2	1L1S104F5LD20	16.402	0.630	0.747	19	0.727	15	
	1L1S104F5LD25	16.424	0.629	0.727	16	0.727	16	
	1L1S104F5LD30	16.324	0.633	0.718	13	0.727	15	
	1L1S104F7LD20	16.394	0.630	0.742	18	0.727	15	
	1L1S104F7LD25	16.392	0.630	0.722	15	0.727	15	
	1L1S104F7LD30	16.504	0.626	0.709	13	0.727	16	
	1L15S104F5LD20	17.210	0.600	0.744	24	0.727	21	
	1L15S104F5LD25	17.244	0.599	0.726	21	0.727	21	
	1L15S104F5LD30	17.348	0.596	0.715	20	0.727	22	
	1L15S104F7LD20	17.306	0.597	0.743	24	0.727	22	
	1L15S104F7LD25	17.342	0.596	0.723	21	0.727	22	
	1L15S104F7LD30	17.444	0.592	0.711	20	0.727	23	
	1L2S104F5LD20	17.480	0.591	0.746	26	0.727	23	
	1L2S104F5LD25	17.440	0.592	0.726	23	0.727	23	
	1L2S104F5LD30	17.458	0.592	0.709	20	0.727	23	
	1L2S104F7LD20	17.566	0.588	0.744	27	0.727	24	
	1L2S104F7LD25	17.560	0.588	0.723	23	0.727	24	
	1L2S104F7LD30	17.494	0.591	0.704	19	0.727	23	
	1L25S104F5LD20	17.474	0.591	0.772	31	0.727	23	
	1L25S104F5LD25	17.378	0.595	0.731	23	0.727	22	
	1L25S104F5LD30	17.304	0.597	0.720	21	0.727	22	
	1L25S104F7LD20	17.528	0.590	0.748	27	0.727	23	
		1L25S104F7LD30	17.386	0.594	0.715	20	0.727	22

Table 6.2. cont'd

	Bridge	FEA Design Factor, D_{df}	FEA DF	AASHTO LRFD DF	Percent Difference between AASHTO LRFD DF and FEA DF	AASHTO Standard DF	Percent Difference between AASHTO Standard DF and FEA DF
Cross-Section 3	1L1S85F5LD20	14.700	0.578	0.644	11	0.727	26
	1L1S85F5LD25	14.495	0.586	0.651	11	0.727	24
	1L1S85F5LD30	14.532	0.585	0.641	10	0.727	24
	1L1S85F7LD20	14.627	0.581	0.652	12	0.727	25
	1L1S85F7LD25	14.608	0.582	0.641	10	0.727	25
	1L1S85F7LD30	14.664	0.580	0.628	8	0.727	25
	1L2S85F5LD20	14.872	0.572	0.674	18	0.727	27
	1L2S85F5LD25	15.028	0.566	0.642	13	0.727	28
	1L2S85F5LD30	15.098	0.563	0.632	12	0.727	29
	1L2S85F7LD20	14.982	0.567	0.654	15	0.727	28
	1L2S85F7LD25	15.100	0.563	0.627	11	0.727	29
	1L2S85F7LD30	15.128	0.562	0.616	10	0.727	29
	1L3S85F5LD20	15.123	0.562	0.675	20	0.727	29
	1L3S85F5LD25	15.228	0.558	0.652	17	0.727	30
	1L3S85F5LD30	15.324	0.555	0.639	15	0.727	31
	1L3S85F7LD20	15.246	0.558	0.674	21	0.727	30
	1L3S85F7LD25	15.471	0.549	0.639	16	0.727	32
	1L3S85F7LD30	15.558	0.546	0.619	13	0.727	33

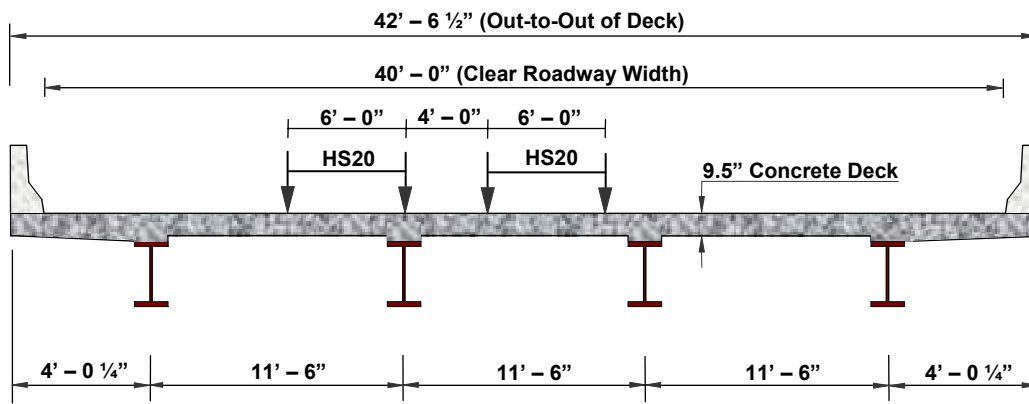


Figure 6.1 Cross-section view and horizontal loading positions for all bridges included in the WVU parametric study for cross-section 1

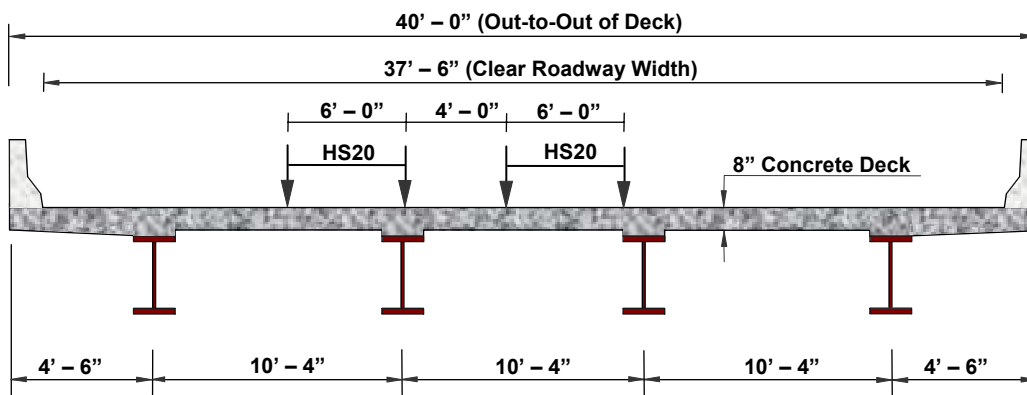


Figure 6.2. Cross-section view and horizontal loading positions for all bridges included in the WVU parametric study for cross-section 2

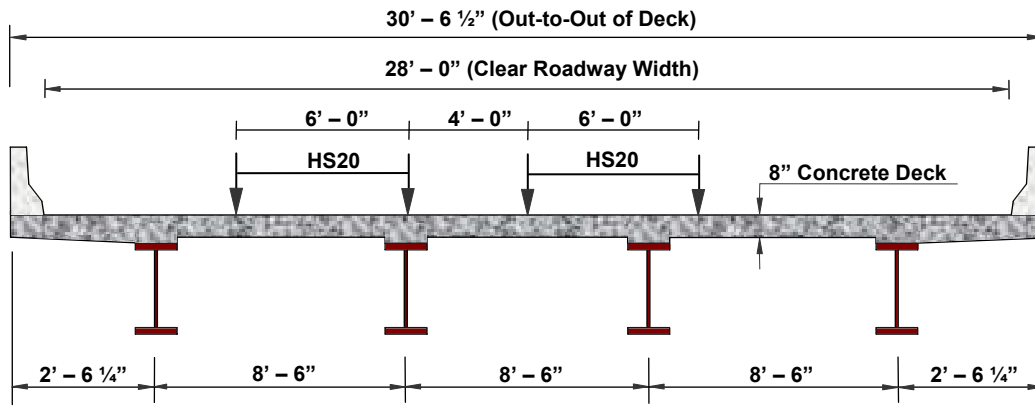


Figure 6.3. Cross-section view and horizontal loading positions for all bridges included in the WVU parametric study for cross-section 3

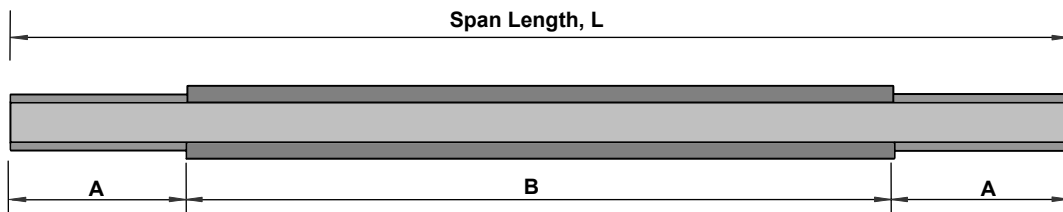


Figure 6.4. Hypothetical girder elevation for girder configurations found in Table 6.1

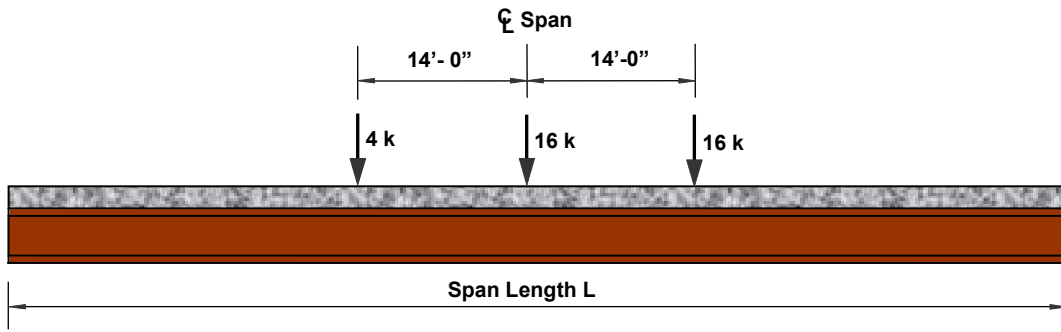


Figure 6.5. Elevation and longitudinal loading positions for girders found in Table 6.1

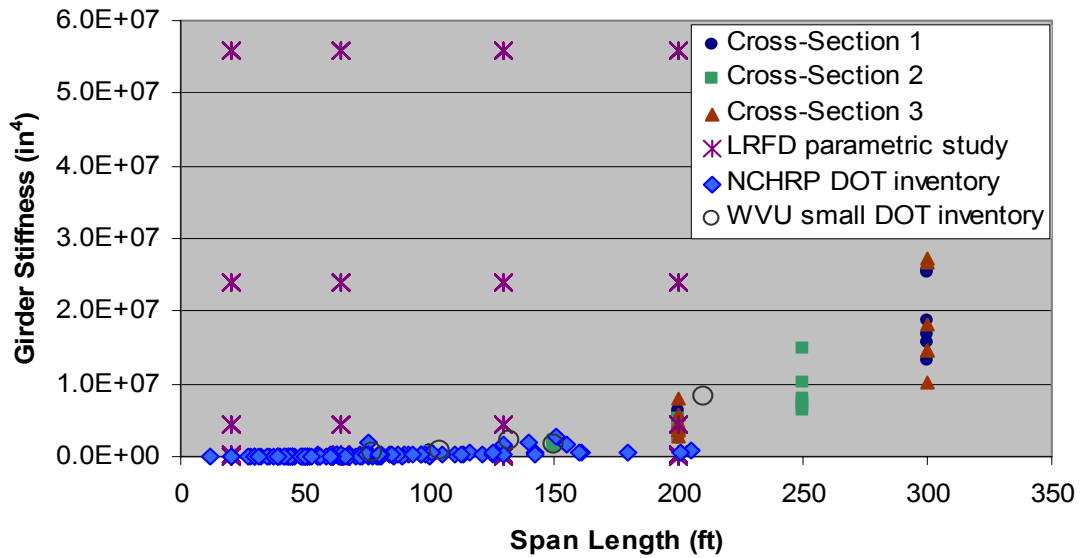


Figure 6.6. Sensitivity study comparing girder stiffness against span length for the WVU parametric study, LRFD parametric study, NCHRP DOT inventory, and WVU small DOT inventory

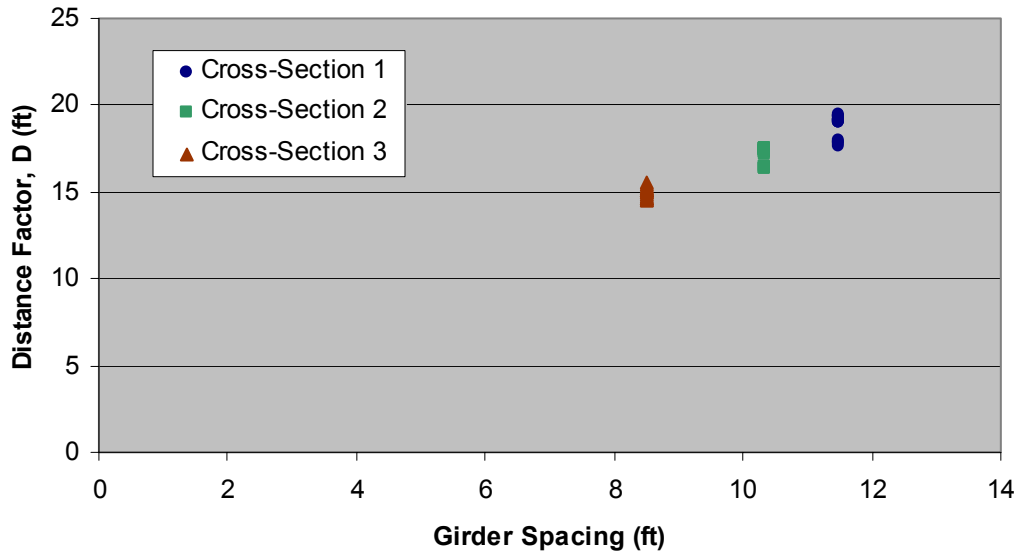


Figure 6.7. Sensitivity study comparing design factor, D, against girder spacing for the WVU parametric study

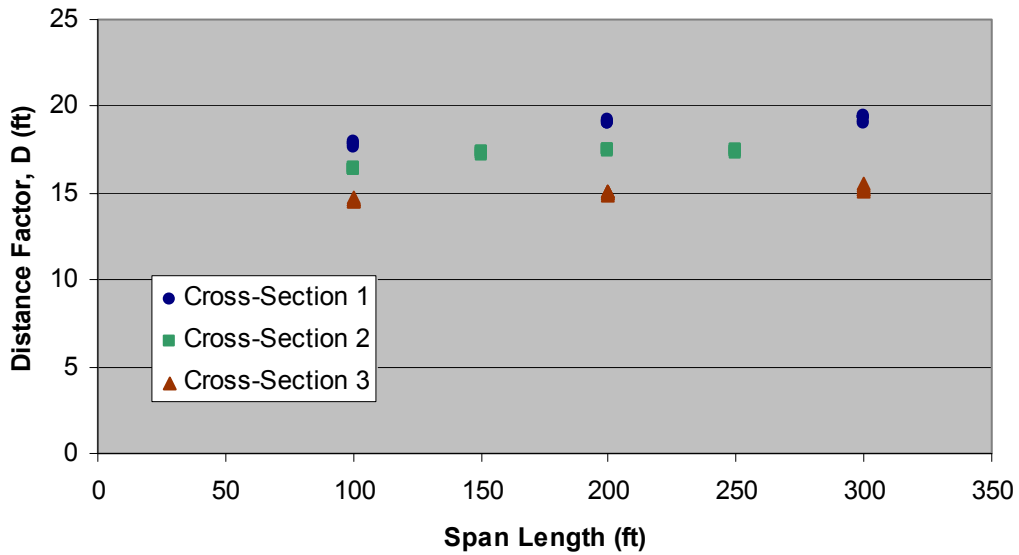


Figure 6.8. Sensitivity study comparing design factor, D, against span length for the WVU parametric study

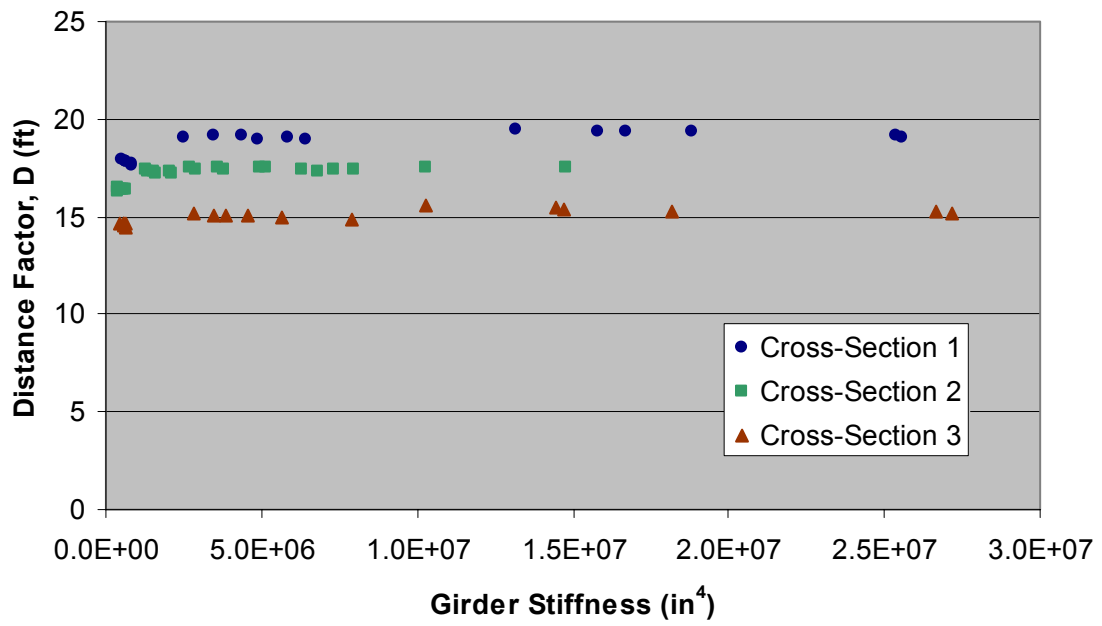


Figure 6.9. Sensitivity study comparing design factor, D, against girder stiffness for the WVU parametric study

CHAPTER 7

GENERAL RESULTS AND DEVELOPMENT OF PROPOSED MOMENT DISTRIBUTION FACTORS

7.1 Introduction

The goal of this chapter is to use the analytical results of the parametric studies conducted in Chapter 6 coupled with the associated trends discussed in that chapter to propose a simplified empirical model for the load distribution factor valid for the range of parameters studied in this effort. Sensitivity studies presented in Chapter 6 showed that the two key parameters influencing the design factor, D_{df} , are girder spacing and span length, subsequent sections in this chapter will present a multivariable regression analysis using these parameters to develop an empirical load distribution factor expression. Also, comparisons will be made between the proposed distribution factor equation and current AASHTO Standard and AASHTO LRFD Specifications (AASHTO, 1996; AASHTO, 2002).

7.2 Development of Proposed Equation

As stated previously, the OHBDC (1991) uses a load distribution factor expression with a similar format to that incorporated in the AASHTO Standard

specification. Which has the form

$$\text{Distribution Factor} = \frac{S}{D_{df}} \quad (\text{Eqn. 7.1})$$

where S = girder spacing (ft)
 D_{df} = design factor (ft).

In the OHBDC, the design factor, D_{df} , is a function of span length, design lane width, and type of superstructure. This parameter was developed by Bakht based on both analytical and parametric studies and was further verified through carefully conducted field tests. This format will be employed in this study with the parameters of girder spacing and span length being used to develop an expression for the design factor, D_{df} , given the analytical results presented in Chapter 6.

The statistical analysis program DataFit 8.0 (2002), created by Oakdale Engineering, was used to aid the process of developing an equation for live load distribution factors. The analysis tool provided accurate results by using multivariable regression to produce an expression for the significant parameters identified in Chapter 6 and determine the accuracy of each expression using a multiple determination value, R^2 . The expression was set up to use the parameters of girder spacing and span length as independent variables with the design factor set as the dependent variable. The resulting model was found to be

$$D_{df} = 5.4 + 1.25S - \frac{170}{L} \quad (\text{Eqn. 7.2})$$

where D_{df} = distance factor (ft)
 S = girder spacing (ft)
 L = span length (ft)

which produced an R^2 value of 0.983. Figure 7.1 shows a comparison between the proposed model (Eqn. 7.2) and the results from the FEA modeling.

7.3 Comparisons of Proposed Equation

The results from the parametric study presented in Chapter 6 were used to compare the load distribution factors from the analytical studies with those predicted by Eqn. 7.2. Also distribution factors predicted by Eqn. 7.2 are compared against those predicted by both the AASHTO Standard and AASHTO LRFD specifications. Figure 7.2 presents a histogram of the proposed distribution factors compared to actual FEA distribution factors. The figure shows Eqn. 7.2 to provide values that compare well to the FEA values observed in bridges modeled from the parametric study. Figures 7.3 and 7.4 present histograms comparing the distribution factors predicted by Eqn. 7.2 with those predicted by the AASHTO Standard and AASHTO LRFD expressions respectively for the bridges in the parametric study. The figures clearly show that both the AASHTO Standard and AASHTO LRFD expressions are found to produce distribution factors that are conservative when compared against the factors calculated using Eqn. 7.2.

Four DOT bridges modeled from the WVU small inventory falling into the range of parameters presented in Section 6.2 were also analyzed and the resulting distribution factors were compared with those predicted by Eqn. 7.2. Table 7.1 presents the results for distribution factors for the FEA model, proposed equation, AASHTO LRFD, and AASHTO Standard specifications. Similar trends to Figs. 7.1, 7.2, and 7.3 are observed from the values presented in Table 7.1.

7.4 Conclusions

Comparisons presented in this chapter show the distribution factors predicted by Eqn. 7.2 to correlate well with the analytical results of the bridges in the parametric study as well as those from a select group of actual bridges. Further, these comparisons show both the AASHTO Standard and AASHTO LRFD specifications to produce conservative distribution factors with respect to both the analytical results of the parametric study and the predictions of Eqn. 7.2. It is important to note that Eqn. 7.2 is only applicable to highway bridges that fall into the range of parameters set in Section 6.2.

Table 7.1. Comparison of distribution factors comparing proposed, AASHTO LRFD, and AASHTO Standard specifications done on four bridges from WVU small bridge inventory, Bakht, and Stallings

Bridge	FEA DF	Proposed DF	AASHTO LRFD	AASHTO Standard
Berks County	0.562	0.597	0.795	0.985
Cedar Creek	0.578	0.569	0.619	0.674
Snyder Street	0.548	0.561	0.626	0.727
Route 20	0.557	0.594	0.701	0.864

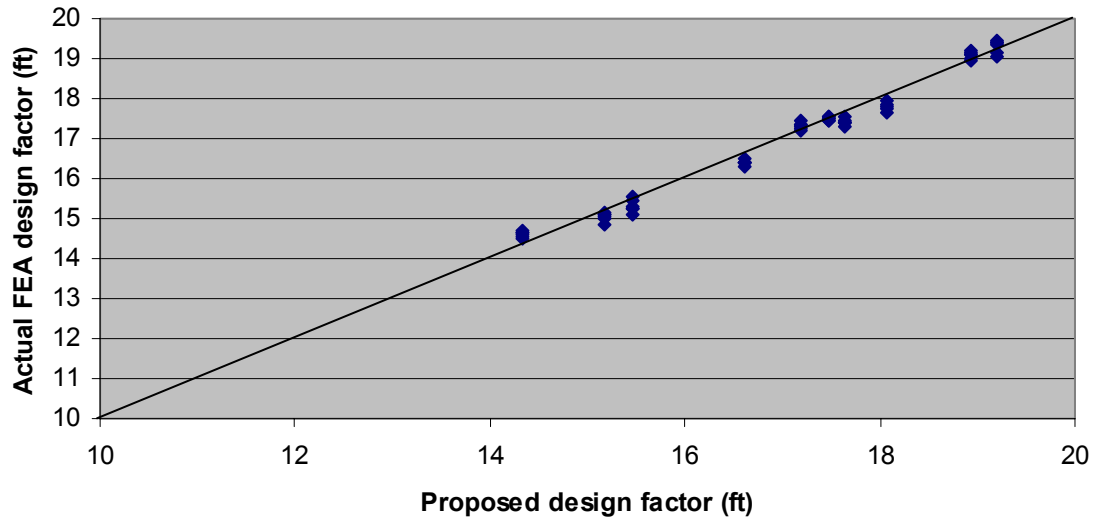


Figure 7.1. Comparison of actual FEA design factor values plotted against proposed design factor values

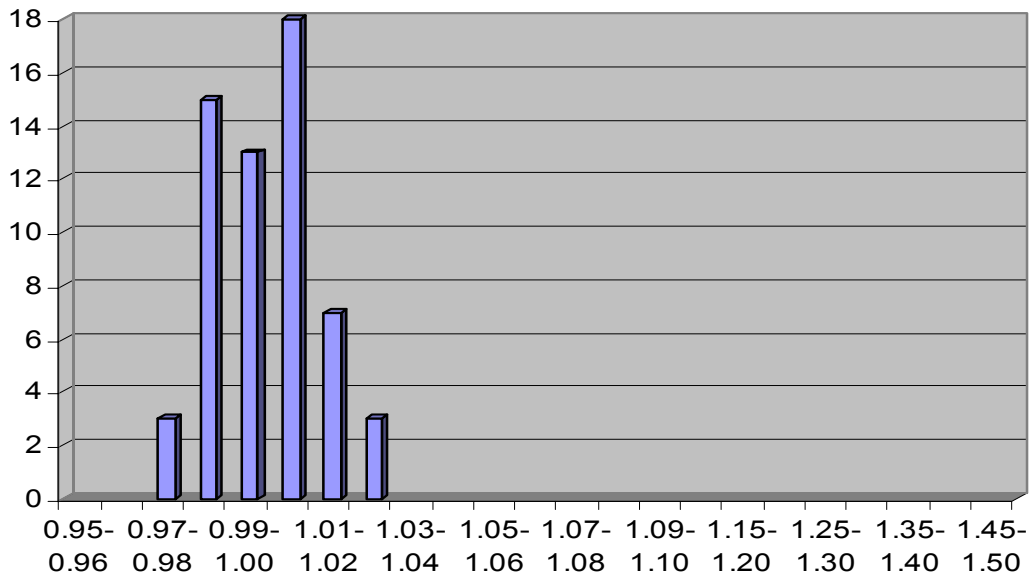


Figure 7.2. Histogram of proposed distribution factors over the actual FEA distribution factors

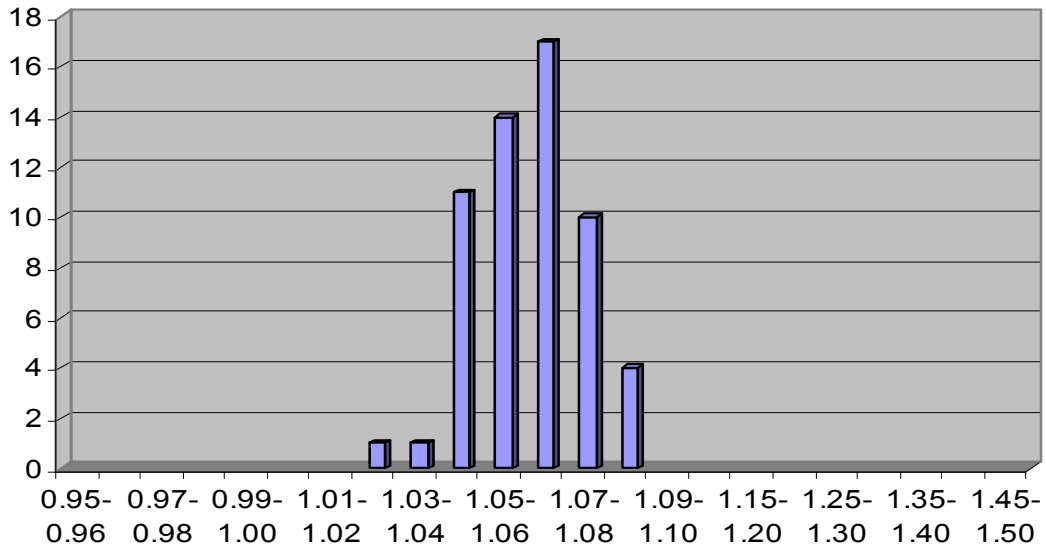


Figure 7.3. Histogram of the AASHTO LRFD distribution factors over the distribution factors calculated from Eqn. 7.2

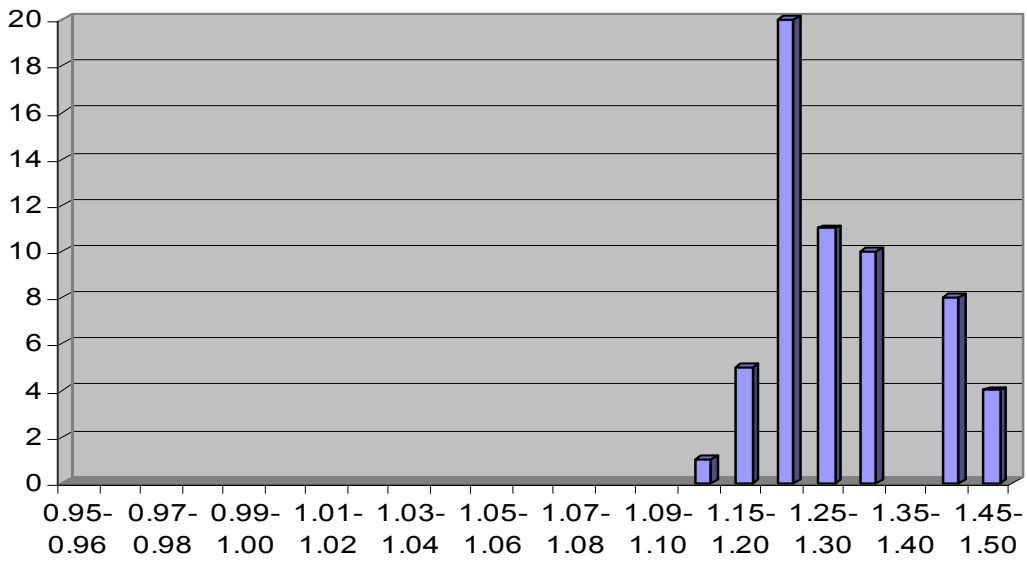


Figure 7.4. Histogram of the AASHTO Standard distribution factors over distribution factors calculated from Eqn. 7.2

CHAPTER 8

SUMMARY AND CONCLUDING REMARKS

8.1 Scope of Work

The primary goal of this effort has been to identify and assess various methods of computing live load distribution factors and to use the results of laboratory and field tests to compare these methods. It has further been a goal of this work to use these methods to perform a parametric study over a wide range of typical slab on steel I-girder bridges to assess the accuracy of both the AASHTO Standard and AASHTO LRFD specifications and to propose an empirical model that correlated better with the analytical results within the range of parameters studied.

A comprehensive literature review was conducted to summarize the background, history, and development of the current AASHTO live load distribution factor equations. Literature from previous investigators was reviewed to obtain procedures for calculating load distribution factors from experimental and analytical data. Results from this literature were used to validate analytical modeling employed in this effort and to compare trends observed in the current modeling with those predicted by current specification equations. The FEA modeling tools were then used to perform a discrete parametric study for simply supported slab on I-girder bridges. Results of this parametric study were also compared with current specification equations and were also used to develop a simplified distribution factor equation applicable to the range of parameters investigated.

8.2 Summary Results

Several models for the computation of live load distribution factors were presented with FEA studies performed to assess these models and verify the accuracy of the analytical tools. A refined parametric study was performed using these analytical tools. The results of the parametric study were assessed to identify the most influential variables within the range of study and these were found to be girder spacing and girder span length. Multivariable regression analysis with these parameters was performed to develop a simplified empirical model for the mid-span moment. The model selected was

$$\text{Distribution Factor} = \frac{S}{D_{df}} \quad (\text{Eqn. 7.1})$$

$$D_{df} = 5.4 + 1.25S - \frac{170}{L} \quad (\text{Eqn. 7.2})$$

where S = girder spacing (ft)
D_{df} = design factor (ft).

This model had an R² value of 0.983.

The results from the analytical models coupled with the results of the simplified prediction model were compared with distribution factors predicted by both the AASHTO Standard and AASHTO LRFD specifications. The comparisons yielded the AASHTO LRFD factors to be 20% conservative compared with the FEA results, while the AASHTO Standard factors were 29% conservative.

8.3 Future Work

While the model presented in this work produced robust comparisons with the analytical studies it is important to extend this work over a broader range of parameters to develop generalized load distribution factor models accurate for a wider range of typical U.S. bridges.

This extended study should include a wider range of girder span lengths with a particular point of assessing (1) shorter span length structures and (2) a more comprehensive range of span lengths between 100 ft. and 300 ft. It should assess a wider range of cross-sections incorporating various girder spacings and numbers of girders in the cross-section. Also it should look at a wider range of loaded lanes.

Additionally it should address such issues as: distribution to exterior girders, specifically looking at edge stiffening effects, girder continuity conditions assessing negative moment distribution, the distribution of shear forces, the influence of skew, and other slab on stringer systems.

Reference Cited

AASHTO LFD Standard Specifications, Fourteenth Edition, American Association of State Highway and Transportation Officials, Washington, D.C., 1996

AASHTO LRFD Specifications, Third Edition, American Association of State Highway and Transportation Officials, Washington, D.C., 2002

ABAQUS v.6.3.1 (2002). Users Manuel. Hibbitt, Karlsson, & Sorensen, Inc., Pawtucket, RI.

AISI Short Span Steel Bridges: Plans and Software. American Iron and Steel Institute. Washington, D.C., 1988

Arockiasamy, M, Amer, A., & Bell, N. B. (1997, February). Load Distribution on Highway Bridges Based on Field Test Data: Phase II. Draft Final Report.

Australian Bridge Design Code, Standards Association of Australia, Sydney, Australia, 1992.

Bakht, B. & Jaeger, L.G. (1988). Bearing Restraint in Slab-on-Girder Bridges. *Journal of Structural Engineering* 114:12, 2724-2740

Bakht, B. (1988, June). Observed Behaviour of a New Medium Span Slab-on-Girder Bridge. *Ministry of Transportation, Ontario, Ontario, Canada.*

Bakht, B. and Moses, F. (1988, Aug). Lateral Distribution Factors for Highway Bridges. *Journal of Structural Engineering*, 114:8, 1785-1803.

- Bakht, B. & Jaeger, L.G. (1990). Bridge Testing – A Surprise Every Time. *Journal of Structural Engineering* 116:5, 1370-1383.
- Barker, M.G., Imhoff, C.M., McDaniel, W. T., & Frederick, T.L (1999, May). *Field Testing and Loading Procedures for Steel Girder Bridges*. Report for Missouri Department of Transportation.
- Barr, P. J., Eberhard, M. O., & Stanton, J. F. (2001, Oct./Sept.). Live-Load Distribution Factors in Prestressed Concrete Girder Bridges. *Journal of Bridge Engineering* 6:5, 298-306.
- Barth, K.E., Clingenpeel, B., Christopher, R., Hevener, W., and Wu, H., (2001). *Unpublished Design Study*, West Virginia University, Morgantown, WV.
- Canadian Highway Bridge Design Code, CSA International, Toronto, Ontario, Canada, 2000.
- Clingenpeel, B. (2001). The Economical use of High Performance Steel in Slab-on-Steel Stringer Bridge Design. MS Thesis, West Virginia University.
- DataFit 8.0 (2002). DataFit v. 8.0®. Oakdale Engineering, Oakdale, PA.
- Eom, J. & Nowak, A. S. (2001, Nov./Dec.). Live Load Distribution for Steel Girder Bridges. *Journal of Bridge Engineering*, 6:6, 489-497.
- Euro Code 2: Steel Bridges, European Committee for Standardization, 2001, Brussels, Belgium.
- FEMap v.8.1 (1999). Users Manuel. Enterprise Software Products, Inc., Exton, PA.

- Fu, C. C., Elhelbawey, M., Sahin, M. A., & Schelling, D. R. (1996, September). Lateral Distribution Factor from Bridge Field Testing. *Journal of Structural Engineering*, 122:9, 1106-1109.
- Hays, C.O., Sessions, L.M., & Berry, A.J. Further Studies on Lateral Load Distribution Using a Finite Element Method. *Transportation Research Record 1072*, 6-14.
- Kim, S. & Nowak, A.S. (1997, August). Load Distribution and Impact Factors for I-Girder Bridges. *Journal of Bridge Engineering*, 2:3, 97-104.
- Mabsout, M.E., Tarhini, K.M., Frederick, G.R., & Tayar, C. (1997, August). Finite-Element Analysis of Steel Girder Highway Bridges. *Journal of Bridge Engineering*, 2:3, 83-87.
- Mabsout, M.E., Tarhini, K.M., Frederick, G.R., & Kobrosly, M. (1997, August). Influence of Sidewalks and Railing on Wheel Load Distribution in Steel Girder Bridges. *Journal of Bridge Engineering*, 2:3, 88-96.
- Mabsout, M.E., Tarhini, K.M., Frederick, G.R., & Kesserwan, A. (1999, May). Effect of Multilanes on Wheel Load Distribution in Steel Girder Bridges. *Journal of Bridge Engineering*, 4:2, 99-106.
- MDX (September 24, 2001). *MDX Curved & Straight Steel Bridge Design and Rating Software*®.
- Moore, M., Strand, K.A., Grubb, M.A., & Cayes, L.R. Wheel-Load Distribution Results from AISI-FHWA Model Bridge Study. *Transportation Research Record 1275*, 34-44.

Newmark, N.M. (1938). A Distribution Procedure for the Analysis of Slabs Continuous over Flexible Girders. *Eng. Exp. Sta. Bull.* 304, 7-118.

Newmark, N.M. (1949). Design of I-Beam Bridges. *Transportation ASC, Vol. 114*, 997-1022.

Newmark, N.M. (1943). Design of Slab and Stringer Highway Bridges. *Public Roads, Vol. 23:7*, 157-166.

Newmark, N.M. & Siess, C.P. (1942). Moments in I-beam Bridges. *Eng. Exp. Sta. Bull.* 336, *Vol. XXXIX, No. 44*, 1-148.

Newmark, N.M. (1946). Studies of Slab and Beam Highway Bridges, Part I: Tests of Simple Span Right I-beam Bridges. *Eng. Exp. Sta. Bull.* 363, 1-130.

Newmark, N.M. (1948). Studies of Slab and Beam Highway Bridges, Part II: Tests of Simple Span Skew I-beam Bridges. *Eng. Exp. Sta. Bull.* 375, 1-61.

Nutt, R.V., Schamber, R.A., & Zokaie, T. (1988). Distribution of Wheel Loads on Highway Bridges. Final Report for National Cooperative Highway Research Program.

Ontario Highway Bridge Design Code, Third Edition, Ontario Ministry of Transportation and Communications, Downsview, Ontario, Canada, 1991.

Sanders, Jr., W.W. (1984). Distribution of Wheel Loads on Highway Bridges. *National Cooperative Highway Research Program Synthesis of Highway Practice 111*.

- Shahawy, M. & Huang, D. (2001, August). Analytical and Field Investigation of Lateral Load Distribution in Concrete Slab-on-Girder Bridges. *ASI Structural Journal*, 590-599.
- Simon v. 8.1 (July 15, 1996). *Simon Systems*®. American Institute of Steel Construction, Chicago, IL.
- Stallings, J.M. and Yoo, C.H. (1991, Feb). Bridge Testing. Final Report: Project Number ST 2019-12 for The State of Alabama Highway Department.
- Tarhini, K.M. & Frederick, G.R. (1992). Wheel Load Distribution in I-Girder Highway Bridges. *Journal of Structural Engineering*, 118:5, 118:5, 1285-1294.
- Tiedeman J.L., Albrecht, P., and Cayes, L.R. (1993, April). Behavior of Two-Span Continuous Bridge under Truck Axle Loading. *Journal of Structural Engineering*, 119:4, 1234-1250.
- Walker, W.H. (1987). Lateral Load Distribution Multi-girder Bridges. *Engineering Journal*, 24:1, 21-28.
- Zokaie, T. (2000, May). AASHTO-LRFD Live Load Distribution Specifications. *Journal of Bridge Engineering*, 5:2, 131-138.